

12-2016

# Quantifying asphalt emulsion-based chip seal curing times using electrical resistance measurements

Miguel A. Montoya Rodriguez  
*Purdue University*

Follow this and additional works at: [https://docs.lib.purdue.edu/open\\_access\\_theses](https://docs.lib.purdue.edu/open_access_theses)



Part of the [Civil Engineering Commons](#)

---

## Recommended Citation

Montoya Rodriguez, Miguel A., "Quantifying asphalt emulsion-based chip seal curing times using electrical resistance measurements" (2016). *Open Access Theses*. 878.  
[https://docs.lib.purdue.edu/open\\_access\\_theses/878](https://docs.lib.purdue.edu/open_access_theses/878)

This document has been made available through Purdue e-Pubs, a service of the Purdue University Libraries. Please contact [epubs@purdue.edu](mailto:epubs@purdue.edu) for additional information.

**PURDUE UNIVERSITY  
GRADUATE SCHOOL  
Thesis/Dissertation Acceptance**

This is to certify that the thesis/dissertation prepared

By Miguel A. Montoya Rodriguez

Entitled

QUANTIFYING ASPHALT EMULSION-BASED CHIP SEAL CURING TIMES USING ELECTRICAL RESISTANCE MEASUREMENTS

For the degree of Master of Science in Civil Engineering

Is approved by the final examining committee:

John E. Haddock

Chair

12/02/2016

Jan Olek

12/01/2016

W. Jason Weiss

12/05/2016

To the best of my knowledge and as understood by the student in the Thesis/Dissertation Agreement, Publication Delay, and Certification Disclaimer (Graduate School Form 32), this thesis/dissertation adheres to the provisions of Purdue University's "Policy of Integrity in Research" and the use of copyright material.

Approved by Major Professor(s): John E. Haddock

Approved by: Dulcy M. Abraham

Head of the Departmental Graduate Program

12/5/2016

Date

QUANTIFYING ASPHALT EMULSION-BASED CHIP SEAL CURING TIMES  
USING ELECTRICAL RESISTANCE MEASUREMENTS

A Thesis

Submitted to the Faculty

of

Purdue University

by

Miguel A. Montoya Rodriguez

In Partial Fulfillment of the

Requirements for the Degree

of

Master of Science in Civil Engineering

December 2016

Purdue University

West Lafayette, Indiana

Dedicated to my parents, Carlos and America; my siblings, Carlos, Arturo, and Herta; my  
grandmother Rosa America, and Jesus, my savior.



## ACKNOWLEDGEMENTS

First, I would like to express my sincere gratitude to my advisor, Prof. John E. Haddock, for his patience, support, motivation, and immense knowledge. His guidance and supervision has helped me throughout the research and writing of this thesis. I could not have imagined a better advisor and mentor for my graduate studies. I would also like to thank my thesis committee members: Prof. W. Jason Weiss for his much appreciated contributions to this research study and his absolutely invaluable discussions, ideas, and feedback, and Prof. Jan Olek for his encouragement and suggestions that encouraged me to widen my research from a different perspective.

I would like to acknowledge the financial support of the Indiana Department of Transportation under the SPR-3801 research project. I am grateful for the incredibly helpful assistance from INDOT transportation officials, Dr. Jusang Lee, Todd Shields P.E., and Clinton Bryant P.E. My sincere thanks also go to the chip seal field inspectors and crews who provided access to the chip seal projects. This thesis could not have been finished without the help and support from my co-workers, Robert Spragg, Cameron Wilson, and Mohammadreza Pouranian. My special appreciation goes to my graduate fellows and colleagues from Purdue University. Last but not least, I would like to thank my family for their unconditional love, encouragement, support, and prayers.

## TABLE OF CONTENTS

	Page
LIST OF TABLES .....	vii
LIST OF FIGURES .....	viii
ABSTRACT .....	xiii
CHAPTER 1. INTRODUCTION .....	1
1.1 Background .....	1
1.2 Problem Statement .....	3
1.3 Research Objectives .....	5
1.4 Thesis Organization.....	6
CHAPTER 2. LITERATURE REVIEW .....	7
2.1 Chip Seal Definition, Cost-effectiveness, and Life Expectancy .....	7
2.2 Chip Seal Best Practices.....	10
2.3 Best Practices Regarding the Construction Sequence Timing .....	13
2.4 Decision-Making Process for Brooming and Opening to Traffic .....	14
2.5 Chip Seal Curing Process and Factors that Affect Curing Time.....	15
2.6 Current Approaches to Determine Chip Seal Curing Times.....	18
2.7 Asphalt Emulsion Electrical Measurement Concept.....	21
2.8 Electrical Resistance Measurements .....	23
CHAPTER 3. EXPERIMENTAL PROGRAM.....	27
3.1 Program Overview .....	27
3.2 Electrical Impedance Spectroscopy Testing .....	28
3.2.1 Materials .....	28
3.2.2 Electrical Impedance Measurements .....	29
3.2.3 Sample Preparation.....	32

3.2.4	Testing Procedures.....	35
3.2.5	Moisture Content Ratio.....	36
3.3	Field Trials and Standardized Mechanical Strength Tests .....	36
3.3.1	Full-Scale Field Trials .....	36
3.3.2	Materials .....	37
3.3.3	Electrical Resistance Measurements.....	38
3.3.4	Water Evaporation Rate.....	40
3.3.5	Development of Mechanical Strength .....	44
3.3.5.1	Sweep Test (ASTM D7000).....	45
3.3.5.2	Vialit Test .....	48
3.4	Field Implementation, Validation, and Calibration.....	51
CHAPTER 4. RESULTS AND DISCUSSION .....		55
4.1	Electrical Impedance Spectroscopy Testing .....	55
4.1.1	Normalized Resistance Index (NRI).....	56
4.1.2	Measurement Concept Validation .....	61
4.1.3	Asphalt Emulsion-Aggregate Combinations .....	63
4.1.4	Multiple Frequency Electrical Response .....	69
4.2	Field Trials and Standardized Mechanical Strength Test.....	71
4.2.1	Statistical Analysis of Chip Seal Curing Process .....	71
4.2.2	Field Trials Using Normalized Resistance Index .....	74
4.2.3	Sweep Test Results .....	77
4.2.4	Vialit Test Results.....	79
4.3	Field Implementation, Validation, and Calibration.....	81
4.3.1	Two-point Probe Configuration.....	82
4.3.2	Distance between Probes .....	83
4.3.3	Frequency of Electrical Current.....	85
4.3.4	Two-point Probe Setting.....	87
4.3.5	Chip Seal Curing Times.....	89
4.3.6	Quality Control Tool.....	91

CHAPTER 5. SUMMARY, CONCLUSIONS, AND FUTURE WORK.....	92
5.1 Summary .....	92
5.2 Conclusions .....	93
5.3 Future Work .....	95
LIST OF REFERENCES.....	98
APPENDICES	
Appendix A. INDOT’s Chip Seal Aggregate Gradation.....	106
Appendix B. Sweep Test Specimens.....	107
Appendix C. Vialit Test Specimens .....	115

## LIST OF TABLES

Table	Page
1.1: INDOT In-house Chip Seal Program, Lane Miles per Fiscal Year between 2009 and 2017 (Tompkins, 2013; Bryant, personal communication October 5, 2016) .....	3
2.1: Typical Unit Costs (Based on 2009 US\$) and Pavement Life for Flexible Pavement Preservation Treatments (Brown and Heitzman, 2013).....	8
3.1: Aggregate Properties.....	38
3.2: Climatic Data .....	42
3.3: Asphalt Emulsion-Aggregate Combinations for Sweep Test.....	46
3.4: Asphalt Emulsion-Aggregate Combinations for Vialit Test Method .....	48
3.5: Materials Used at Each Pavement Section .....	52
4.1: Regression Equations Relating NRI and MCR for Asphalt Emulsions.....	61
4.2: Asphalt Emulsion-Aggregate Combinations .....	64
4.3: Regression Results for Asphalt Emulsion-Aggregate Combinations .....	67
4.4: Stepwise Variable Selection Output .....	73
4.5: Piecewise Regression Analysis for ASTM D7000 Data .....	79
4.6: Piecewise Regression Analysis for Vialit Test Results at 37°C .....	80
4.7: Quantified Chip Seal Curing Times at Field Sites.....	90
Appendix Table	
A.1: INDOT's Chip Seal Aggregate Gradation.....	106

## LIST OF FIGURES

Figure	Page
2.1: Life-cycle benefits of preventive maintenance; PCI = pavement condition index (Galehouse et al., 2003). .....	9
2.2: Desirable chip seal design (Wood et al., 2006). .....	11
2.3: Chip seal equipment: (a) asphalt emulsion distributor, (b) aggregate spreader, (c) roller, and (d) broom. ....	12
2.4: Importance of chip seal curing time on surface treatment success, performance, and life expectancy. ....	14
2.5: Stages in the curing process of asphalt emulsions (James, 2006). ....	16
2.6: Relationship between chip seal strength gain and moisture loss using frosted marble test (Howard et al., 2011).....	19
2.7: Correlation between sweep test chip loss and emulsion moisture loss for field test site aggregates and emulsions (Shuler, 2011).....	20
2.8: Dielectric properties of water-in-oil emulsions at different water contents (Sowa et al., 1995). ....	21
3.1: Flow chart of experimental program. ....	28
3.2: Phasor diagram of impedance measurement of asphalt emulsion specimen. ....	30
3.3: Nyquist plot of impedance measurement of asphalt emulsion specimen. ....	30

3.4: Bode plots of impedance measurements of asphalt emulsion specimen: (a) impedance vs. frequency and (b) phase angle vs. frequency.....	31
3.5: Schematic of two-point uniaxial EIS sample holder. ....	33
3.6: Pure asphalt emulsion binder specimens. ....	34
3.7: Asphalt emulsion-aggregate combination specimen. ....	35
3.8: Location of full-scale field trials (source: <a href="http://d-maps.com">http://d-maps.com</a> ). ....	37
3.9: Electrical resistance two-point probe.....	39
3.10: Schematic representation of proper electrical connection. ....	40
3.11: Plywood plate prior to construction sequence. ....	41
3.12: Plate sample placed on balance. ....	41
3.13: Plate sample mass as a function of curing time for SR 8 chip seal. ....	43
3.14: Shear force simulation using broom. ....	44
3.15: Aggregate loss at area subjected to broom's shear force.....	45
3.16: ASTM D7000 brooming simulation. ....	46
3.17: Electrical resistance measurement of sweep test specimen. ....	48
3.18: Vialit test specimen, AE-90S SC 16 gravel.....	49
3.19: Specimen temperature after freezer conditioning, $0 \pm 2^{\circ}\text{C}$ . ....	50
3.20: Specimen used to relate electrical properties to Vialit test sample trays.....	51
3.21: Location of field implementation sites (source: <a href="http://d-maps.com">http://d-maps.com</a> ). ....	52
3.22: Two-point probe: (a) using plastic spacer, (b) using felt and stainless steel washers, and using plywood pad supports spaced at (c) 7.6 cm, (d) 15.2 cm, and (e) 30.4 cm. ....	53
4.1: MCR vs. curing time in days at $23 \pm 0.5^{\circ}\text{C}$ and $50 \pm 2\% \text{ RH}$ : (a) AE-90S and (b) CRS-2P. ....	56

4.2: Bulk resistance vs. MCR at $23 \pm 0.5^\circ\text{C}$ and $50 \pm 2\%$ RH: (a) AE-90S and (b) CRS-2P. ....	58
4.3: NRI vs. MCR at $23 \pm 0.5^\circ\text{C}$ and $50 \pm 2\%$ RH: (a) AE-90S and (b) CRS-2P. ....	60
4.4: NRI as a function of $D$ at $23 \pm 0.5^\circ\text{C}$ and $50 \pm 2\%$ RH: (a) AE-90S and (b) CRS-2P. ....	62
4.5: MCR vs. curing time in days: CRS-2P limestone combination at $23 \pm 0.5^\circ\text{C}$ and $50 \pm 2\%$ RH. ....	65
4.6: Bulk resistance vs. MCR: CRS-2P limestone combination at $23 \pm 0.5^\circ\text{C}$ and $50 \pm 2\%$ RH. ....	65
4.7: NRI vs. MCR trends of asphalt-emulsion aggregate specimens: (a) limestone and (b) gravel at $23 \pm 0.5^\circ\text{C}$ and $50 \pm 2\%$ RH. ....	66
4.8: Schematic illustration of the theoretical relationships in emulsion-based chip seal systems. ....	68
4.9: Bode plot, AE-90S gravel 1.8 L/m <sup>2</sup> OD: (a) impedance vs. frequency and (b) phase angle vs. frequency. ....	70
4.10: Moisture content ratio as a function of curing time profiles. ....	73
4.11: Electrical resistance measurements during chip seal curing. ....	74
4.12: Normalized resistance indices as a function of curing time. ....	75
4.13: Relationship between normalized resistance index values and water evaporation rate. ....	76
4.14: Aggregate dislodgement potential correlated to the normalized resistance index... ..	77



4.15: Piecewise linear regression between aggregate mass loss and normalized resistance index.....	78
4.16: Vialit test results at 37°C: aggregate mass loss vs. normalized resistance index. ....	80
4.17: Vialit test results at $0 \pm 2^\circ\text{C}$ : aggregate mass loss vs. normalized resistance index.	81
4.18: NRI vs. curing time at US 52 in Metamora: two-point probe comparison between using plywood pad supports and plastic spacer. ....	83
4.19: Electrical resistance vs. curing time at SR 827 in Angola: probes spaced at different distances.....	84
4.20: NRI vs. curing time at SR 827 in Angola: probes spaced at different distances. ....	84
4.21: Phase angle vs. curing time at SR 827 in Angola: probes spaced at different distances.....	85
4.22: Bode plots at SR 352 in Oxford: (a) electrical resistance vs. frequency and (b) phase angle vs. frequency. ....	86
4.23: Setting probe in fresh chip seal system.....	87
4.24: Tapping steel rod probes.....	88
4.25: NRI vs. Curing time, measured at five-different spots on the fresh chip seal at SR 827 Angola.....	89
4.26: MCR vs. Curing time, plate sample (1) at SR 827 Angola. ....	90
Appendix Figure	
B.1: AE-90S SC 16 Limestone. ....	107
B.2: AE-90S SC 16 Dolomite.....	108
B.3: AE-90S SC 11 Limestone. ....	109
B.4: AE-90S SC 16 Gravel. ....	110

B.5: CRS-2P SC 16 Limestone.....	111
B.6: CRS-2P SC 16 Dolomite.....	112
B.7: CRS-2P SC 11 Limestone.....	113
B.8: CRS-2P SC 16 Gravel.....	114
C.1: AE-90S SC 16 Limestone.....	115
C.2: AE-90S SC 16 Dolomite.....	116
C.3: AE-90S SC 11 Limestone.....	117
C.4: AE-90S SC 11 Gravel.....	118
C.5: CRS-2P SC 11 Limestone.....	119
C.6: CRS-2P SC 16 Gravel.....	120

## ABSTRACT

Montoya Rodriguez, Miguel A. M.S.C.E., Purdue University, December 2016. Quantifying Asphalt Emulsion-Based Chip Seal Curing Times Using Electrical Resistance Measurements. Major Professor: Prof. John Haddock.

Chip seals are among the most cost-effective surface treatments available for asphalt pavement preventive maintenance. Chip sealing typically consists of covering a pavement surface with asphalt emulsion into which aggregate chips are embedded. The asphalt emulsion cures through the evaporation of water, which helps to provide mechanical strength for the chip seal. Ultimately, the curing process enables the emulsion to adhere to the pavement while keeping the aggregate chips in place. The curing time for the chip seal depends on many factors, such as the asphalt emulsion and aggregate types, aggregate moisture content, emulsion and aggregate application rates, and environmental conditions (e.g., temperature, wind speed, relative humidity, and solar radiation).

Currently, no field technique is available that can quantify when sufficient mechanical strength has developed in the binder to allow traffic on a newly sealed roadway or to remove the surplus aggregate from a fresh chip seal. Such decisions are made by empirical factors that rely on the experience of field personnel. Consequently, frequent problems associated with the lack of early mechanical strength development of asphalt emulsion, which can result in premature surface treatment failure, have led to the need to improve the characterization of the chip seal curing process. As such, this study

investigated the use of an electrical resistance measurement to develop a sound construction methodology to prevent common failures that occur soon after construction.

First, full frequency, two-point, uniaxial electrical impedance spectroscopy was used to characterize the electrical properties of asphalt emulsions and various asphalt emulsion-aggregate combinations. The laboratory test results suggest a relationship between the changes in the electrical resistance of an asphalt emulsion and the amount of curing that has occurred in a chip seal system. In addition, standardized mechanical strength tests and full-scale field trials were conducted using a variety of materials. The electrical properties of the fresh seal coats were quantified by employing a handheld electrical device with a two-point probe to measure resistance. The findings suggest that chip seal systems gain significant mechanical strength when the initial electrical resistance measurement increases by a factor of 10. Finally, the implementation of the methodology for five full-scale chip seal systems in Indiana indicates that curing times for the chip seal projects range from 3.5 to 4.0 hours.

Electrical resistance measurements can provide a rapid, nondestructive, low-cost indication of the amount of curing that has occurred in a chip seal. The application of this methodology will result in more accurate, robust, and timely decisions with regard to when a chip seal has gained sufficient mechanical strength to allow brooming or opening to unrestricted traffic without undue loss of cover aggregate. Furthermore, implementing this construction technique could positively impact chip seal construction quality as well as extend the service life of the chip seal. Lastly, the findings of this study can be extended to include a variety of asphalt emulsion applications.

## CHAPTER 1. INTRODUCTION

### 1.1 Background

In the United States, over 3.95 million miles of public roads must be maintained, conserved, and protected. The quality of these roads plays a critical role in the nation's economy, having a considerable impact on agriculture, industry, commerce, and recreation (FHWA, 2003). Accordingly, most highway agencies have implemented pavement preservation programs to address pavement needs and improve ride quality, as well as to reduce vehicle operating costs for the transportation industry and general public. 'Pavement preservation' refers to the sum of all the activities required to provide and maintain serviceable highways, including preventive maintenance, minor rehabilitation, and routine maintenance (FHWA, 2005).

Among these three major components, preventive maintenance is the keystone of any pavement preservation program. Preventive maintenance is a planned strategy of cost-effective treatments for an existing roadway system and its appurtenances that preserves the system, retards future deterioration, and maintains or improves the functional condition of the system. Just \$1 spent on preventive maintenance can save \$6 to \$14 on future repairs (Geoffroy, 1996). Chip sealing is one of the most widely used preventive maintenance treatments for flexible pavements due to its ease of use, favorable economic benefits, and effectiveness (TxDOT, 2003).

Since the 1920s, chip seals have been used to provide cost-effective riding surfaces. The early uses were predominantly as wearing courses in the construction of low-volume gravel roads. Over the past 75 years, chip seals have evolved into maintenance treatments that can be successful for both low-volume and high-volume pavements (Gransberg and James, 2005). However, the last two decades have seen growing popularity among highway transportation agencies to use chip seals as a pavement preservation technique. The popularity of chip seals is a direct outcome of their low initial costs in comparison with those of thin asphalt overlays and other preservation options (Gransberg and James, 2005).

As a result, chip seals have become increasingly important in the nation's pavement preservation programs, leading to seemingly constant revision by many state and local highway agencies of both maintenance policies and construction specifications to improve chip seal performance (Mahoney et al., 2014). Transportation officials have established ongoing chip seal research programs with the purpose of delivering longer-lasting surface treatments (Cole and Wood, 2014). The goal is to develop new methodologies that contribute to lengthening the service life of chip seal treatments and thus maximize the available funding for pavement preservation.

One of the states that uses chip sealing as its most common pavement preservation technique and has implemented innovative chip seal practices is Indiana. In 2009, the Indiana Department of Transportation (INDOT) established an in-house chip seal program to maintain the statewide pavement network at the lowest possible cost (Tompkins, 2013). As part of this program, a three-year study was conducted to develop a software program to determine the asphalt emulsion and aggregate application rates for

each chip seal project (Lee et al., 2011). In 2013, a research project was launched to find ways to improve the efficiency of the chip seal process by identifying and sharing best practices across the six INDOT districts (Padfield et al., 2014). As shown in Table 1.1, INDOT currently completes between 1,400 and 1,500 lane miles of chip sealing per fiscal year at a cost of approximately \$12 to \$14 million (INDOT, 2012).

Table 1.1: INDOT In-house Chip Seal Program, Lane Miles per Fiscal Year between 2009 and 2017 (Tompkins, 2013; Bryant, personal communication October 5, 2016)

Fiscal Year	Lane Miles
2009	444
2010	705
2011	1161
2012	1424
2013	1445
2014	1272
2015	1548
2016	1499
2017	1475

## 1.2 Problem Statement

Chip seals are applied to pavements that show minimal distress in order to waterproof the surface, seal small cracks, improve friction, and prolong the life of the roadway surface for at least four years (Moulthrop, 2003; Sinha, 2005). The quality and performance of chip seal treatments during their service life are driven primarily by the construction phase (Gransberg and James, 2005). Chip seals typically are constructed by spraying an asphalt emulsion film on the surface of an existing pavement, spreading a layer of cover aggregate, rolling the aggregate onto the fresh asphalt emulsion's surface to seat the aggregate chips firmly into the emulsion, brooming the surplus aggregate particles, and opening the pavement to unrestricted traffic (Asphalt Institute, AEMA, 2008).

To a great extent, the timing of this construction sequence determines the success or failure of the surface treatment. Although rapid-set emulsions are used for chip seals, these emulsions still require some amount of time to sufficiently cure (WSDOT, 2003). The actual curing time is jobsite-specific and depends on several factors, which include the types of emulsion and aggregate, the temperature, humidity, wind speed, and cloud cover, as well as several less quantifiable factors. Sometimes, uncontrollable variables that affect the chip seal curing process can make the seal coat performance unpredictable and may even lead to surface treatment failures, such as aggregate loss and bleeding, and to vehicle damage that can compromise human safety (Shuler, 1999).

The methodology for determining the optimal time for brooming or the opening of a newly chip-sealed pavement to unrestricted traffic has been more an art than a science (Wegman, 1991). More recent approaches to predict chip seal curing times are difficult to transfer to the field and may fail to account for the inherent variability that exists within all chip seal projects. As a result, such decisions are still made by empirical factors that rely on experienced field personnel. References in the literature have termed this decision-making process a ‘subjective decision’ or ‘judgment call’ (Schuler, 2011; Testa et al., 2014). State and local highway agencies must be able to rely on sound construction techniques to achieve the pavement preservation benefits of chip sealing.

From a performance perspective, the best practice would be to allow the chip seal to sufficiently cure to prevent damage caused by brooming or subsequent vehicular traffic. However, this approach is in contrast with the desire to open the roadway to the travelling public as quickly as possible. As a result, there are cases where the chip seal may be opened to traffic too early, resulting in diminished pavement performance. Consequently,



there is a need to develop quantitative tools that can be used to determine when a fresh chip seal has cured properly and the road can be returned to service.

Therefore, as an alternative methodology, this research proposes the use of electrical property measurements to aid the chip seal construction decision-making process. In particular, this novel technique will contribute fundamentally to the determination of when asphalt emulsion-based chip seals can be broomed and opened to unrestricted traffic. Electrical resistance measurements can provide a rapid, effective, reliable, and nondestructive indication of the amount of curing that has occurred. The implementation of this technique could potentially positively impact chip seal construction quality as well as service life performance.

### 1.3 Research Objectives

The primary objective of this research is to develop a practical field measurement technique that can consistently determine when a chip seal system has sufficiently cured and, therefore, if the chip seal can tolerate the shear forces of brooms and traffic. The following specific objectives were identified for the successful accomplishment of the work:

1. Develop an experimental set-up that simulates chip seal geometry and ensures repeatable electrical impedance spectroscopy (EIS) measurements for the proper electrical characterization of asphalt emulsions and various asphalt emulsion-aggregate combinations.
2. Evaluate the relationship between the electrical resistance properties and curing process of asphalt emulsion specimens and chip seal systems.

3. Investigate the correlations among the electrical resistance properties, rate of moisture removal, and mechanical performance of full-scale chip seal systems.
4. Establish a quantifiable method that estimates the mechanical resistance to aggregate brooming or shearing due to traffic via electrical resistance measurements.
5. Conduct field experiments to validate the proposed electrical resistance measurement technique.

#### 1.4 Thesis Organization

This thesis is composed of five chapters. Chapter 1 is an introduction that includes the background, problem statement, and research objectives. Chapter 2 presents a literature review of chip seal best practices about when to broom or open to traffic a fresh chip seal and the current approaches used to determine chip seal curing times. This chapter also provides information about the asphalt emulsion curing process and factors that affect this phenomenon as well as the feasibility of using electrical resistance measurements to quantify chip seal curing times. Chapter 3 describes the materials, test procedures, electrical resistance measurement techniques, water evaporation rate (WER) assessments, and mechanical performance tests that were employed to accomplish the research objectives. In Chapter 4, the experimental results of this study are reported and discussed. This chapter also presents the development of the field measurement technique, from preliminary laboratory testing to the application of this methodology for full-scale chip seal projects. Finally, conclusions from this research and future research recommendations are outlined in Chapter 5.

## CHAPTER 2. LITERATURE REVIEW

### 2.1 Chip Seal Definition, Cost-effectiveness, and Life Expectancy

Numerous guidelines, specifications, and research studies have been published worldwide about chip sealing, also referred to in the literature as a seal coat, asphalt surface treatment, single surface treatment, bituminous surface treatment, sprayed seal, surfacing seal, and surface dressing (Wood et al., 2006; NCDOT, 2015; RSTA, 2014; VICROADS, 2004; NZTA, 2012). A chip seal is defined as a single layer of asphalt emulsion binder that is covered by embedded aggregate, with its primary purpose to seal the fine cracks in the underlying pavement's surface and prevent the intrusion of water into the base and subgrade. The aggregate's purpose is to protect the asphalt residue layer from damage and to develop a macrotexture that results in a skid-resistant surface for vehicles (Gransberg and James, 2005).

Chip seals are employed as a preventive maintenance treatment for flexible pavements for at least one of the following reasons: (a) to provide a water-resistant, skid-resistant surface over an existing pavement structure, (b) as an interim measure pending the application of an asphalt mixture, and (c) to correct surface raveling and oxidation of old pavements (Asphalt Institute, AEMA, 2008). The common usage of chip seals as a pavement preservation tool is based on their beneficial cost-effectiveness in comparison

with thin asphalt and other preventive maintenance treatments. The cost for a single chip seal typically is slightly more than \$1 per square yard, which is far less than the \$3 to \$9 per square yard for other pavement preservation treatments and resurfacing projects (INDOT, 2016). Table 2.1 presents average cost estimates of preservation treatment options based on analysis of responses provided to the Federal Highway Administration (FHWA) by five selected state departments of transportation (DOTs) (Brown and Heitzman, 2013).

Table 2.1: Typical Unit Costs (Based on 2009 US\$) and Pavement Life for Flexible Pavement Preservation Treatments (Brown and Heitzman, 2013)

Pavement Preservation Treatment	Initial Costs, US\$/yd <sup>2</sup>	Expected Extended Life of Pavement, year	Annualized Cost, US\$/ yd <sup>2</sup> -year
Crack Treatment	0.32	2	0.16
Fog Seals	0.99	4	0.25
Chip Seals	1.85	6	0.31
Microsurfacing	3.79	6	0.63
Slurry Seals	4.11	5	0.82
Thin HMA Overlay	5.37	13	0.41

Chip seals enhance pavement conditions and extend the pavement service life when they are applied on pavements that show minimal distress (Moulthrop, 2003). It is important to note that chip seals cannot restore evenness to a deformed road nor do they contribute to the structural strength of the road (Read and Whiteoak, 2010). The average life of a seal coat is about six to eight years (TxDOT, 2003). As illustrated in Figure 2.1, three or four chip seals may be necessary for a pavement to reach its design life expectancy (Gransberg and James, 2005). These life-cycle benefits can be accomplished only if the chip seal treatments are constructed properly (AZAGC, 2013).

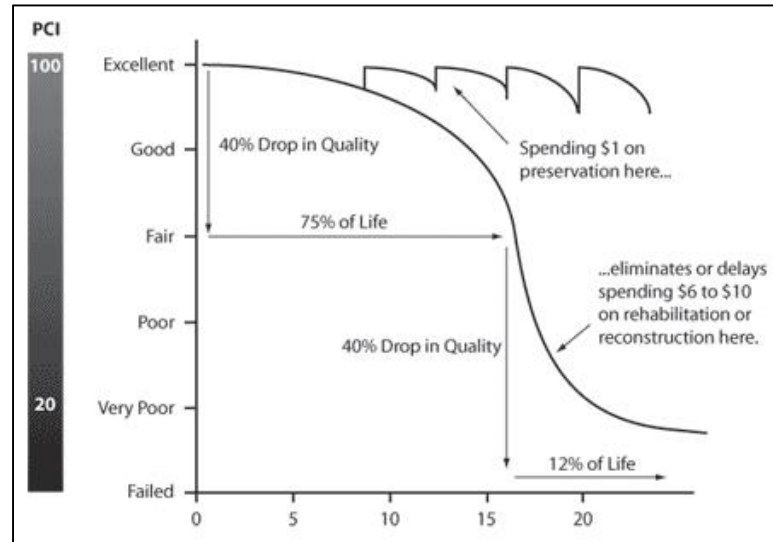


Figure 2.1: Life-cycle benefits of preventive maintenance; PCI = pavement condition index (Galehouse et al., 2003).

In North America, the traditional method used for designing and constructing chip seals is based mostly on local empirical experience (Wegman, 1991). Such empirical design methods can lead to lower than expected performance (Wood and Olson, 2007). Sometimes, the uncertainties of a chip seal project, such as the use of local materials, design and construction experience, and equipment availability, can make the chip seal's performance unpredictable and even lead to pavement failure due to problems such as bleeding and loss of aggregate, and may cause vehicle damage, thus compromising driver and passenger safety (Schuler, 1999). In order to deliver reliable and durable chip seal projects, state DOTs must rely on chip seal best practices. By implementing sound construction techniques, chip seal life expectancy, which is typically between 6 to 8 years, can be prolonged to 12 or even 15 years (Cole and Wood, 2014).

## 2.2 Chip Seal Best Practices

Chip seal best practices have been identified as a set of maintenance policies, design specifications, and construction techniques that determine the service life of a chip seal project. Gransberg and James grouped chip seal best practices into four main categories (Gransberg and James, 2005):

1. Contract administration, warranties, and performance measures,
2. Pavement selection, design, and material selection,
3. Construction, and
4. Chip seal equipment and quality assurance and quality control.

Any of these four best practices can play a pivotal role in the success or failure of a chip seal project. First, the administrative policies have an enormous impact on the cost of the treatment as well as the chip seal's ultimate performance. Chip seals designed and installed by state DOT's in-house maintenance forces are believed to produce the best final results (Gransberg and James, 2005). The process continues in the planning stage when the pavement surface is analyzed to determine whether a chip seal is an appropriate preventive maintenance treatment. This candidate generation depends on several attributes of the pavement section, such as the age of the pavement, wearing surface condition parameters (i.e., roughness, friction, rutting, cracking), and the average daily traffic (Tompkins, 2013).

Once the decision to use a chip seal has been made, the next step is to select the proper materials and determine suitable application rates. It is crucial to highlight that asphalt emulsion binders and cover aggregate make up the finished chip seal treatment.

Several theoretical procedures are available for chip seal design. As shown in Figure 2.2, a desirable design is based on 60 percent to 70 percent of the aggregate voids being filled with asphalt emulsion residue. This process usually involves determining the average least dimension of the aggregate shape, the voids in the aggregate, and the loose unit weight of the cover aggregate (Asphalt Institute, AEMA, 2008).

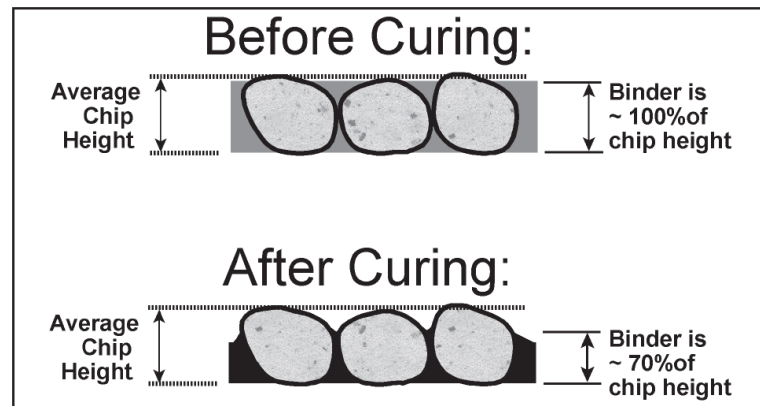


Figure 2.2: Desirable chip seal design (Wood et al., 2006).

The application of a chip seal involves essentially four pieces of equipment: the asphalt emulsion distributor, aggregate spreader, rollers, and brooms (Gransberg and James, 2005), as shown in Figure 2.3. The equipment should be calibrated properly and in good operating condition to distribute the asphalt emulsion and cover aggregate in a consistent manner. Chip seals typically are constructed by employing the following operation sequence:

1. Patch potholes and repair damaged areas in the existing pavement,
2. Clean the surface with a rotary broom or by another approved method,
3. Spray the asphalt emulsion binder at the specified rate and proper temperature,

4. Spread the cover aggregate at the specified rate immediately after the asphalt emulsion application to achieve maximum possible chip wetting,
5. Roll the cover aggregate adequately to thoroughly seat the particles in the asphalt film,
6. Develop a good traffic control plan, and
7. Remove loose and surplus aggregate particles with a rotary broom after the treatment is completed (Asphalt Institute, AEMA, 2008).

For optimal performance, chip seals must be applied during the warmest and driest weather possible. Finally, an aggressive quality control testing program, combined with close inspection, contribute to the chip seal project's success (Gransberg and James, 2005).

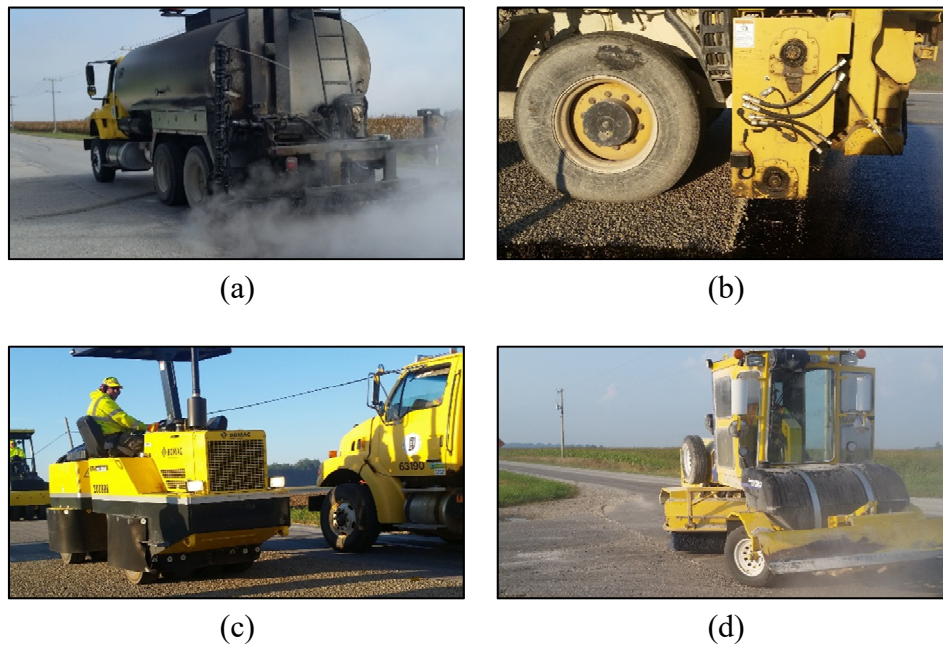


Figure 2.3: Chip seal equipment: (a) asphalt emulsion distributor, (b) aggregate spreader, (c) roller, and (d) broom.



### 2.3 Best Practices Regarding the Construction Sequence Timing

The quality and performance of chip seals during their service life are driven mainly by the construction phase (Gransberg and James, 2005). Furthermore, if the material and equipment best practices are satisfied and the climatic conditions are favorable, the success of the chip seal hinges on the timing of the construction process (NCDOT, 2015). Therefore, chip seal best practices regarding construction sequence timing are a key aspect of a surface treatment's success.

To begin the process, it is recommended that patching be completed at least six months before and cracks repaired at least three months before the application of a chip seal (Gransberg and James, 2005). Once chip sealing initiates, as soon as the asphalt emulsion is sprayed, the aggregate must be spread. Aggregate should be spread within one minute after applying the emulsion to avoid aggregate debonding due to significant emulsion curing and breaking. Equally important, the rollers should follow the chip spreader as closely as practical. Pneumatic tire rollers should cover the area three times within 30 minutes after the aggregate application. The first roller application should be completed within two minutes after aggregate application.

When rolling has been completed, traffic control should be maintained until the surplus aggregate has been swept away. This sweeping is done once the asphalt emulsion has sufficiently cured to hold the aggregate in place (Lee and Shield, 2010). The curing time thus regulates the timing of key chip seal construction operations, such as removing excess aggregate and allowing traffic on the newly sealed pavement. Consequently, the

chip seal curing time is a decisive input element to attain chip seal best practices, as presented in Figure 2.4.

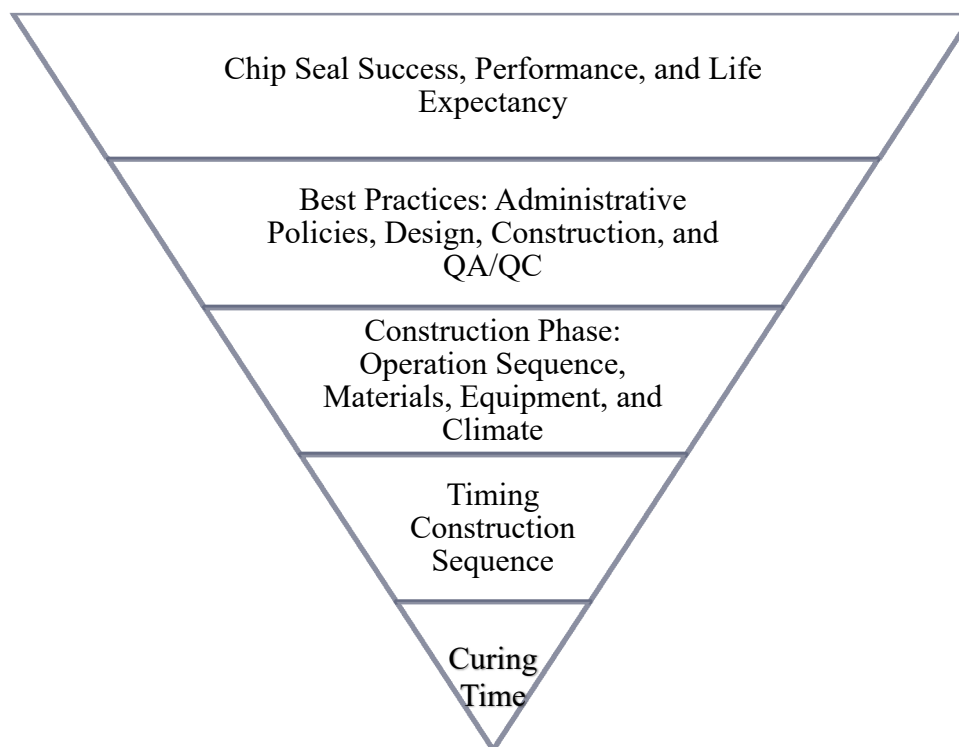


Figure 2.4: Importance of chip seal curing time on surface treatment success, performance, and life expectancy.

#### 2.4 Decision-Making Process for Brooming and Opening to Traffic

The decision-making process for brooming and opening the newly sealed pavement to unrestricted traffic is a critical stage of the construction sequence. If done too soon, brooming itself might damage the chip seal by dislodging embedded aggregate particles (WSDOT, 2003). Similarly, uncontrolled traffic before the fresh seal has sufficiently cured may trigger aggregate particle loss and lead to chip orientation and embedment beyond rolling (Connor, 1984). Aggregate particle loss due to brooming or early trafficking is detrimental to the quality and performance of the surface treatment, as

the aggregate provides resistance to skidding, polishing, and abrasion (Griffith and Hunt, 2000). Furthermore, aggregate particle loss can increase the chance of chip particles becoming airborne under traffic, which can lead to windshield breakage and possible accidents. Traditionally, it is recommended that brooming should take place on the morning following the application of the chip seal (Lee and Shield, 2010), which often delays the completion of construction and increases public dissatisfaction (Caltrans, 2014).

The decision-making process depends on factors such as engineering experience, climatic conditions, traffic volume, types of equipment, and material properties (Gransberg and Zaman, 2002). Any one of these factors can have a significant effect on how long it takes the chip seal to cure enough to retain the aggregate and support the brooming operation and opening to traffic. To date, there is no quantitative method available that can determine when the binder has sufficiently cured. Such decisions are made by empirical factors that rely on experienced field personnel. Limited research has been undertaken on this topic, and Austroads identified this topic as one of the most fertile areas in pavement engineering for further study and development (Alderson, 2009). A quantitative methodology that can accurately determine chip seal curing times would be useful to improve the overall chip seal construction process.

## 2.5 Chip Seal Curing Process and Factors that Affect Curing Time

The use of asphalt emulsion in chip seals allows for application temperatures that are well below those needed for hot applied asphalt binder, which is positive from the perspective of both environmental and safety aspects (Baumgardner, 2006). However, one inherent

concern that is related to emulsion-based chip seals is the curing process. The asphalt emulsion curing process refers to the development of the residual asphalt mechanical properties (Asphalt Institute, AEMA, 2008), particularly the formation of enough binder adhesive strength to bond the emulsion to the existing pavement while keeping the aggregate chips in place.

As shown in Figure 2.5, the curing process involves a series of steps that must occur to achieve a continuous asphalt cohesive film. Asphalt emulsions contain a significant water portion, and curing is governed primarily by the amount of water that evaporates (Banerjee et al., 2012). As such, after emulsion is placed it must break to initiate the evaporation of water. The asphalt emulsion breaking process refers to the separation of the emulsion components (i.e., asphalt and water). The chemical reactions between the aggregate and the emulsion are the main breaking mechanisms. As the water evaporates, the asphalt particles move closer together and begin to flocculate (James, 2006). At this early stage of the curing process, a considerable amount of water may have evaporated, but no appreciable mechanical strength has yet developed (Howard et al., 2011).

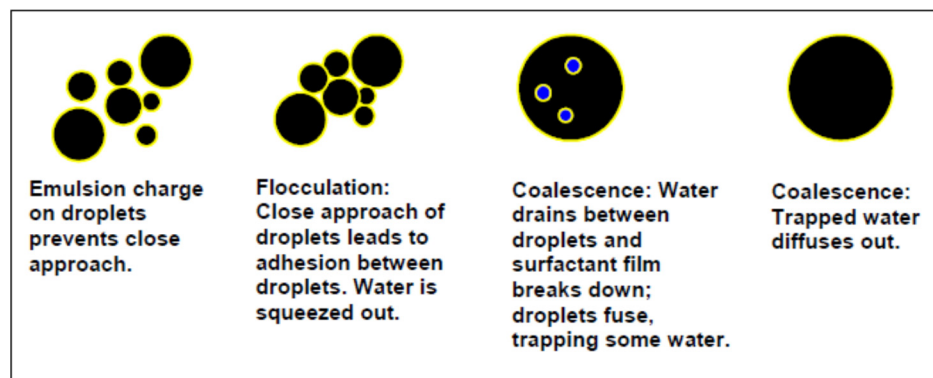


Figure 2.5: Stages in the curing process of asphalt emulsions (James, 2006).

As more water evaporates, the asphalt emulsion particles begin to coalesce and the mechanical strength improves. After a sufficient amount of water has evaporated, the emulsion reverts from layer-emulsified asphalt particles dispersed in water to predominantly an asphalt film with some entrapped water molecules (James, 2006). This transition to a continuous asphalt film leads to a significant increase in the adhesive strength of the binder, and the asphalt emulsion can then be considered sufficiently cured to retain aggregate particles. Once the aggregate particles are satisfactorily embedded in the emulsion, brooming operations can begin and uncontrolled traffic can be allowed onto the fresh seal coat (Shuler, 2011). However, it should be noted that water pockets may continue to move through the asphalt film and leave residue material. Once the total amount of water in the emulsion evaporates, the asphalt emulsion is considered completely cured (James, 2006).

The actual curing time is project-specific and depends on several factors, such as material properties and climatic conditions, as well as several other less quantifiable factors. Such uncertainties have stymied the development of a standard, quantifiable method to ascertain when a fresh chip seal can withstand the forces of brooming or unrestricted traffic. Some of the most significant factors that affect the curing rate of chip seal systems include the types of asphalt emulsion and aggregate, climatic conditions, aggregate moisture content, asphalt emulsion-aggregate compatibility, material application rates, and rolling pressure (Asphalt Institute, AEMA, 2008).

## 2.6 Current Approaches to Determine Chip Seal Curing Times

Traditionally, the methodology used to determine the optimal time for brooming or the opening of a newly chip-sealed pavement to unrestricted traffic has been more an art than a science (Wegman, 1991). Recently, several statistical models have been developed to predict the amount of water that is lost under field conditions that incorporate different aspects of the prevailing weather conditions, namely, the ambient temperature, relative humidity (RH), wind speed, and solar radiation (Banerjee et al., 2012; Yaacob et al., 2015).

Shuler and others (2011; Howard et al., 2011) have reported a strong relationship between the moisture content and binder strength in a chip seal system. Howard et al. (2011) measured chip seal binder adhesive strength gain as a function of moisture loss using three laboratory test methods: the sweep test (ASTM D7000), modified sweep test, and frosted marble test. Although all three tests are different, the results were similar and indicated that the strength in emulsion residue increases as the total moisture in the system is reduced, as shown in Figure 2.6.

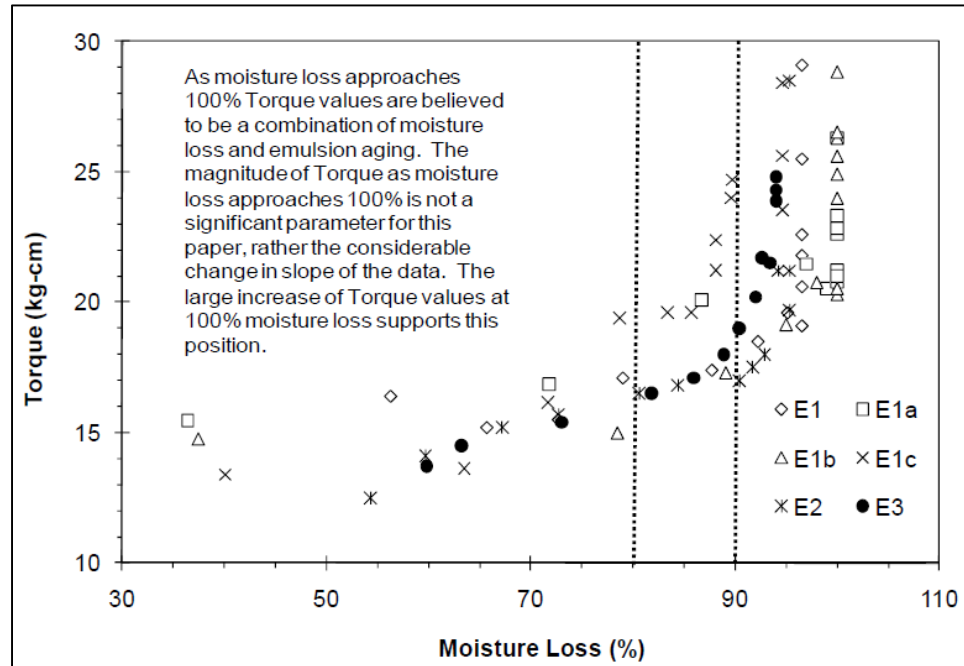


Figure 2.6: Relationship between chip seal strength gain and moisture loss using frosted marble test (Howard et al., 2011).

Shuler (2011) conducted full-scale pavement tests under different climatic conditions and modified laboratory sweep tests (Figure 2.7). The results of these field and laboratory tests were comparable and revealed a relationship between moisture content and binder strength. As a result, *The Manual for Emulsion-Based Chip Seals for Pavement Preservation* (Shuler et al., 2011) recommends the initial brooming operation be undertaken when the moisture content of the chip seal reaches approximately 25 to 15 percent of the total moisture present in the chip seal system.

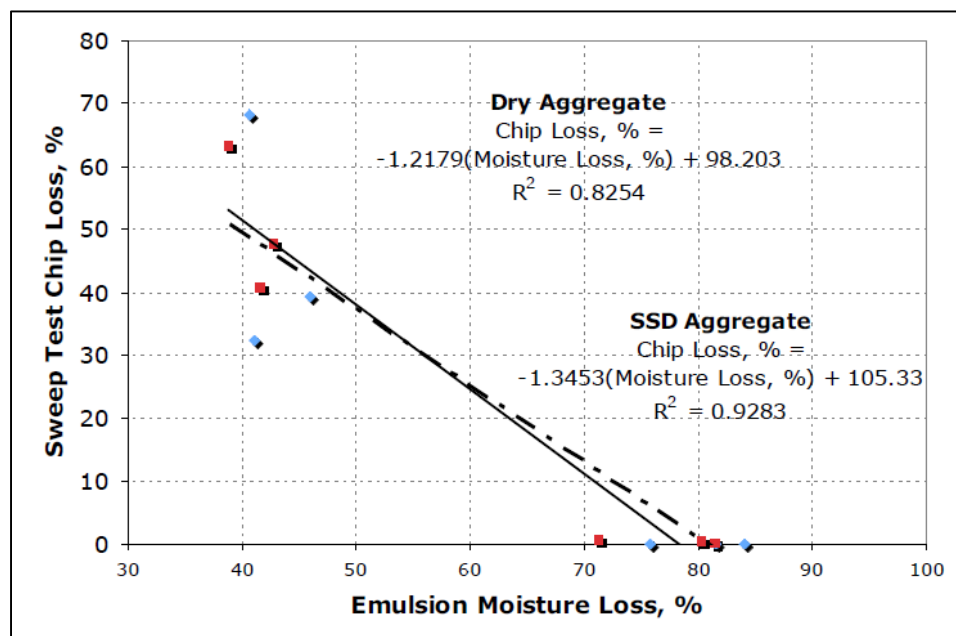


Figure 2.7: Correlation between sweep test chip loss and emulsion moisture loss for field test site aggregates and emulsions (Shuler, 2011).

The total moisture content consists of water in the emulsion plus moisture in the aggregate chips. To perform this procedure, it is suggested preliminary laboratory sweep tests be conducted to determine the moisture content at which the chip seal test specimen reaches 10 percent aggregate mass loss (AML). The moisture content of the chip seal should be measured in areas of the project where moisture loss is expected to be slowest, such as in shady or cooler locations (Shuler et al., 2011).

In principle, these current approaches are comprehensive and statistically sound. However, these methodologies are difficult to transfer to the field and therefore are not widely used in practice.



## 2.7 Asphalt Emulsion Electrical Measurement Concept

As an alternative, this research proposes the use of electrical property measurements to quantify chip seal curing times and aid the construction decision-making process. The correlation between moisture loss and strength gain can be used as the central premise to develop practical specification guidelines that are related to brooming and traffic opening (Howard et al., 2011). Schuler (2011) emphasized that research is needed to identify a quantitative measure for evaluating chip seal binder adhesive strength. As shown in Figure 2.8, previous studies in the petroleum industry have reported a relationship between the electrical properties of water-in-oil (w/o) emulsions and the water volume fraction (Sowa et al., 1995). However, this relationship has not been extended to the use of electrical properties to quantify the curing time, moisture content, or binder adhesive strength for chip seals.

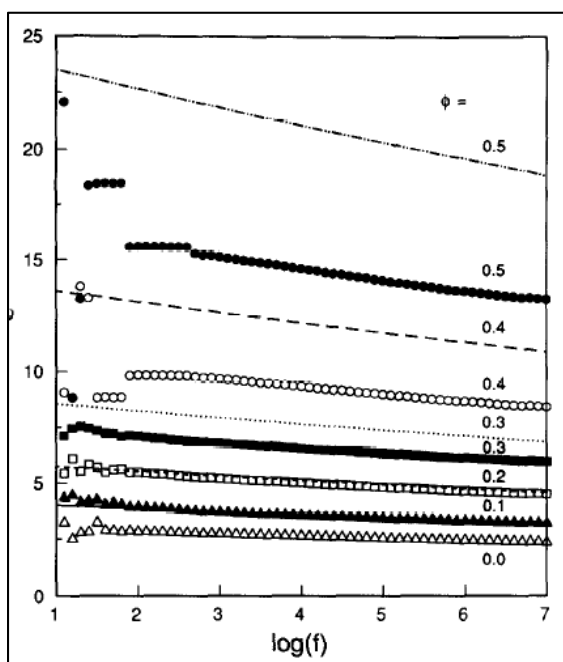


Figure 2.8: Dielectric properties of water-in-oil emulsions at different water contents (Sowa et al., 1995).

In light of this information, the current research investigates the feasibility of using electrical resistance measurements to quantify the moisture content of a chip seal system, or the extent of the curing process. As the emulsion reverts from emulsified asphalt particles dispersed in water to a continuous asphalt film, the residue increasingly will tend to oppose the passage of an electric current. This hypothesis is based on two main concepts: the significant amount of water that is contained in emulsions and the stages of the water evaporation process in the system.

Standard asphalt emulsions normally contain 40% to 75% bitumen, 25% to 60% water, and 0.1% to 2.5% emulsifier plus some minor components (James, 2006). These primary constituents can be grouped by their molecular arrangement into polar and nonpolar components. According to Needham (1996), bitumen is a complex material that contains some polar elements; however, overall, it is considered nonpolar. Conversely, water is a polar medium that consists of various ionic species (Needham, 1996).

It is well known that polar compounds are reasonable conductors of electricity, whereas nonpolar compounds typically behave as insulators. As such, it can be assumed that most conduction occurs through the ionic species of the water portion in the emulsion. The electrical properties of the emulsifiers are neglected, as they have separated into nonpolar and polar portions in a single molecule (Takamura and James, 2015) and represent a marginal portion of the asphalt emulsion products.

Considering the ions in water are the primary mode of conduction, the passage of an electric current through bitumen emulsion is dictated by the remaining volume of water in the system. James (2006) described the evaporation of water in emulsions as a four-stage breakdown process. Initially, the emulsified asphalt particles are dispersed in

water and an electrostatic barrier prevents asphalt droplets from approaching each other. The electrical current path is governed by the interconnection of the water layer. Eventually, the droplets achieve enough energy to overcome this barrier and gradually adhere to each other while water is squeezed out. The water layer becomes thinner, and the passage of electric current is driven by the tortuosity of the water layer path.

At the third stage, water drains between the asphalt droplets and the surfactant film breaks down; the droplets then fuse, thereby trapping some water. Thus, the electrical path is governed by the size and distribution of the trapped water molecules. Finally, the trapped water diffuses out, leaving a continuous asphalt film (James, 2006). As the emulsion breaks, it is expected that the electrical resistance, a measure of the difficulty to pass an electrical current through the residue, gradually increases over time.

## 2.8 Electrical Resistance Measurements

Electrical resistance measurements can evaluate the ability of a material to tolerate the transfer of ions subjected to an electric field (Spragg, 2013). As a result, electrical resistance measurements have shown potential to detect water and its connectivity in a wide range of materials, such as concrete, wood, and soil (Stamm, 1927; Waters, 1974; Williams, 1980). Although the use of electrical resistance measurements to quantify chip seal curing times seems straightforward at first glance, it is extremely important to develop an appropriate method that captures the nature of the material and specific application of the measurement technique (Singh, 2013).

Ohm's law defines resistance as the ratio of voltage to current (Equation 2.1). Accordingly, the selection of an electric current source has a considerable impact on the

electrical output. Previous studies suggest that, for the electrical characterization of construction materials, alternating current (AC) is preferable to direct current (DC). DC can induce polarization effects on the electrode-material interface and inside the specimen. Also, DC-based techniques fall short in eliminating the ability of the material to hold an electric charge (Spragg, 2013; Layssi et al., 2015).

$$R = \frac{V}{I} \quad [2.1]$$

where:

R = resistance,  $\Omega$ ,

V = voltage, V, and

I = current, A.

Electrical resistance measurements are also affected by the cross-sectional area, length, temperature, and resistivity of the material. The geometry and degree of heat of a sample directly impact the ions' ability to move freely and carry the electric current (Spragg, 2013). Resistivity is an intrinsic property that quantifies how strongly a given material opposes the flow of electric current. Asphalt emulsion electrical properties depend on a set of material attributes that includes the emulsion's viscosity, surface potential, and dielectric of the medium and strength of the electric field. Also, for a given type of emulsion, the electrical measurements are sensitive to factors such as water content and partial breaking due to mechanical agitation (Banerjee, 2012). Equation 2.2 is generally used to relate the cross-sectional area, length, resistivity, and resistance of a material.

$$R = \frac{\rho L}{A} \quad [2.2]$$

where:

R = resistance,  $\Omega$ ,

$\rho$  = resistivity,  $\Omega\text{-m}$ ,

L = length of the material, m, and

A = cross-sectional area of the material measured,  $\text{m}^2$ .

In addition, the electrical response is dependent upon the measurement technique employed (Spragg, 2013). Several configurations have been proposed for performing resistance measurements in construction materials. The most commonly used techniques are the uniaxial method and two- and four-point probe methods. In the uniaxial method, the material sample is placed between two electrodes. AC is applied through the cross-sectional area perpendicular to the electrodes, and the drop in the potential between the electrodes is measured. This technique is suitable for measuring the electrical resistance in laboratory-based tests.

Two-point methods usually measure electrical resistance by embedding two electrodes in a substance or material at a fixed distance. Four-point probes measure the surface electrical resistance using four electrodes. The electrodes are located in a straight line and equally spaced. The two inner electrodes measure the electrical potential generated when the exterior electrodes apply AC. Due to their configurations, the two-point and four-point methods are nondestructive, which makes them ideal for field evaluations of construction materials (Layssi et al., 2015).

Other factors that affect electrical resistance measurements include electrode contact properties, current frequency, and user variability. Therefore, to establish an effective, reliable, and simple electrical resistance measurement technique, the effects of all these factors need to be taken into account (Spragg, 2013).

## CHAPTER 3. EXPERIMENTAL PROGRAM

### 3.1 Program Overview

A three stage experimental program was developed to investigate the potential use of electrical resistance measurements to quantify chip seal curing times (Figure 3.1). The first stage involved identifying an approach that could correlate the amount of curing in a fresh chip seal system to the electrical properties of the residual material. Full frequency, two-point, uniaxial EIS testing was used to examine the electrical properties of the asphalt emulsions and various asphalt emulsion-aggregate combinations. This part of the study fundamentally evaluated the relationship between the electrical properties and the volumetrics of the asphalt emulsion (i.e., the volume of water and asphalt).

The second stage was focused on fully understanding three primary factors related to the curing of full-scale chip seal systems: 1) an increase in electrical resistance, 2) water loss due to evaporation, and 3) development of mechanical strength. In 2015, five full-scale field trials were completed in Indiana and the field experimental results compared with laboratory test results obtained using materials collected at the field sites.

The third stage comprised the field validation and the implementation and calibration of the electrical resistance methodology. In 2016, the methodology was implemented at five different pavement sections to refine the electrical resistance

technique and develop a simple procedure that can be used by field inspectors, technicians, and contractors.

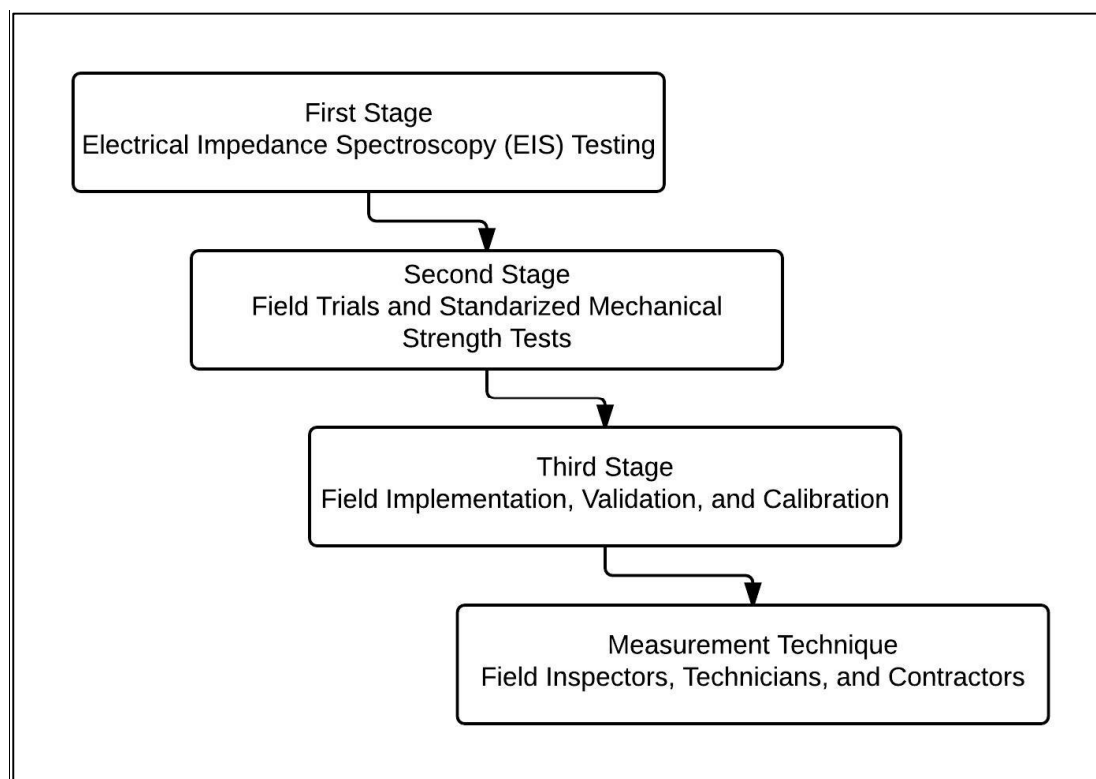


Figure 3.1: Flow chart of experimental program.

## 3.2 Electrical Impedance Spectroscopy Testing

### 3.2.1 Materials

The chip seal materials used for this study were selected in accordance with work by Lee et al. (2011) that specified the most common bitumen emulsions and cover aggregate used for surface treatment projects in the INDOT in-house chip seal program. AE-90S and CRS-2P emulsions were obtained from an Indiana asphalt emulsion supplier. AE-90S and CRS-2P are both polymer-modified, rapid-set emulsions, the former anionic and the latter cationic. Limestone and gravel aggregate were utilized because they are by far the



most common aggregate types used for Indiana chip seals (Lee et al., 2011). Limestone particles generally have a high affinity for liquid asphalt and possess a positive surface electrical charge (INDOT 2013). Conversely, gravel aggregate typically has an electronegative surface charge. The aggregate particles were sized between 6.3 mm and 9.5 mm, with a flakiness index of zero percent.

### 3.2.2 Electrical Impedance Measurements

Electrical impedance measurements were employed to monitor how strongly the residual material opposed the flow of an alternating electric current. Standard bitumen emulsions are typically considered to be oil-in-water (o/w) types of suspensions (James, 2006), which means that emulsified asphalt particles are dispersed in water. An EIS test is a powerful tool for the electrical characterization of such o/w systems (Shahidi, 2013). In this study, an impedance/gain-phase analyzer was used to assess the electrical properties of the asphalt emulsions and asphalt emulsion-aggregate combinations. This test equipment applies AC and measures the drop in the potential between electrodes, or the impedance quantity ( $Z$ ). Figure 3.2 illustrates impedance as a complex number, where the imaginary term is the capacitance ( $Z''$ ) and the real component is the resistance ( $Z'$ ).

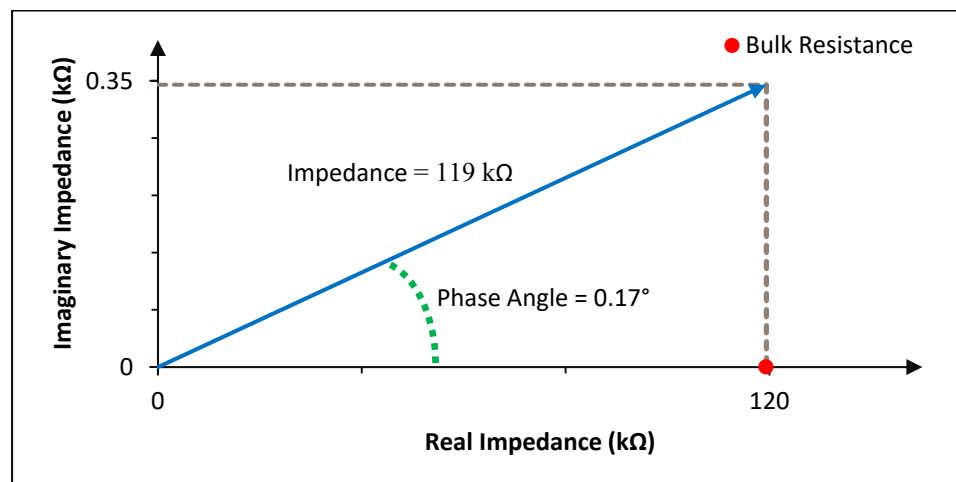


Figure 3.2: Phasor diagram of impedance measurement of asphalt emulsion specimen.

The magnitude and phase angle of the impedance will vary depending on the frequency of the applied electrical current. For this study, a frequency range between  $10^7$  and  $10^{-1}$  Hz was employed. Within this frequency range, the impedance measurement (with the minimum imaginary term and phase angle) was taken as the bulk resistance. Figure 3.3 shows a typical Nyquist plot (imaginary versus real impedance), which helps to identify the bulk resistance.

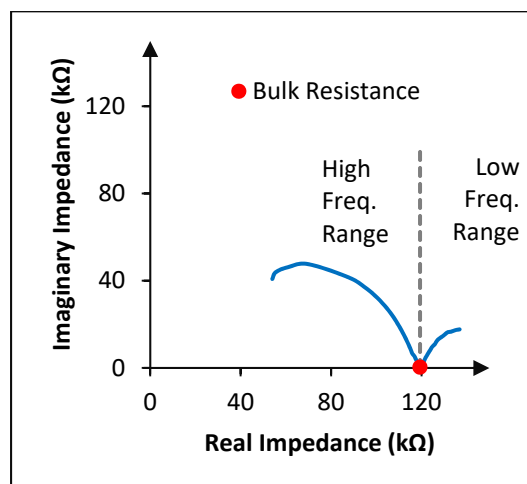
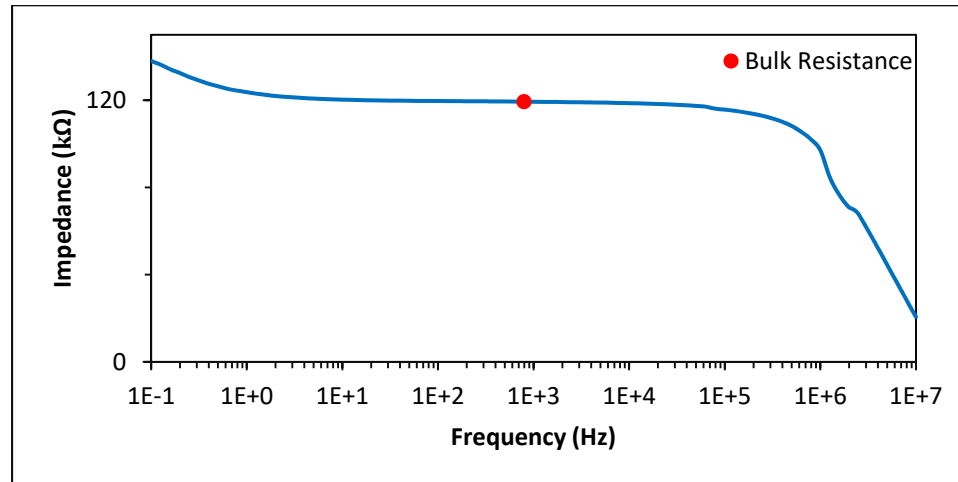
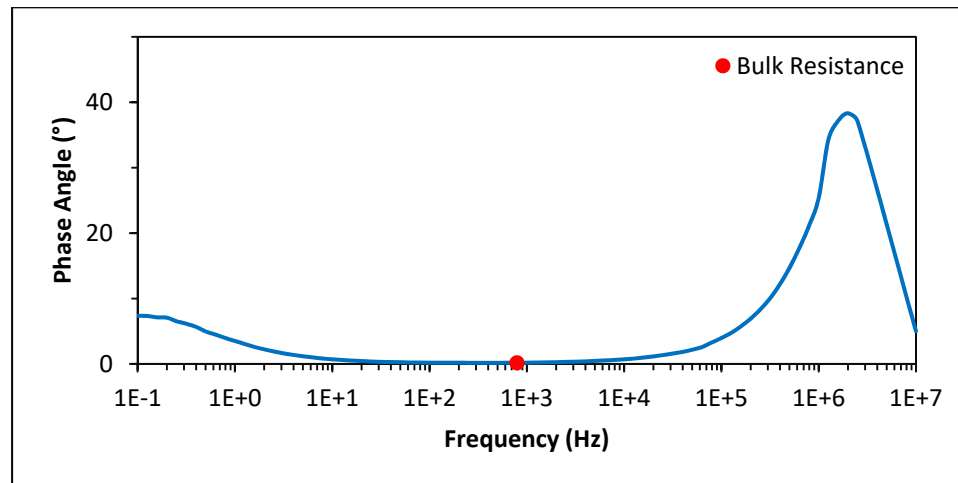


Figure 3.3: Nyquist plot of impedance measurement of asphalt emulsion specimen.

Figures 3.4 (a) and 3.4 (b) present the Bode plots for impedance versus frequency and phase angle versus frequency of the electrical current, respectively. The Bode plots characterize the electrical response over the frequency spectrum.



(a)



(b)

Figure 3.4: Bode plots of impedance measurements of asphalt emulsion specimen: (a) impedance vs. frequency and (b) phase angle vs. frequency.

### 3.2.3 Sample Preparation

A robust experimental set-up that simulates the chip seal geometry and ensures repeatable EIS experiments was established for proper electrical characterization. Figure 3.5 shows the schematic representation of the experimental set-up for performing the two-point uniaxial EIS tests. The sample mold preparation started by using a 58-mm by 134-mm  $\pm$  2 mm, 19-mm thick, marine-grade high-density polyethylene (HDPE) frame. This material provides an excellent electrically insulated mold. The frame was cut using a vertical band saw.

Once the frame was cut to size, a rectangular pocket, 32 mm by 108 mm  $\pm$  1 mm, was milled using a computerized numerical control milling machine that employed a 13-mm diameter tool (speed: 1300 RPM, feed: 1585 mm/min). The tool was controlled using a code system that enables it to be monitored by a computer and with a great deal of repeatability. Because the milling tool was 13 mm in diameter, the final sample holder was a rounded corner rectangular pocket with a 6.5-mm corner radius. A similar process was undertaken to manufacture molds with five different pocket depths (3 mm, 5 mm, 6 mm, 10 mm, and 13 mm). The milling machine digitally probed the frame before the milling operation to meet conformance specifications.

Electrodes were placed at either end of the specimen. The electrodes were made of copper woven wire cloth with 0.30-mm wire diameter. A rectangular mesh (58 mm by 32 mm  $\pm$  2 mm) was placed on top of the frame at each end. A segment of the mesh was notched and bent toward the pocket in order to make an electrical connection with the specimen placed in the mold. The dimensions of the mesh-bent fraction were equivalent to the sample's initial axial surface (width by thickness). The clear distance between

electrodes was 95 mm. The span between electrodes was shorter than the specimen length to ensure that the electrodes were embedded thoroughly, thus allowing a proper electrical connection. The electrodes were fixed in the designed position by tightening plastic screws. The copper mesh was connected to the EIS equipment through a 152-mm stranded wire, 300V AC, 22-gauge, which was joined to the electrode using solder wire without flux.

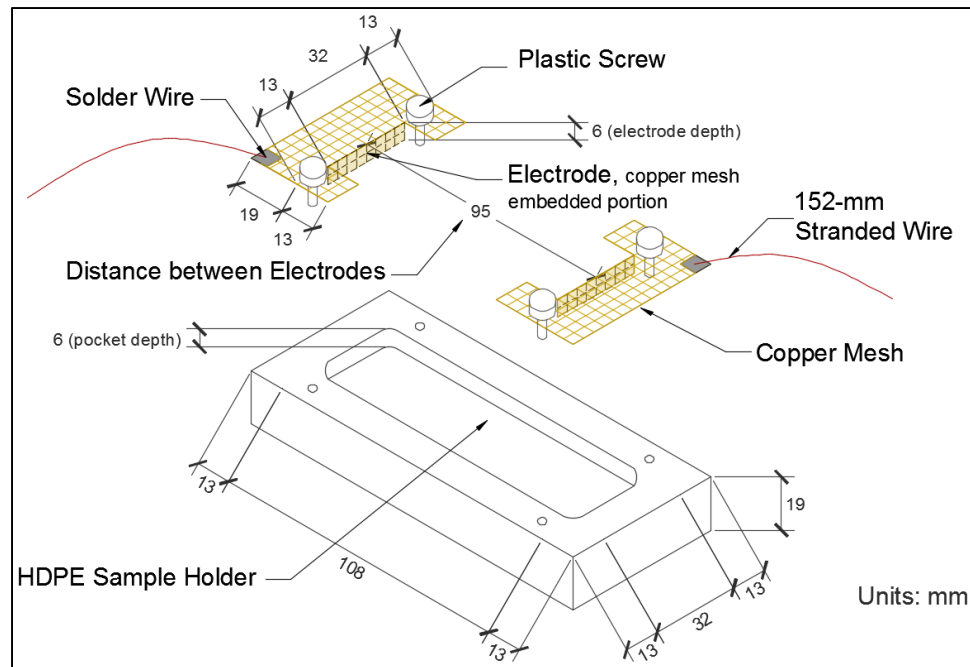


Figure 3.5: Schematic of two-point uniaxial EIS sample holder.

As shown in Figure 3.6, asphalt emulsion specimens for both AE-90S and CRS-2P emulsions were prepared by pouring the emulsion into the sample molds until the total volume of each pocket was filled. Asphalt emulsion molds were cast at five different sample thicknesses: 3 mm, 5 mm, 6 mm, 10 mm, and 13 mm.



Figure 3.6: Pure asphalt emulsion binder specimens.

Asphalt emulsion-aggregate samples were also prepared. Calculations were performed to replicate the asphalt emulsion application rates typically used in the field, 1.4 and 1.8 L/m<sup>2</sup>. It was found that 4.8 and 6.3 g were equivalent to placing 1.4 and 1.8 L/m<sup>2</sup> of emulsion, respectively. The corresponding asphalt emulsion quantities were poured into a 6-mm depth pocket mold. The sample holder was tilted back and forth to enable the sample to develop a uniform thickness. The aggregate was spread until a prevalent interlocking mosaic pattern was achieved. Lastly, a tamping rod was rolled six times along the longitudinal side of the sample to provide consistent chip embedment and orientation and to simulate rolling operations at chip seal projects, as shown in Figure 3.7.

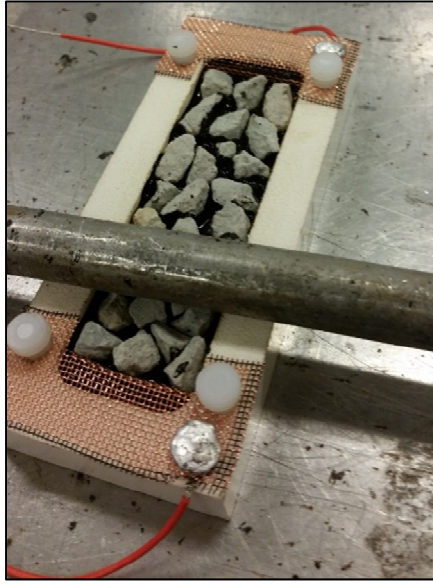


Figure 3.7: Asphalt emulsion-aggregate combination specimen.

#### 3.2.4 Testing Procedures

After the sample preparation, the specimens were connected immediately to the EIS analyzer to acquire the impedance data. The monitoring process was automated using impedance data analysis software. The electrical properties of the samples were monitored at 10-minute intervals for 16 hours. Similarly, the mass of each sample was measured constantly while the specimen cured using a balance and data logger. The readings were logged at 1-minute intervals. Subsequently, the electrical properties and mass of the samples were point-measured on a periodic basis until no mass change was observed ( $0.0002 \text{ g/h}$ ). At this point, the samples were considered to be completely cured. The experimental procedure was conducted at  $23 \pm 0.5^\circ\text{C}$  and  $50 \pm 2$  percent Relative Humidity in an environmental chamber. EIS data files were scanned to extract the bulk resistance measurement at each interval.

### 3.2.5 Moisture Content Ratio

For this stage of the study and during the course of this research program, a moisture content ratio (MCR) was adopted to estimate the amount of curing that an asphalt emulsion or chip seal specimen experienced. This percentage was computed using Equation 3.1.

$$MCR = \left( \frac{m_t - m_f}{m_i - m_f} \right) \times 100 \quad [3.1]$$

where:

MCR = moisture content ratio, %,

$m_i$  = initial sample mass, g,

$m_t$  = sample mass at any given curing time, g, and

$m_f$  = final sample mass, specimen completely cured, g.

## 3.3 Field Trials and Standardized Mechanical Strength Tests

### 3.3.1 Full-Scale Field Trials

As shown in Figure 3.8, field trials were performed on Indiana SR 19 (approximately 3 miles north of Mentone, IN), SR 8 (approximately 5 miles west of Auburn, IN), SR 1 (approximately 1 mile north of Farmland, IN), and at two locations on SR 39 (one near Lizton, IN and one near Lebanon, IN). At each location, electrical resistance measurements were taken to examine how strongly the residual material opposed the flow of the AC. Fresh plate samples were extracted from the surface treatment to monitor the amount of water loss over time. The electrical resistance and mass loss of the chip seal were monitored until the asphalt residue gained enough binder adhesive strength to keep the aggregate chips in place. The chip seal's mechanical strength development was



evaluated by simulating the shear forces that are applied by brooms and uncontrolled traffic to fresh seal coats.

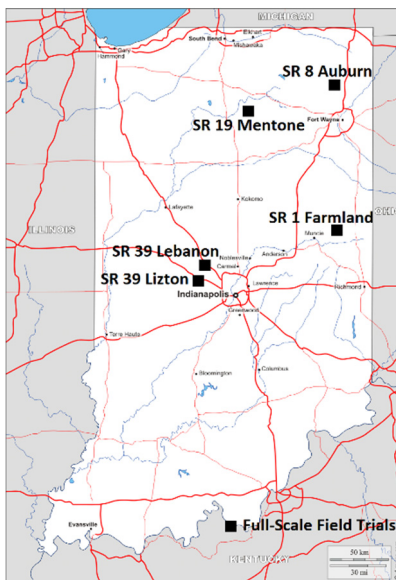


Figure 3.8: Location of full-scale field trials (source: <http://d-maps.com>).

### 3.3.2 Materials

The selection of the chip seal projects was based on the availability of pavement sections. As a result, only chip seal systems that used AE-90S (anionic, rapid-set, polymer-modified) emulsions were tested in the full-scale field trials. However, CRS-2P (cationic, rapid-set, polymer-modified) emulsion chip seal samples were evaluated under laboratory conditions. The cover aggregate types used in these projects and in the laboratory tests were SC 16 limestone, SC 16 dolomite, SC 11 limestone, and SC 16 gravel. Table 3.1 presents the aggregate properties. *SC* is the INDOT designation for aggregates produced primarily for use in chip seal applications (INDOT, 2015).

Table 3.1: Aggregate Properties

Sieve Analysis (AASHTO T 27)	Indiana State Road			
	SR 19 Mentone	SR 8 Auburn	SR 1 Farmland	SR 39 Lizton- Lebanon
Sieve Size (mm)	Type of Aggregate			
	SC 16 Limestone	SC 16 Dolomite	SC 11 Limestone	SC 16 Gravel
12.500	100.0	100.0	100.0	100.0
9.500	92.2	95.6	86.2	88.2
8.000	72.6	83.2	62.0	55.1
6.300	48.0	62.2	38.7	25.1
4.750	21.0	32.0	15.0	1.8
2.360	6.2	10.9	3.9	0.5
1.180	1.8	2.7	1.2	0.4
0.600	0.9	1.1	0.9	0.4
0.300	0.5	0.7	0.8	0.4
0.150	0.4	0.5	0.7	0.4
0.075	0.3	0.4	0.6	0.3
Bulk Specific Gravity (AASHTO T 85)	2.667	2.681	2.653	2.656
Flakiness Index % (ITM 224)	11.0	13.0	10.0	6.0

### 3.3.3 Electrical Resistance Measurements

Once the chip seal rolling process was completed at each site, a two-point probe was fixed in the fresh seal coat. As seen in Figure 3.9, two 0.64-cm diameter, 7.60-cm long threaded stainless steel probes were fitted into a plastic spacer, with 7.60-cm clearance between the electrodes. The probes were seated into the chip seal by gently tapping the top of the steel rods.

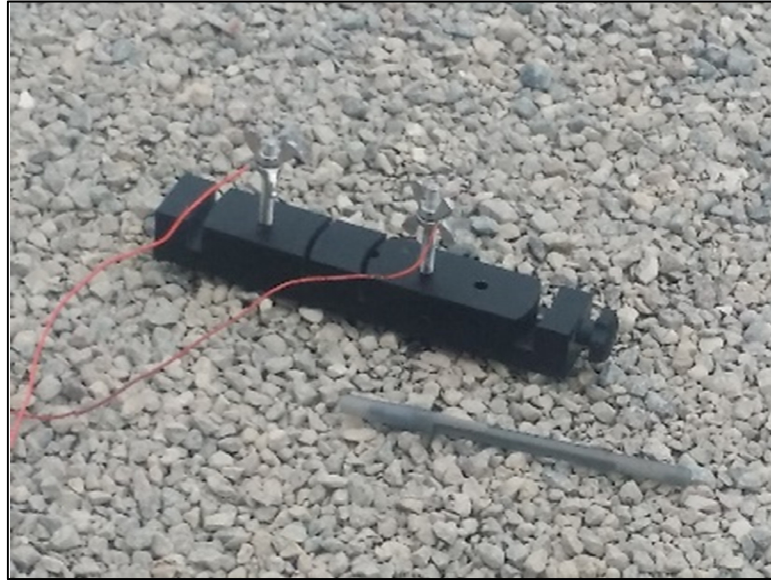


Figure 3.9: Electrical resistance two-point probe.

Figure 3.10 illustrates how the probes were positioned to ensure a proper electrical connection. Each probe had a 7.5-m copper wire lead attached to it using stainless steel wing nuts. These leads were then attached to a handheld inductance (L), capacitance (C), and resistance (R) (LCR) meter. This electronic test equipment is capable of applying AC at five frequencies, 100 Hz and 120 Hz, and 1 kHz, 10 kHz, and 100 kHz. The LCR meter measures the potential difference between the two probes and automatically calculates the resistance from the measured voltage and applied current values.

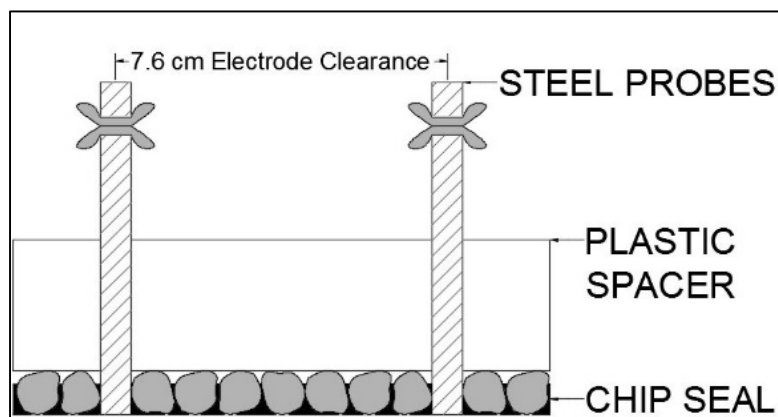


Figure 3.10: Schematic representation of proper electrical connection.

The LCR meter also provides detailed component analysis by including, as a secondary reading, the phase angle value of the electrical measurement at each designated frequency. By selecting the frequency that generates the lowest phase angle, a stable electrical resistance measurement can be acquired. The LCR meter can provide continual recordings for data logging purposes; for the results reported in this part of the study, measurements were logged at 1-minute intervals.

#### 3.3.4 Water Evaporation Rate

Prior to the initiation of the chip seal operation, an aluminum foil-covered plywood plate (20 cm x 10 cm x 1 cm) was placed on the existing pavement surface (Figure 3.11). The chip seal was applied to the existing pavement surface and allowed to cover the plate, which was then extracted as a plate sample and placed on an electronic balance to record the mass loss due to water evaporation (Figure 3.12). The plate sample mass was logged at 10-second intervals throughout the curing process.



Figure 3.11: Plywood plate prior to construction sequence.



Figure 3.12: Plate sample placed on balance.

A handheld weather station and thermocouple were placed on the pavement surface to monitor the ambient temperature, RH, wind speed, cloud cover, and pavement temperature at 15-minute intervals. Table 3.2 summarizes the climatic data documented at each pavement section. Upon completion of the field tests, each plate sample was sealed in plastic and relocated to a laboratory environmental chamber ( $23 \pm 0.5^\circ\text{C}$  and  $50 \pm 2\%$  RH) in order to cure the specimen completely and determine the final sample mass.

Table 3.2: Climatic Data

Pavement Section	Ambient Temperature Range ( $^\circ\text{C}$ )	Relative Humidity Range (%)	Wind Speed Range (m/s)	Prevalent Cloud Cover	Pavement Temperature Range ( $^\circ\text{C}$ )
SR 19 Mentone	27.3 – 35.1	49.3 – 76.5	2.3 – 6.6	Sunny	25.0 – 33.0
SR 8 Auburn	20.7 – 35.1	23.6 – 64.1	1.0 – 6.1	Sunny	20.0 – 30.0
SR 1 Farmland	13.6 – 36.9	22.1 – 96.4	0.2 – 4.6	Sunny	19.0 – 37.0
SR 39 Lizton	15.7 – 24.6	56.5 – 91.5	1.1 – 4.3	Cloudy	18.0 – 30.0
SR 39 Lebanon	21.6 – 38.5	17.6 – 66.2	1.1 – 3.1	Sunny	24.0 – 34.0

When the mass loss testing of the field samples was completed, a plot was developed for the dataset with the mass of the specimens plotted as a function of curing time, as shown in Figure 3.13. In addition to the recorded mass measurements, a regression model was applied to the data. Figure 3.13 presents the SR 8 data.

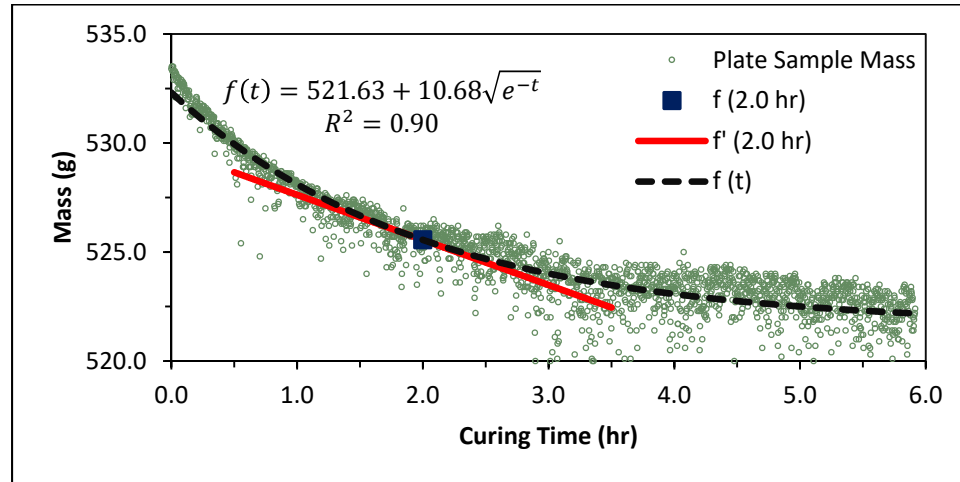


Figure 3.13: Plate sample mass as a function of curing time for SR 8 chip seal.

In addition, WERs and MCRs were calculated at 15-minute intervals. The MCRs were estimated using Equation 3.1. Equation 3.2 describes the computation of the WER. The WER is equivalent to the absolute value of the slope of the mass loss regression equation at a particular curing time, divided by the plate sample area. Consequently, the WER has a unit of grams per square centimeter-hour ( $\text{g}/\text{cm}^2\text{-hr}$ ).

$$WER = \frac{|f'(t)|}{A} \quad [3.2]$$

where:

WER = water evaporation rate,  $\text{g}/\text{cm}^2\text{-hr}$ ,

$f(t)$  = slope of the mass drop regression equation at a particular curing time,  $\text{g}/\text{hr}$ ,

and

$A$  = area of the plate sample,  $200 \pm 5 \text{ cm}^2$ .

The WER and MCR values relate directly to the climatic condition data and electrical resistance measurements. By combining the five mass loss datasets, 111 observations were created for further statistical analysis. For example, the measurements



that correspond to the slope displayed in Figure 3.13 are the following: WER = 0.010 g/cm<sup>2</sup>-hr, MCR = 49.23%, wind speed = 3.08 m/s, RH = 44.50%, ambient temperature = 27.3°C, cloudiness = sunny, pavement temperature = 23.0°C, and electrical resistance = 155,920  $\Omega$ .

### 3.3.5 Development of Mechanical Strength

Chip seal mechanical strength gain was analyzed in terms of aggregate loss, which is one of the most common failures of fresh chip seals. During the full-scale chip seal trials, the seals were periodically and manually swept using a broom with a 61-cm long medium-duty bristle, as pictured in Figure 3.14.



Figure 3.14: Shear force simulation using broom.

An aggregate dislodgement potential (DP) was determined on a scale of 0 percent to 100 percent, with 0 percent indicating no aggregate loss and 100 percent indicating complete failure of the surface treatment. The DP was established based on visual



inspections that in turn were based on the percentage of chips that were dislodged at the area subjected to the broom's shear force, as shown in Figure 3.15.



Figure 3.15: Aggregate loss at area subjected to broom's shear force.

Because this mechanical strength parameter was based on a non-standardized test procedure, the chip seal specimens also were evaluated in the laboratory using sweep tests and Vialit tests.

#### 3.3.5.1 Sweep Test (ASTM D7000)

As illustrated in Figure 3.16, the ASTM D7000 test measures the curing characteristics of chip seals by simulating the brooming of a surface treatment in the laboratory (ASTM D7000, 2011).



Figure 3.16: ASTM D7000 brooming simulation.

As detailed in Table 3.3, four different asphalt emulsion-aggregate combinations were evaluated using AE-90S emulsions and cover aggregate collected at the field test sites. CRS-2P emulsion also was used in combination with the four aggregate types to make four additional emulsion-aggregate combinations.

Table 3.3: Asphalt Emulsion-Aggregate Combinations for Sweep Test

Chip Seal Combination ID	Asphalt Emulsion		Cover Aggregate	
	Type	Application Quantity (g)	Type	Application Quantity (g)
1	AE-90S	83.0 ± 5	SC 16 Limestone	471.2 ± 1
2	AE-90S	83.0 ± 5	SC 16 Dolomite	461.5 ± 1
3	AE-90S	83.0 ± 5	SC 11 Limestone	485.6 ± 1
4	AE-90S	83.0 ± 5	SC 16 Gravel	489.9 ± 1
5	CRS-2P	83.0 ± 5	SC 16 Limestone	471.2 ± 1
6	CRS-2P	83.0 ± 5	SC 16 Dolomite	461.5 ± 1
7	CRS-2P	83.0 ± 5	SC 11 Limestone	485.6 ± 1
8	CRS-2P	85.0 ± 5	SC 16 Gravel	489.9 ± 1

Eight specimens were prepared for each chip seal combination and tested at different curing times (0.5, 1, 1.5, 2, 3, 4, 5 and 7 hours). The fresh seal coat samples were cured in an oven at  $37 \pm 2^\circ\text{C}$  prior to testing. The AML percentage was estimated according to ASTM D7000 (Equation 3.3).

$$\% AML = \left( \frac{A - B}{A - C} \right) \times 100 \times 1.33 \quad [3.3]$$

where:

% AML = aggregate mass loss as a percentage of the area exposed to the abrading force, %,

A = initial specimen mass, g,

B = final specimen mass, g, and

C = asphalt sample disk mass, g.

As shown in Figure 3.17, the electrical resistance properties of the chip seal specimens also were monitored during the tests by employing a two-point probe and LCR meter, and the electrical resistance measurements related to the mechanical performance of the chip seal specimens.

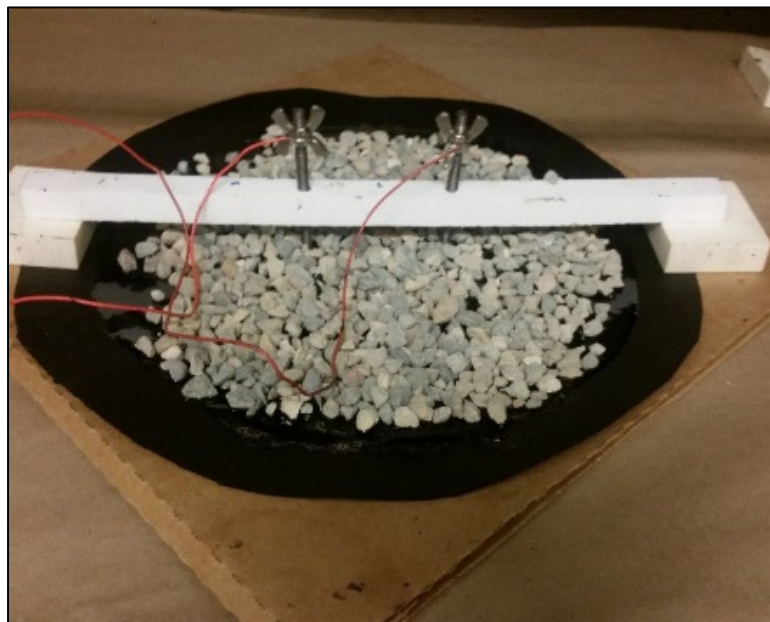


Figure 3.17: Electrical resistance measurement of sweep test specimen.

### 3.3.5.2 Vialit Test

The Vialit test provides an indication of aggregate loss for chip seals. Table 3.4 reports the six asphalt emulsion-aggregate combinations that were evaluated using the Vialit test method, i.e., British Standard EN 12272-3 (BSI, 2003). Two asphalt emulsion-aggregate combinations, CRS-2P SC 16 Limestone (ID: 5) and CRS-2P SC 16 Dolomite (ID: 6), were not evaluated due to the lack of enough chip particles to perform the Vialit test.

Table 3.4: Asphalt Emulsion-Aggregate Combinations for Vialit Test Method

Chip Seal Combination ID	Asphalt Emulsion	Cover Aggregate
	Type	Type
1	AE-90S	SC 16 Limestone
2	AE-90S	SC 16 Dolomite
3	AE-90S	SC 11 Limestone
4	AE-90S	SC 16 Gravel
7	CRS-2P	SC 11 Limestone
8	CRS-2P	SC 16 Gravel

As shown in Figure 3.18, 52 g of asphalt emulsion were applied to standard sized stainless-steel pans (304 stainless-steel, 2 mm-thick, 20 cm by 20 cm). Exactly 196 particles were embedded into the emulsion in rows with even spacing. The aggregate particles that were used for testing passed the 9.5-mm sieve and were retained on the 6.3-mm sieve.



Figure 3.18: Vialit test specimen, AE-90S SC 16 gravel.

After the sample preparation, the specimens were cured in an oven at  $37 \pm 2^\circ\text{C}$ . Eight specimens were prepared for each asphalt emulsion-aggregate combination and cured at different times (0.5, 1, 1.5, 2, 3, 4, 5 and 7 hours). Following this curing process, the specimens were inverted onto a testing frame and a 500 g ball was dropped three times from a distance of 50 cm onto the inverted pans. The aggregate loss was determined at  $37 \pm 2^\circ\text{C}$  using Equation 3.4.

$$\% AL = \frac{NP_i - NP_f}{NP_i} \times 100 \quad [3.4]$$

where:

% AL = percentage of aggregate loss, %,

$NP_i$  = number of particles before testing, unit, and

$NP_f$  = number of particles retained, unit.

After this initial assessment, the samples were conditioned for one hour in a freezer at  $-10 \pm 2^\circ\text{C}$ . The samples were then removed from the freezer, reaching a temperature equivalent to  $0 \pm 2^\circ\text{C}$  (Figure 3.19). The Vialit impact force was applied again to the pans by dropping the 500-g ball three times onto the inverted metal trays. The aggregate loss was determined at  $0^\circ\text{C} \pm 2^\circ\text{C}$  using Equation 3.4. Evaluating the low-temperature performance is imperative in predicting long-term performance. Most aggregate loss failure in chip seals occurs during the first frost season of the chip seal's life (Lee and Shields, 2010).



Figure 3.19: Specimen temperature after freezer conditioning,  $0 \pm 2^\circ\text{C}$ .



In order to measure the electrical resistance of the asphalt emulsion-aggregate combinations, 13 g of asphalt emulsion were poured into a HDPE mold (10 cm by 10 cm, pocket depth equal to 6 mm). This mold was fabricated in accordance with the specifications used for the EIS sample holders. Forty-nine aggregate particles were embedded into the emulsion (Figure 3.20). The electrical resistance was measured by using a two-point probe while the specimen cured in an oven at  $37 \pm 2^\circ\text{C}$ . The electrical properties related to the Vialit mechanical performance of the specimens.

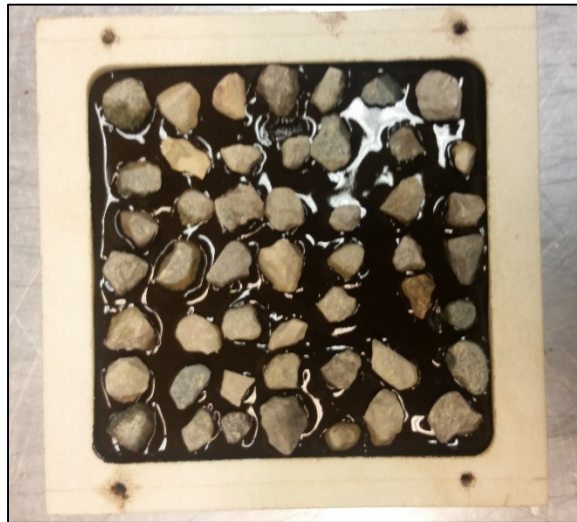


Figure 3.20: Specimen used to relate electrical properties to Vialit test sample trays.

### 3.4 Field Implementation, Validation, and Calibration

Figure 3.21 shows the locations where the electrical measurement methodology was implemented in 2016 on SR 352 (approximately 2 miles west of Oxford, IN), SR 38 (approximately 1 mile east of Kirklin, IN), at two locations on US 52 (one near Brookville, IN and one near Metamora, IN), and on SR 827 (approximately 3 miles north

of Angola, IN). Table 3.5 shows the asphalt emulsion and cover aggregate used at each location.

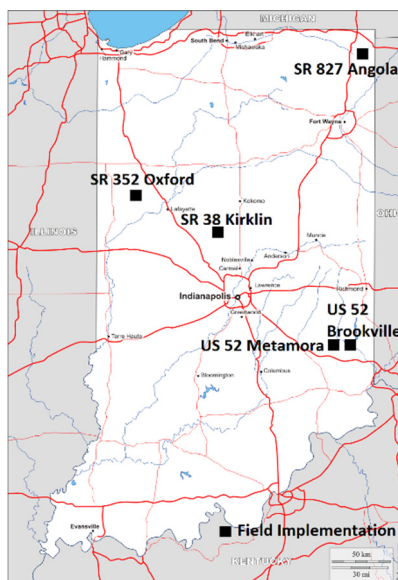


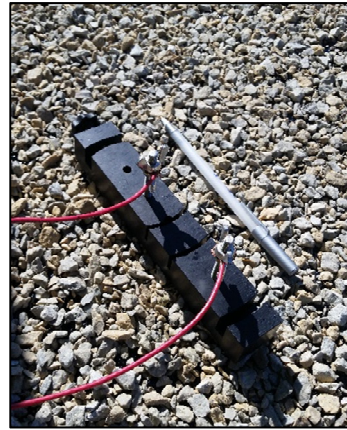
Figure 3.21: Location of field implementation sites (source: <http://d-maps.com>).

Table 3.5: Materials Used at Each Pavement Section

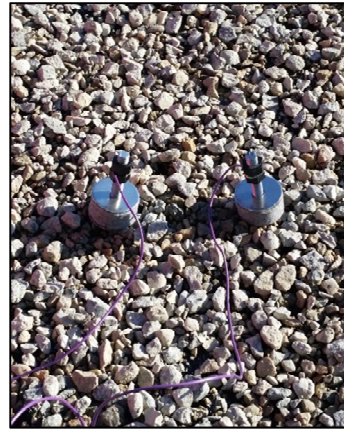
Pavement Section	Asphalt Emulsion	Cover Aggregate
SR 352 Oxford	AE-90S	SC 16 Limestone
SR 38 Kirklin	AE-90S	SC 16 Gravel
US 52 Brookville	CRS-2P	SC 11 Dolomite
US 52 Metamora	CRS-2P	SC 11 Dolomite
SR 827 Angola	AE-90S	SC 16 Dolomite

Figure 3.22 shows that the electrical resistance measurements taken to quantify the chip seal curing times involved various two-point probe configurations, namely a two-point probe using plastic spacers (spacing 7.6 cm), felt and stainless steel washers (probes spaced at 7.6 cm), and plywood pad supports (probes spaced at 7.6 cm, 15.2 cm, and 30.4 cm). The resistance measurements were taken at different locations on the newly placed surface treatment.





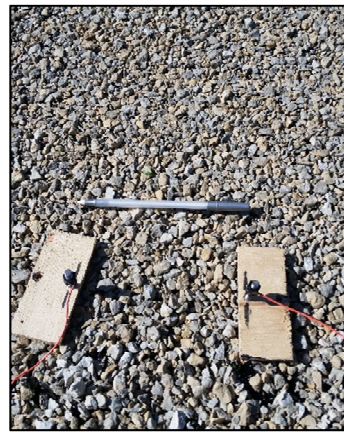
(a)



(b)



(c)



(d)



(e)

Figure 3.22: Two-point probe: (a) using plastic spacer, (b) using felt and stainless steel washers, and using plywood pad supports spaced at (c) 7.6 cm, (d) 15.2 cm, and (e) 30.4 cm.

The measured curing times were validated by monitoring the water loss due to evaporation and the mechanical strength gain at each field site. Two plate samples were extracted from the fresh chip seal, and the shear forces caused by sweeping were simulated manually using a broom. These procedures were performed in the same way as in Stage 2 of the study. Finally, the advantages and disadvantages of each two-point probe configuration were evaluated in order to recommend an effective, reliable, and simple measurement technique.

## CHAPTER 4. RESULTS AND DISCUSSION

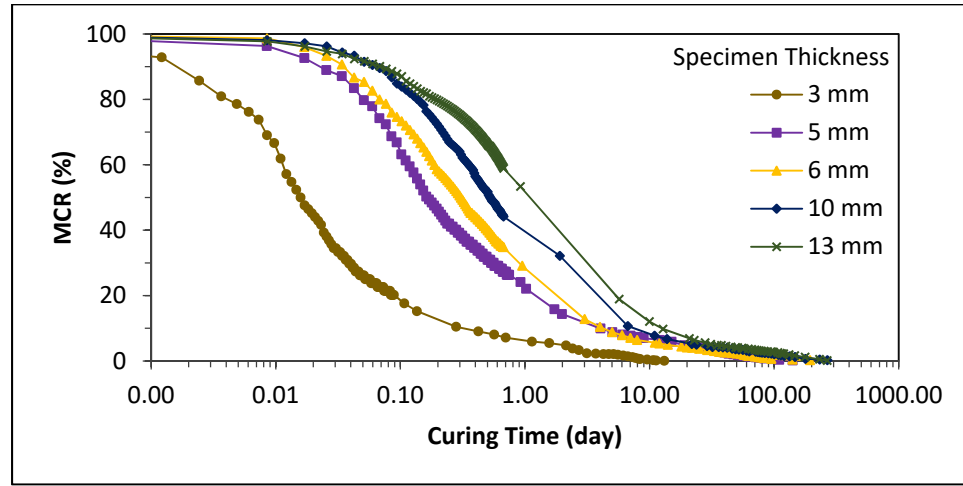
### 4.1 Electrical Impedance Spectroscopy Testing

To a great extent, the emulsion curing process is a function of the water that evaporates from the emulsion. Therefore, the first objective was to evaluate the relationship between the asphalt emulsion electrical properties and the amount of moisture in the emulsion. The initial water volume fraction in chip seal systems comes from two sources: the water portion of the asphalt emulsion and the moisture in the aggregate (Shuler et al., 2011). These two aspects were evaluated to develop a reliable correlation between the electrical properties and the amount of curing in an emulsion.

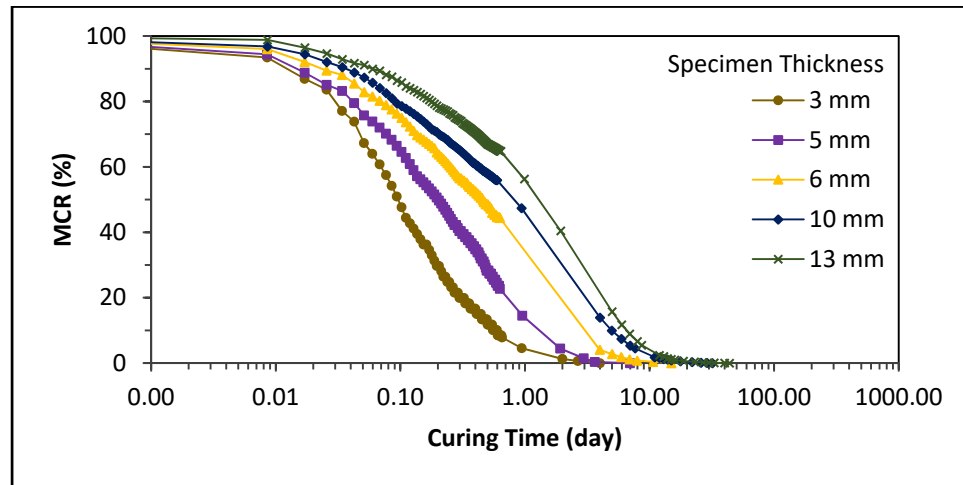
First, the curing process of two asphalt emulsions, AE-90S and CRS-2P, was examined by molding specimens with dissimilar sample volumetrics (i.e., the volume of water and asphalt). Then, four typical asphalt emulsion-aggregate chip seal combinations were tested using two emulsion application rates, 1.4 and 1.8 L/m<sup>2</sup>, and two aggregate moisture conditions, oven-dried (OD) and saturated surface-dried (SSD).

#### 4.1.1 Normalized Resistance Index (NRI)

Figure 4.1 presents the MCRs versus curing times for the asphalt emulsion samples of different thicknesses. The MCRs were calculated using Equation 3.1 to determine the amount of curing experienced by each specimen, and relate to the specimen's electrical response.



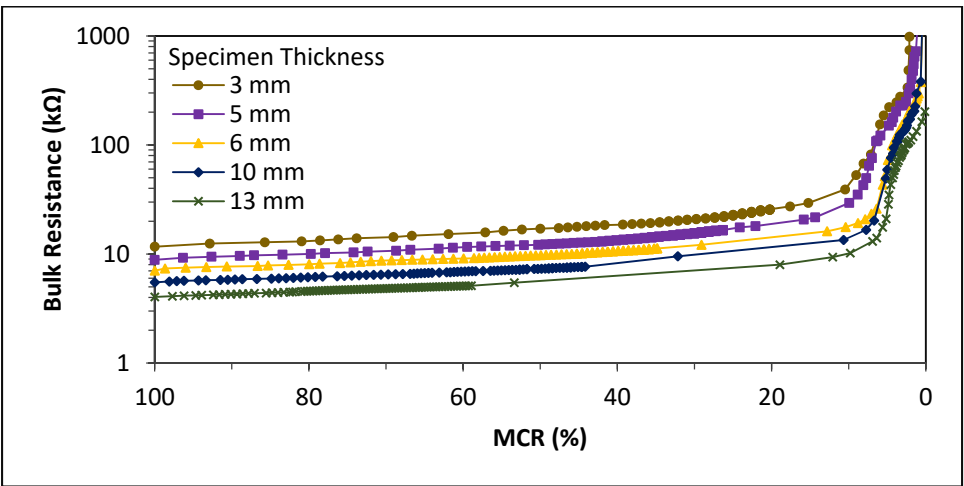
(a)



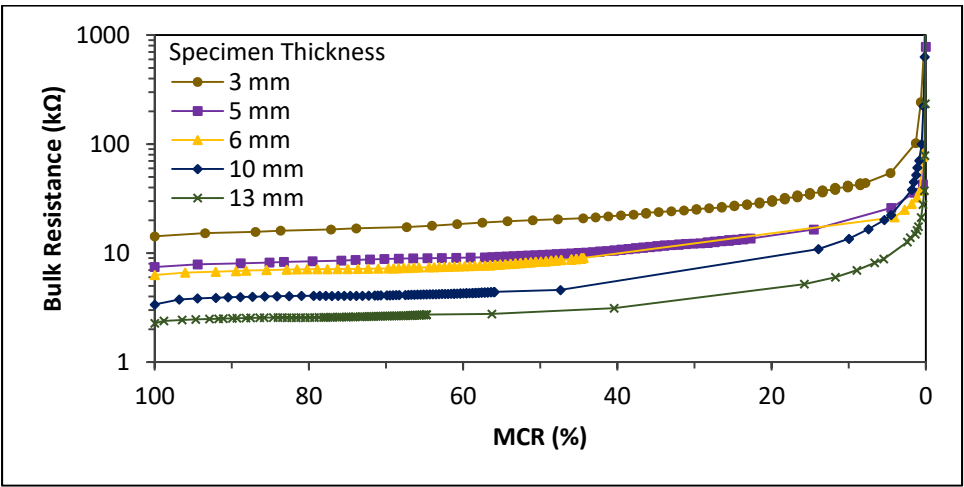
(b)

Figure 4.1: MCR vs. curing time in days at  $23 \pm 0.5^\circ\text{C}$  and  $50 \pm 2\%$  RH: (a) AE-90S and (b) CRS-2P.

Figure 4.2 shows that the bulk resistance of the asphalt emulsion specimens increased during the curing process. This electrical response reflects the connectivity of the water molecules and the ionic species as the material cures. However, it is evident that the specimen thickness had a pronounced effect on the electrical response of the residual material. Thicker specimens exhibited lower bulk resistance measurements. These electrical responses are attributable mainly to the effects of the cross-sectional area on the ions' ability to move freely and carry the electric current. Indeed, any material with a uniform cross-section has a resistance that varies inversely with its cross-sectional area.



(a)



(b)

Figure 4.2: Bulk resistance vs. MCR at  $23 \pm 0.5^\circ\text{C}$  and  $50 \pm 2\%$  RH: (a) AE-90S and (b) CRS-2P.

Generally, a normalized resistivity factor is used to address the dependence of the resistance on the cross-sectional area. Whereas resistance is measured, resistivity is an intrinsic property that quantifies how strongly a given material opposes the flow of electric current. Resistivity is calculated by dividing the resistance and cross-sectional area by the distance between electrodes. However, the cross-sectional area of a chip seal can vary significantly in practice due to the quantity of asphalt, quantity of aggregate,

nominal size of aggregate, aggregate gradation, percentage of voids filled, rolling operation protocol (i.e., rolling type and pattern, number of coverages, aggregate embedment depth), and the amount of curing that has occurred. In this context, a normalized resistance index (NRI) was developed to greatly reduce the impact of the cross-sectional area characteristics of the chip seal system. As illustrated in Equation 4.1, the NRI is determined as a quotient of the initial bulk resistance that corresponds to each sample.

$$NRI = \frac{R_t}{R_i} \quad [4.1]$$

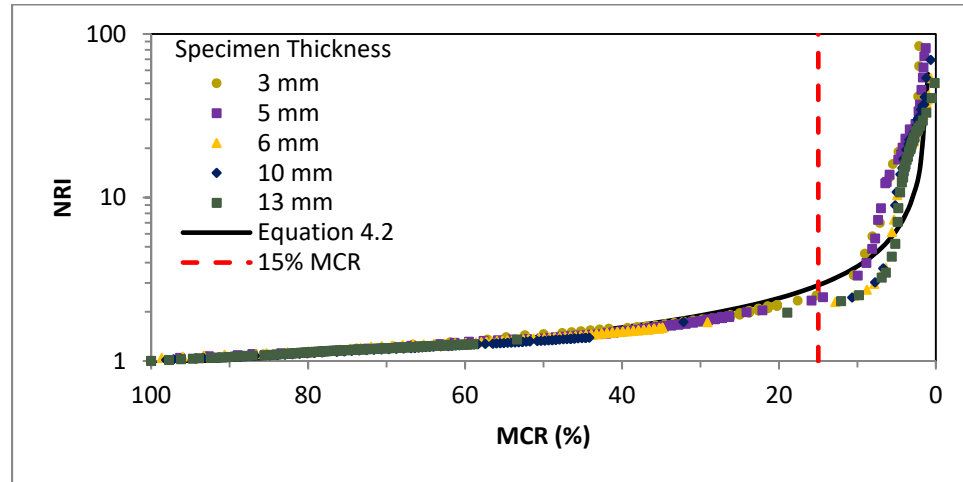
where:

NRI = normalized resistance index, unitless,

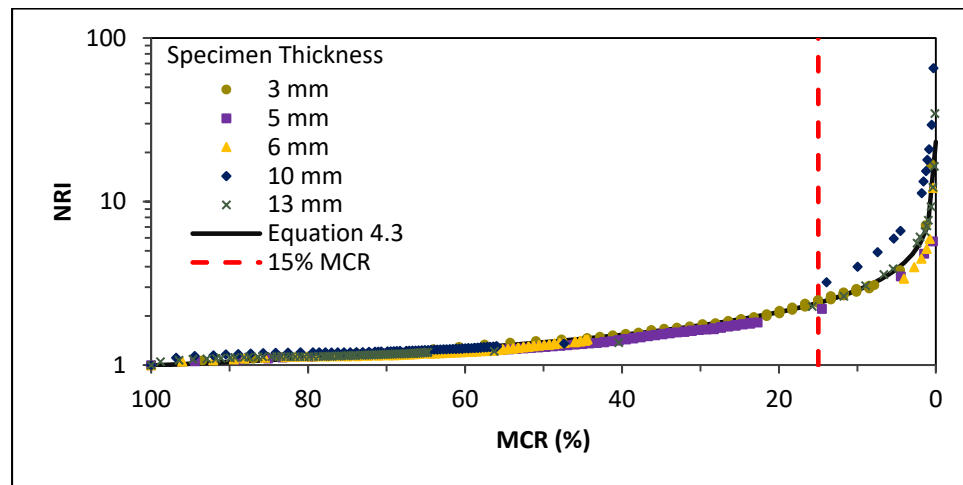
$R_t$  = bulk resistance at any given MCR,  $k\Omega$ , and

$R_i$  = initial bulk resistance at 100% MCR,  $k\Omega$ .

Figure 4.3 presents the relationships between the NRI and MCR. Linear regression analysis was performed to quantify the NRI within the critical moisture content range, i.e., between 15 and 25 percent. Shuler (2011) defined ‘critical moisture content’ as the ratio of the mass of water to very high residue strength. When the critical moisture content is reached, uncontrolled traffic and broom operations can be allowed onto the fresh seal coat. Statistical analysis of the data indicates that the coefficients of determination ( $R^2$ ) are 0.98 and 0.97 for the AE-90S and CRS-2P emulsions, respectively.



(a)



(b)

Figure 4.3: NRI vs. MCR at  $23 \pm 0.5^\circ\text{C}$  and  $50 \pm 2\%$  RH: (a) AE-90S and (b) CRS-2P.

Table 4.1 summarizes the developed regression equations (Equations 4.2 and 4.3) and the NRI values estimated at MCRs of 25, 20, and 15 percent. Hypothetically, the emulsion has transformed from emulsified asphalt particles dispersed in water to a predominantly asphalt film at the MCR of 15 percent. For both emulsion types, the NRI value starts to increase significantly after the MCR reduces to 15 percent, indicating poor connectivity and high tortuosity of the water phase. As shown in Figure 4.1, the cationic



emulsion cured faster than the anionic emulsion. All the CRS-2P samples cured completely before 100 days, whereas the AE-90S specimens achieved the same condition after 200 days.

Table 4.1: Regression Equations Relating NRI and MCR for Asphalt Emulsions

Asphalt Emulsion	AE-90S	CRS-SP
X =	$\sqrt{MCR}$	$\sqrt{MCR}$
Y =	$\frac{1}{NRI}$	$\frac{1}{NRI}$
Regression Equation	$Y = 0.11371X - 0.09608$ [4.2]	$Y = 0.09632X + 0.04319$ [4.3]
R <sup>2</sup>	0.98	0.97
NRI at MCR = 25%	2.18	1.99
NRI at MCR = 20%	2.51	2.22
NRI at MCR = 15%	3.03	2.56

#### 4.1.2 Measurement Concept Validation

The electrical measurement concept is based on the mass loss, or evaporation of water. As emulsion samples cure, the water diffuses from areas with high moisture concentrations to the drying surface (or areas of low moisture concentrations) and then evaporates. A diffusivity coefficient ( $D$ ) can capture the movement speed of the water molecules over a distance. The diffusivity coefficient is conveyed in units of squared length per time. For this study,  $D$  is defined arithmetically in Equation 4.4. Figure 4.4 reveals that NRI is reasonably dependent on  $D$ .

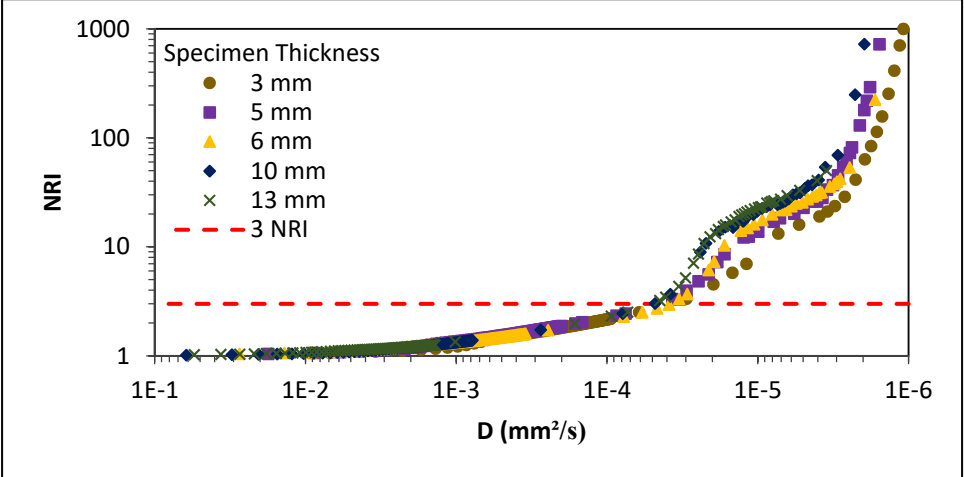
$$D = \frac{x^2}{2t} \tag{4.4}$$

where:

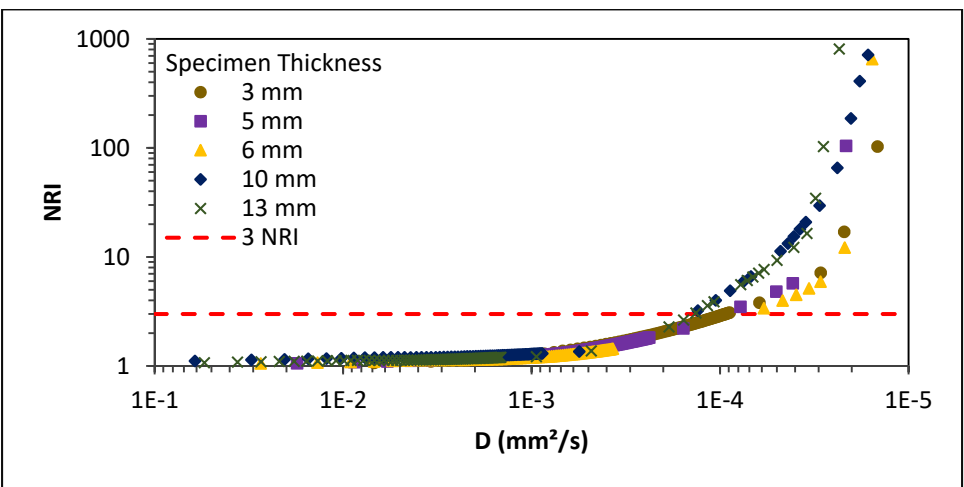
D = diffusivity coefficient, mm<sup>2</sup>/s,

x = distance from the starting point that a molecule diffuses in time, mm, and

t = curing time, s.



(a)



(b)

Figure 4.4: NRI as a function of *D* at 23 ± 0.5°C and 50 ± 2% RH: (a) AE-90S and (b) CRS-2P.

Once the residual material achieves a critical moisture content threshold (approximately at a 3.0 NRI value for a pure binder specimen), the asphalt emulsion samples experience minimal water movement. This occurrence can be attributed to the asphalt emulsion phase transition from o/w to a continuous asphalt film and the decrease in the amount of moisture available in the specimen (Banerjee et al., 2012). Accordingly, the electrical resistance of the material residue abruptly increases. The straightforward connection between the NRI and  $D$  validates the proposed measurement concept. Evidently, the electrical response of the material is fundamentally associated with the asphalt emulsion curing process.

#### 4.1.3 Asphalt Emulsion-Aggregate Combinations

The asphalt emulsion-aggregate test results indicate that NRI can quantify the amount of curing that occurs in four typical asphalt emulsion-aggregate combinations. As detailed in Table 4.2, 16 combination specimens were tested.

Table 4.2: Asphalt Emulsion-Aggregate Combinations

No.	Asphalt Emulsion-Aggregate Combination	Asphalt Emulsion Application Rate	Aggregate Moisture Condition
1	AE-90S Limestone	1.4 L/m <sup>2</sup>	Oven Dry (OD)
2			Saturated Surface Dry (SSD)
3		1.8 L/m <sup>2</sup>	Oven Dry (OD)
4			Saturated Surface Dry (SSD)
5	CRS-2P Limestone	1.4 L/m <sup>2</sup>	Oven Dry (OD)
6			Saturated Surface Dry (SSD)
7		1.8 L/m <sup>2</sup>	Oven Dry (OD)
8			Saturated Surface Dry (SSD)
9	AE-90S Gravel	1.4 L/m <sup>2</sup>	Oven Dry (OD)
10			Saturated Surface Dry (SSD)
11		1.8 L/m <sup>2</sup>	Oven Dry (OD)
12			Saturated Surface Dry (SSD)
13	CRS-2P Gravel	1.4 L/m <sup>2</sup>	Oven Dry (OD)
14			Saturated Surface Dry (SSD)
15		1.8 L/m <sup>2</sup>	Oven Dry (OD)
16			Saturated Surface Dry (SSD)

Figures 4.5 and 4.6 present the results obtained for the CRS-2P gravel combination. Figure 4.5 shows that chip seal replicas that contain 1.4 L/m<sup>2</sup> emulsion cured earlier than replicas with 1.8 L/m<sup>2</sup> emulsion. Figure 4.5 also shows that chip seal systems with SSD cover aggregate cured faster than the systems with OD aggregate. These results highlight the fact that any single variable can delay or accelerate the chip seal curing process. Figure 4.6 shows that a lower electrical resistance measurement was observed for the samples with 1.8 L/m<sup>2</sup> of emulsion. This observation is due to a larger conductive region in the water layer of the specimen. Similar observations can be made for the four asphalt emulsion-aggregate combinations.

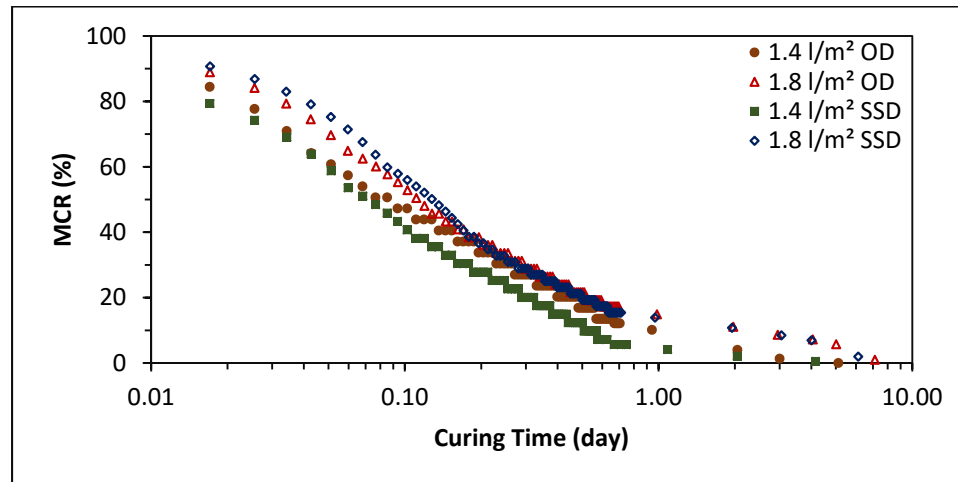


Figure 4.5: MCR vs. curing time in days: CRS-2P limestone combination at  $23 \pm 0.5^\circ\text{C}$  and  $50 \pm 2\%$  RH.

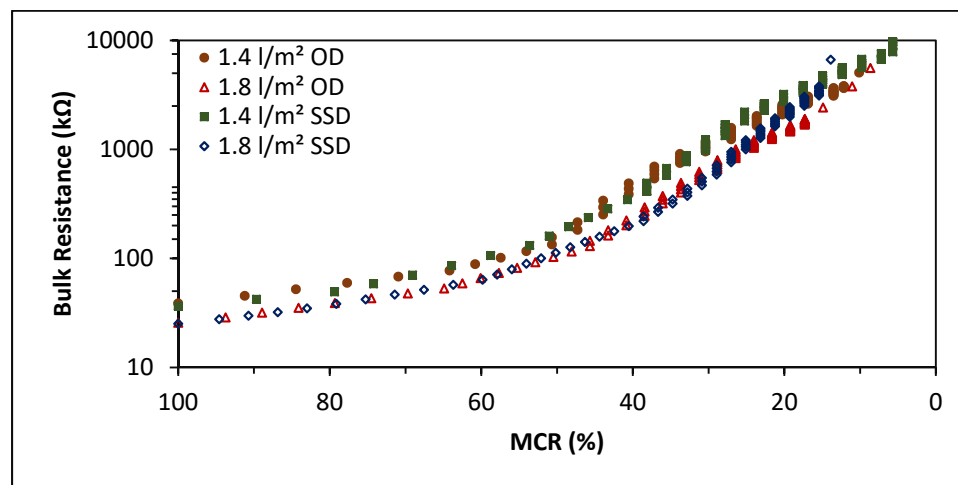
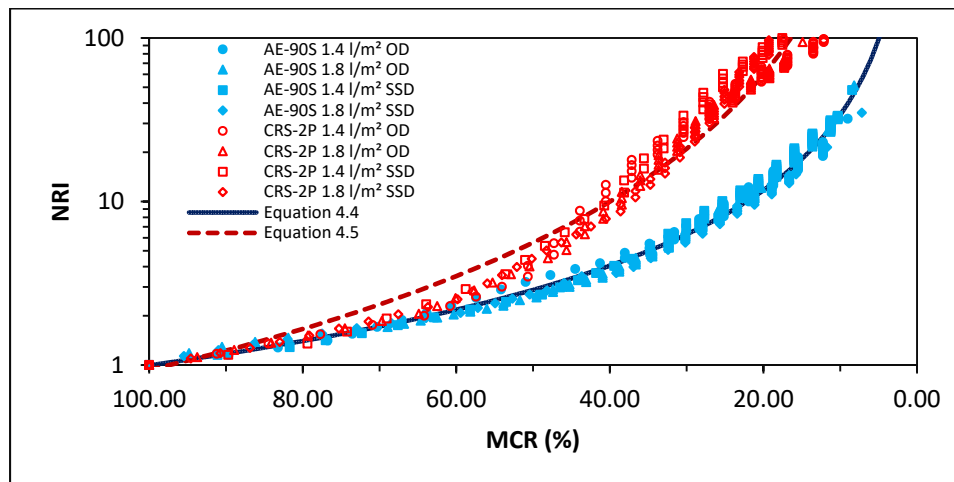
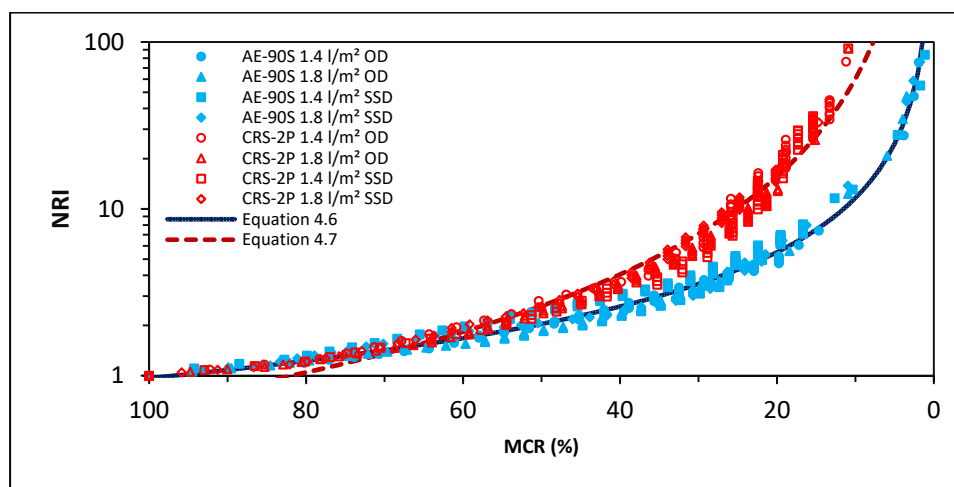


Figure 4.6: Bulk resistance vs. MCR: CRS-2P limestone combination at  $23 \pm 0.5^\circ\text{C}$  and  $50 \pm 2\%$  RH.

Figure 4.7 shows the normalized electrical response for each asphalt emulsion-aggregate combination. As detailed in Table 4.3, power functions (Equations 4.4 – 4.7) were formulated for each chip seal emulsion-aggregate combination, and NRI values were calculated at MCRs of 25, 20, and 15 percent.



(a)



(b)

Figure 4.7: NRI vs. MCR trends of asphalt-emulsion aggregate specimens: (a) limestone and (b) gravel at  $23 \pm 0.5^\circ\text{C}$  and  $50 \pm 2\%$  RH.

The results suggest the NRI approach is relatively constant, regardless of the variations in the primary moisture sources (the water portion of the asphalt emulsion or the moisture condition of the aggregate). The aggregate augments the tortuosity of the electrical current path in comparison to the pure asphalt emulsion specimens, which causes the bulk resistance to increase more quickly.

Table 4.3: Regression Results for Asphalt Emulsion-Aggregate Combinations

Chip Seal Combination	AE-90S Limestone	CRS-2P Limestone	AE-90S Gravel	CRS-2P Gravel
X =	MCR	MCR	MCR	MCR
Y =	NRI	NRI	NRI	NRI
Regression Equation	$Y = 1150X^{-1.53}$ [4.4]	$Y = 140058X^{-2.59}$ [4.5]	$Y = 140X^{-1.08}$ [4.6]	$Y = 5410X^{-1.95}$ [4.7]
R <sup>2</sup>	0.98	0.95	0.98	0.97
NRI at MCR = 25%	8.32	33.76	4.32	10.13
NRI at MCR = 20%	11.71	60.15	5.50	15.66
NRI at MCR = 15%	18.19	126.64	7.30	27.45

The trends in the NRI as a function of MCR data are in agreement with strength gain as a function of moisture loss patterns found in the literature. Howard et al. (2011) correlated the binder strength gain and moisture loss by conducting frosted marble tests (FMTs). FMTs are used in an attempt to quantify binder adhesive behavior and identify when chip seals are ready to accept uncontrolled traffic and brooming operations. The FMT is conducted using a tray that consists of 15 glass etched marbles that are torqued after curing in a 57°C environmental chamber.

Howard et al. (2011) reported that during the early stage of the curing process, high levels of initial moisture loss can be measured, but appreciable mechanical properties do not develop. As the material approaches the critical moisture content range, relatively moderate strength improvement is attained. Once the critical moisture content range is reached, the relationship curves rise sharply and the system gains substantially higher mechanical strength (Figure 2.6). This trend is conceptually similar to the electrical responses that were obtained in this study. As shown in Figure 4.8, it can be

hypothesized that the NRI approach can determine when a chip seal has sufficiently cured to withstand the shear forces of sweeping and uncontrolled traffic.

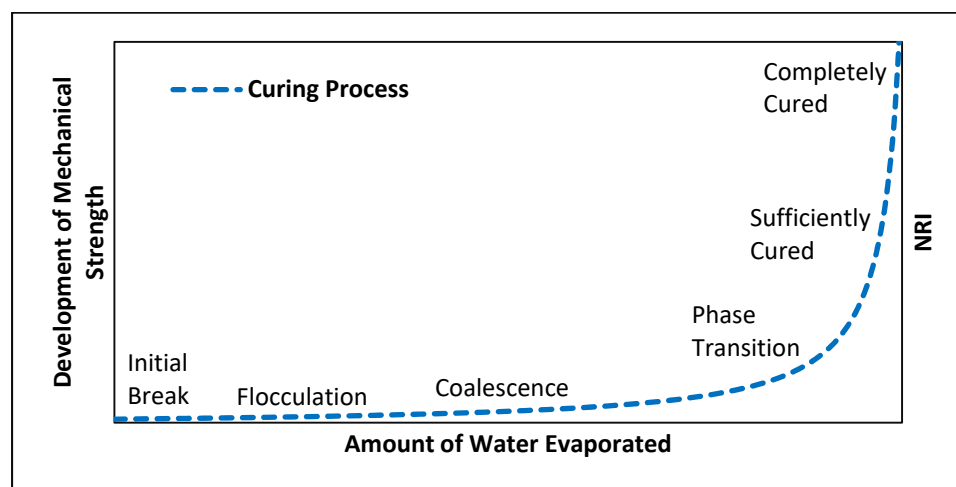


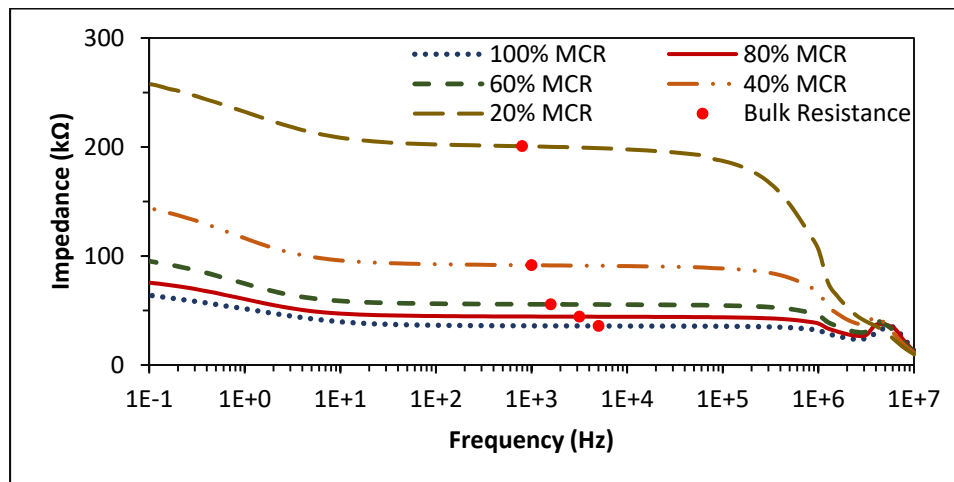
Figure 4.8: Schematic illustration of the theoretical relationships in emulsion-based chip seal systems.

It is important to note that the moisture content at which the electrical resistance starts to significantly increase varies depending on the asphalt emulsion-aggregate combination. Table 3 reports different NRI values for each combination at the critical moisture content range of MCRs at 25, 20, and 15 percent. This system response can be caused principally by the asphalt emulsion and cover aggregate properties (i.e., absorption, porosity) in addition to the asphalt emulsion-aggregate compatibility. Any of these factors can impact how the water molecules lose connectivity and leave the system, and how the emulsion gains strength. The current methodology to determine when to allow brooms and traffic onto a fresh seal coat uses the critical moisture content. These results highlight the importance of an electrical resistance measurement to quantify chip seal curing times, as such a measurement can provide a consistent evaluation of the asphalt emulsion curing process.

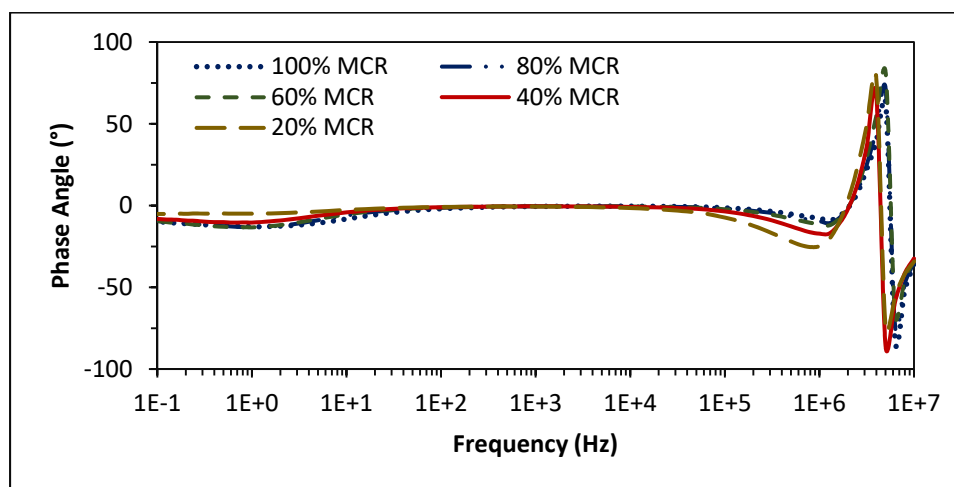


#### 4.1.4 Multiple Frequency Electrical Response

Figure 4.9 shows the multiple frequency electrical responses of the AE-90S gravel, 1.8 L/m<sup>2</sup> OD specimen. The Bode plots show the impedance, and thus the bulk resistance can be overestimated or underestimated at low or high frequencies, respectively. In addition, the bulk resistance frequency tends to decrease as the material cures, oscillating between 10 kHz and 100 Hz. However, the electrical response remains stable over a broad number of frequency decades (between 10<sup>1</sup> and 10<sup>5</sup>) and throughout the curing process. This outcome was consistent for the 16 asphalt emulsion-aggregate combinations that were tested. From an electrical point of view, the constant material response across multiple frequencies reinforces the measurement's reliability and encourages a move toward field evaluations that employ portable devices.



(a)



(b)

Figure 4.9: Bode plot, AE-90S gravel 1.8 L/m<sup>2</sup> OD: (a) impedance vs. frequency and (b) phase angle vs. frequency.

## 4.2 Field Trials and Standardized Mechanical Strength Test

### 4.2.1 Statistical Analysis of Chip Seal Curing Process

Typical approaches to determine when to broom or open to traffic a fresh surface treatment tend to predict chip seal curing times as a function of climatic conditions or amount of moisture loss. However, these methodologies may fail to address the uncertainties and variability that exist within all chip seal projects. It is believed that water evaporation is affected by wind velocity, humidity, and ambient temperature, in that order of importance (Read and Whiteoak, 2010). Moreover, once these methodologies are applied in the field, the presence of solar radiation also contributes to the moisture loss from asphalt emulsions (Yaacob et al., 2015). Climatic conditions can vary greatly and interact with each other during the curing process.

Recent evidence suggests the magnitude of the water evaporation rate is driven mainly by the moisture content that is available in the system (Banerjee et al., 2012). Nevertheless, quantifying the amount of moisture, or moisture loss in the field is often time-consuming and impractical. To demonstrate this point, a statistical analysis was performed using the climatic condition factors and moisture loss measurements gathered from the field experiments completed for this project. Considering that an asphalt emulsion's development of stiffness is governed by the rate of moisture removal from the system (Banerjee et al., 2012), a multiple linear regression analysis was employed to predict the WER based on the available explanatory variables: wind velocity, RH, ambient temperature, pavement temperature, cloud cover, and the moisture content remaining in the system. Equation 4.8 expresses the resulting fitted model ( $R^2 = 0.70$ ).

$$WER = -0.070 + 0.0004(MCR) + 0.0008(PT) + 0.0004(RH) - 0.0007(CC) + 0.0007(AT) \quad [4.8]$$

where:

WER = water evaporation rate, g/cm<sup>2</sup>-hr,

MCR = moisture content ratio, %,

PT = pavement temperature, °C,

RH = relative humidity, %,

CC = cloud cover, qualitative, and

AT = ambient temperature, °C.

The regression equation includes the independent variables that met the significance level ( $p < 0.05$ ) for entry into the model. Contrary to expectations, the data suggest that wind speed is statistically insignificant and that higher RH values trigger faster WERs, although the effect is slight. Given that these findings are contrary to observations, they should be interpreted with caution and warrant additional investigation.

The regression results presented in Table 4.4 show that MCR is the variable that contributes the most to explain the WER (partial R-squared = 0.52). Figure 4.10 shows that a high level of moisture loss was experienced during the early stage of the curing process. The WER is shown to accelerate or slow down depending on the climatic conditions. However, once the fresh seal coat reaches a critical moisture content, the rate of the mass loss drops substantially with time. This decrease in the rate of evaporation can be attributed to the asphalt emulsion phase transition as well as to the decrease in the amount of moisture that is available in the system (Banerjee et al., 2012). After the asphalt emulsion phase transition, the evaporation of water is diffusion-controlled due to

the fact that the water moves passively through the asphalt binder to the drying surface in order to evaporate (James, 2006).

Table 4.4: Stepwise Variable Selection Output

Step	Variable Entered	Partial R-Squared	Model R-Squared	F-value	p-value
1	MCR	0.52	0.52	117.85	<.0001
2	PT	0.05	0.57	13.68	0.0003
3	RH	0.03	0.60	6.87	0.0100
4	CC	0.06	0.66	18.59	<.0001
5	AT	0.04	0.70	14.05	0.0003

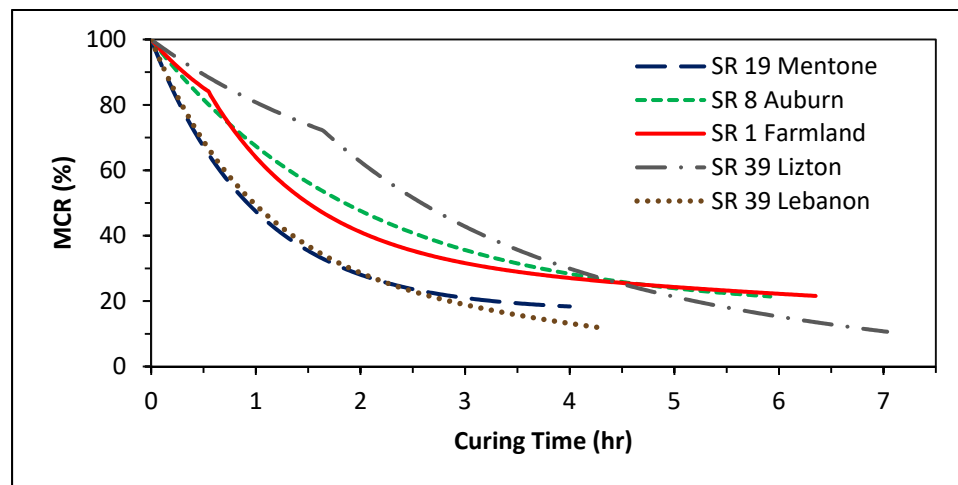


Figure 4.10: Moisture content ratio as a function of curing time profiles.

For the aforementioned reasons, the amount of moisture remaining in a chip seal system is a reasonable predictor to determine traffic opening times (Howard et al., 2011). However, the critical MCR at which the chip seal has adequately cured can vary considerably. A field electrical measurement technique might more accurately and consistently predict chip seal curing times compared to the MCR.

#### 4.2.2 Field Trials Using Normalized Resistance Index

Figure 4.11 shows the electrical resistance measurements as a function of curing time for each of the field test pavement sections. Each dataset shows different trends with curing time, highlighting the variability between projects due to the impact of the environmental conditions on the evaporation rate. The average initial electrical resistance measured ( $n = 5$ ) was  $28.7 \text{ k}\Omega$  (with a coefficient of variation of 31%). This initial variability can be attributed mostly to the asphalt emulsion properties (i.e., viscosity and water volume fraction) and cover aggregate features (i.e., gradation and dampness), and to the application rates.

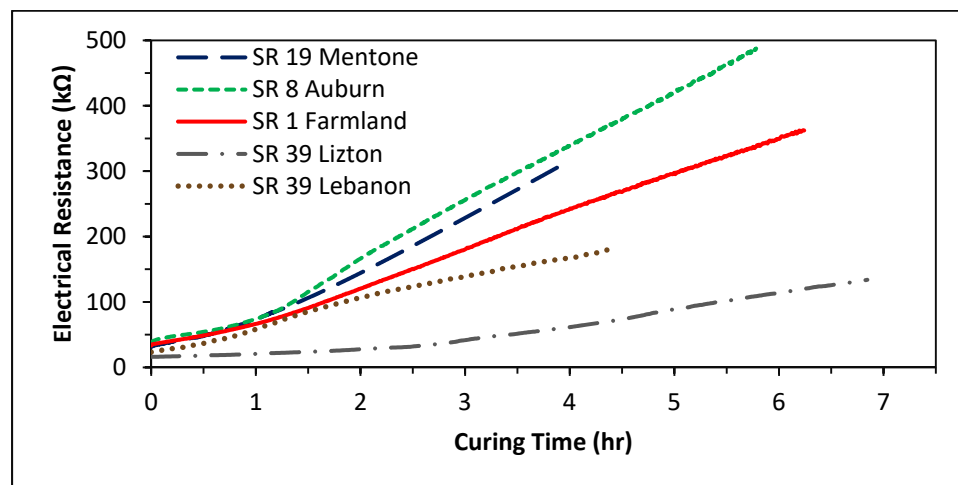


Figure 4.11: Electrical resistance measurements during chip seal curing.

In order to minimize the variability that is due to the application rates, aggregate properties, and mechanical action, the time-dependent resistance was normalized by the initial electrical resistance measurement (see Equation 4.1). During the course of this study, the NRI approach demonstrated great potential to serve as a quantifiable method to

determine when a fresh chip seal can withstand the shear forces of brooms and traffic.

Figure 4.12 shows the NRI as a function of curing time for the various field projects.

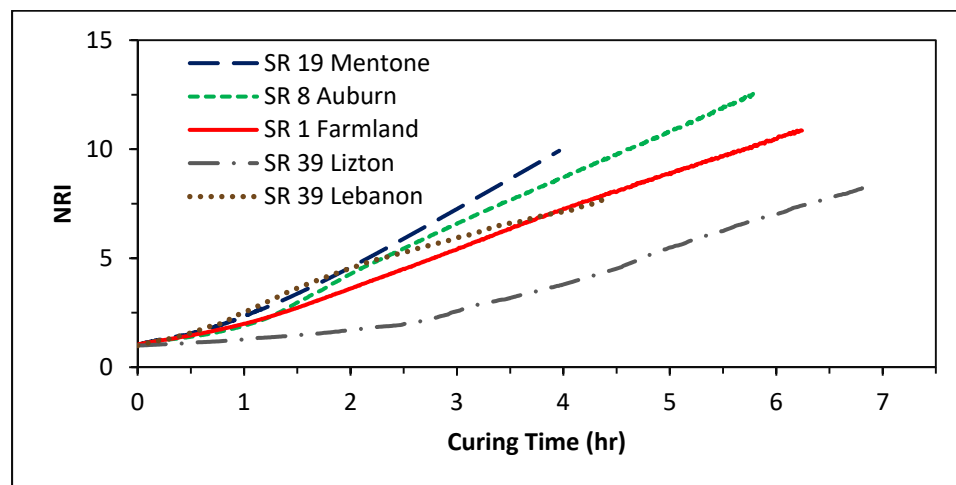


Figure 4.12: Normalized resistance indices as a function of curing time.

The data clearly illustrate the impact of environmental conditions. For example, the chip seal projects at Lizton and Lebanon used identical materials and were constructed by the same chip seal crew on consecutive days. The project at Lizton was constructed on a day that was mostly overcast, whereas the project at Lebanon was constructed on a sunny day with high temperatures and low humidity. These different conditions explain the difference in curing rate and electrical resistance between the Lizton and Lebanon projects. The NRI seems well correlated to water evaporation.

Figure 4.13 presents the NRI as a function of the WER. The plot suggests the lower the NRI value, the higher and more dispersed are the WER observations. The observed variability is attributable mainly to the material and climatic factors that affect the WER. Chip seal systems experience different moisture removal mechanisms, especially during the early stages of the curing process. For example, the strength of the

asphalt emulsion-aggregate reaction is in many cases sufficient to squeeze the water from the chip seal system (James, 2006). However, it is evident that as the fresh seal coat cures and the NRI value increases, the WER and error variance both decrease. In short, the electrical resistance measurement increments are in good agreement with the minimal moisture loss experienced by the chip seal system.

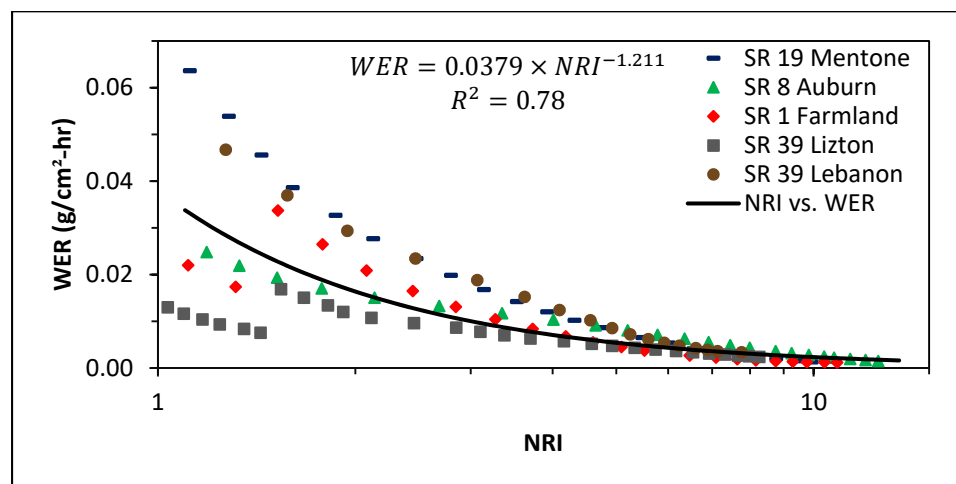


Figure 4.13: Relationship between normalized resistance index values and water evaporation rate.

Despite the fact that several variables affect chip seal aggregate loss (i.e., aggregate gradation, flakiness index, etc.), a positive correlation was established between the NRI and the aggregate's dislodgement potential (DP). Figure 4.14 reveals that as the NRI value increases, the aggregate's DP markedly decreases. This result supports the finding that NRI values are well correlated to the formation of asphalt residue film and the development of binder adhesive strength for asphalt emulsions. Based on the NRI correlation with both the WER and DP, it can be hypothesized that, once the chip seal system's initial electrical resistance increases by a factor of 10, no significant water loss or aggregate dislodgement are to be expected.



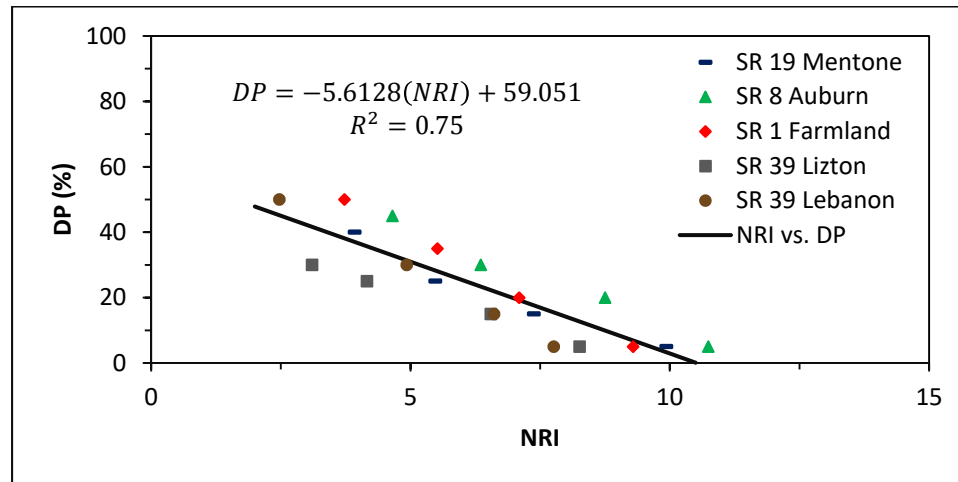


Figure 4.14: Aggregate dislodgement potential correlated to the normalized resistance index.

#### 4.2.3 Sweep Test Results

Figure 4.15 presents the ASTM D7000 test results showing the percentage of aggregate mass loss (AML) from the chip seal specimens as a function of the NRI. The lower the AML value, the higher the mechanical strength that is developed within the chip seal system. The plot clearly shows that the mechanical performance of the samples reaches a consistent value once the NRI value exceeds 10; as such, this value appears to correlate to a sufficiently mature seal coat.

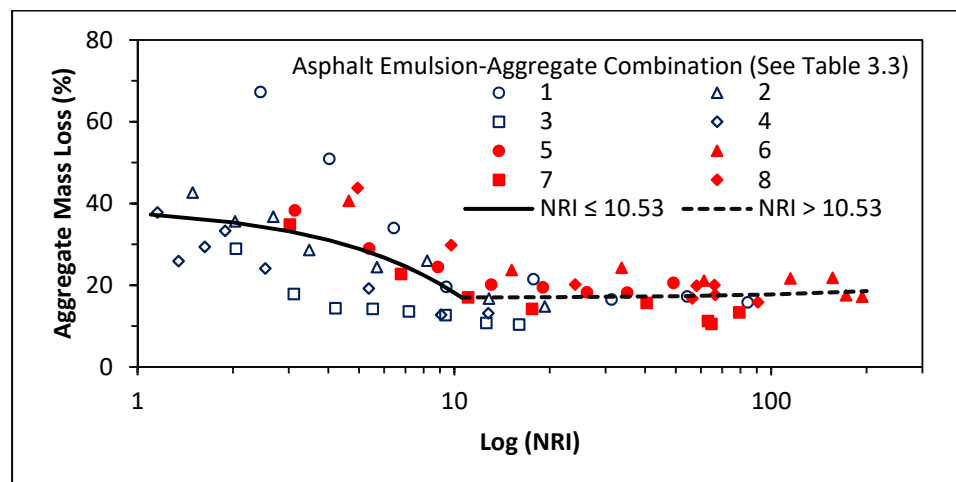


Figure 4.15: Piecewise linear regression between aggregate mass loss and normalized resistance index.

Piecewise linear regression analysis was used to analyze the chip seal mechanical performance as a function of the NRI. It was found that when the NRI equals 10.53, the relationship between the NRI and AML experiences a shift in the slope. Table 4.5 reports how the different functions fit the AML data over varying ranges of the NRI. Below an NRI value of 10.53, the AML value substantially decreases as the NRI value increases ( $p < 0.05$ ). Once the NRI value reaches and exceeds 10.53, the chip seal specimens achieve a threshold at which the aggregate loss variation is insignificant ( $p > 0.05$ ). This mechanical performance obtained using ASTM D7000 is in excellent agreement with the field experimental results and suggests the emulsion in a chip seal system has sufficiently cured once the NRI value exceeds approximately 10. At this NRI level, a fresh seal coat has gained significant mechanical strength to withstand the shear forces of brooms and uncontrolled traffic.

Table 4.5: Piecewise Regression Analysis for ASTM D7000 Data

R <sup>2</sup>		0.47	
p-value		<0.0001	
Breakpoint		10.53	
Breakpoint 95% Confidence Interval		6.89 - 14.17	
NRI Range	Regression Equation	R <sup>2</sup>	p-value
NRI ≤ 10.53	AML = 39.68 - 2.1500 (NRI)	0.23	0.01
NRI > 10.53	AML = 16.94 + 0.0082(NRI)	0.01	0.57

#### 4.2.4 Vialit Test Results

Figure 4.16 presents the Vialit test results at 37°C. Piecewise linear regression analysis was performed to evaluate the changes in AML over the varying ranges of the NRI. As shown in Table 4.6, the piecewise linear regression analysis results suggest that the transition from relatively high AML percentages to minimum or no AML occurs at a NRI value of 4.66. This NRI value differs from the previous sweep test findings that suggest that the AML transition (breakpoint) happens at the NRI value of 10.53. This lack of agreement is attributable mainly to the differences between the test methods, such as their sample preparation, loading mechanism, and applied energy. However, apart from these differences, the Vialit test results confirm that consistent AML percentages can be achieved once a specific NRI value is reached.

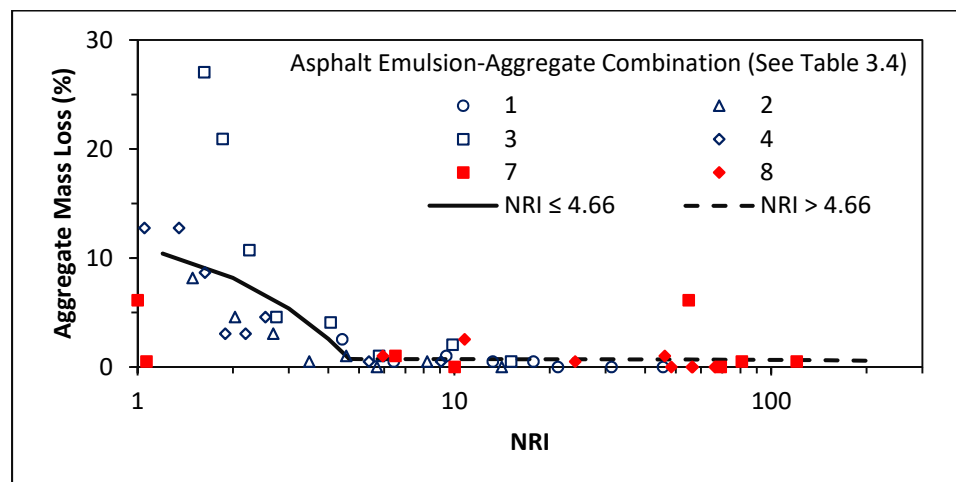


Figure 4.16: Vialit test results at 37°C: aggregate mass loss vs. normalized resistance index.

Table 4.6: Piecewise Regression Analysis for Vialit Test Results at 37°C

R <sup>2</sup>		0.47	
p-value		<.0001	
Breakpoint		4.66	
Breakpoint 95% Confidence Interval		2.85 – 6.47	
NRI Range	Regression Equation	R <sup>2</sup>	p-value
NRI ≤ 4.66	AML = 13.75 - 2.79 (NRI)	0.19	0.06
NRI > 4.66	AML = 0.74 - 0.0008 (NRI)	0.00	0.92

Figure 4.17 shows the Vialit test results at 0°C. The data suggest that the aggregate's DP at low temperatures decreases as the chip seal cures. This finding reinforces the importance of allowing chip seal systems time to sufficiently cure. The curing process could have a significant impact on the chip seal performance at low temperatures and, thus, on the service life. Further Vialit testing at lower temperatures and different freezing times as well as various freeze-thaw cycles could provide more informative data (Jordan and Howard, 2011). However, the correlation found between the NRI and chip seal performance at low temperatures seems promising.

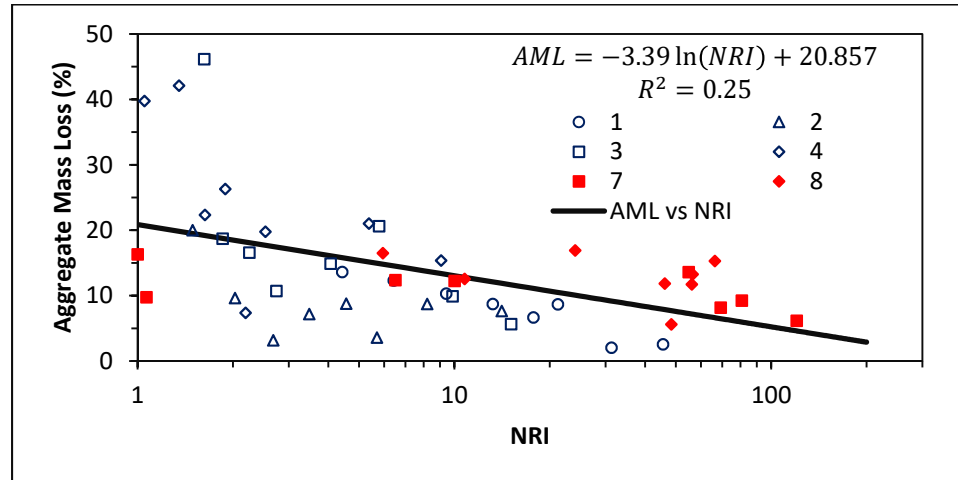


Figure 4.17: Vialit test results at  $0 \pm 2^\circ\text{C}$ : aggregate mass loss vs. normalized resistance index.

### 4.3 Field Implementation, Validation, and Calibration

The electrical resistance measurement technique was implemented, validated, and calibrated based on the following criteria: measurement effectiveness, measurement reliability, and ease of use. The effectiveness of the technique was evaluated on the basis of the results obtained compared to the water mass loss measured and aggregate DP that was observed. Measurement reliability was assessed in terms of the electrical measurement phase angle and proper electrical connection. Finally, ease of use refers to the user-friendliness of the measurement technique such that it can be performed easily by field inspectors, technicians, and contractors. Within the framework of these criteria, the following observations and recommendations were made to refine the measurement technique.

### 4.3.1 Two-point Probe Configuration

Previous findings in the literature indicate that shady spots in a chip-sealed pavement section undergo lower moisture removal than sunny spots (Shuler et al., 2011). In this context, it was noticed that a two-point probe measurement using a plastic spacer might provide some shade (beyond the actual shade or solar radiation experienced by a full-scale chip seal system) to the area subjected to the electrical field. This effect could delay the increase in the resistance of a chip seal system to moisture loss, as solar radiation significantly contributes to moisture loss. In order to improve measurement effectiveness, two-point probes supported by felt and stainless steel washers and plywood pads were evaluated.

Figure 4.18 shows the NRI over curing time results obtained at US 52 in Metamora for two-point probes using plywood pad supports and using a plastic spacer. It is believed that the shade provided by the plastic spacer delayed the increase in the resistance measurements in comparison to the electrical measurements using plywood pad supports. Consequently, using plywood pad supports provided a better representation of the chip seal curing process. Also, these results suggest that electrical resistance should be measured in areas of the project where moisture loss is expected to be slowest (Shuler et al., 2011).

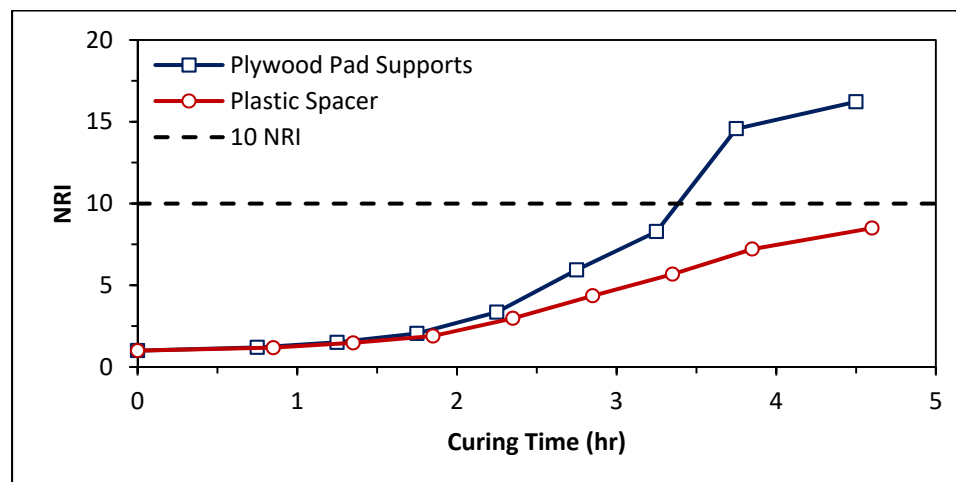


Figure 4.18: NRI vs. curing time at US 52 in Metamora: two-point probe comparison between using plywood pad supports and plastic spacer.

#### 4.3.2 Distance between Probes

Of particular interest was measuring the electrical resistance at different distances between probes. This research effort was undertaken in order to validate that a normalized 7.6-cm two-point probe measurement is an accurate and significant representation of a full-scale chip seal. Figure 4.19 presents the electrical resistance measured over curing time for two-point probe measurements using plywood pad supports at SR 827 in Angola. The probes were spaced at 7.6 cm, 15.2 cm, and 30.4 cm. As expected, when the spacing was increased, the electrical resistance measurement was higher. For any material, the measured resistance will vary directly with the distance between electrodes.

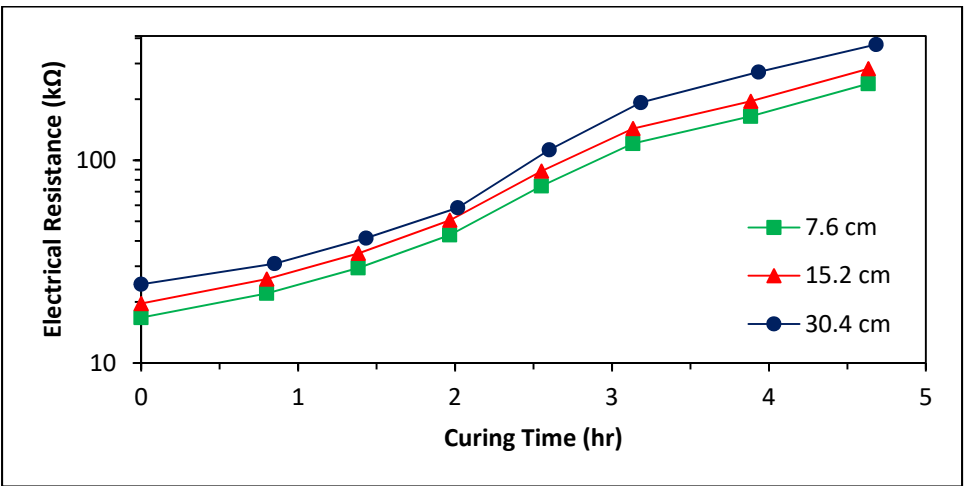


Figure 4.19: Electrical resistance vs. curing time at SR 827 in Angola: probes spaced at different distances.

Figure 4.20 shows the NRI over curing time for the electrical measurements taken at different distances between electrodes. As shown, the normalized approach significantly reduces the variability due to the distance between the probes. These results validate the normalized approach suggested in this study.

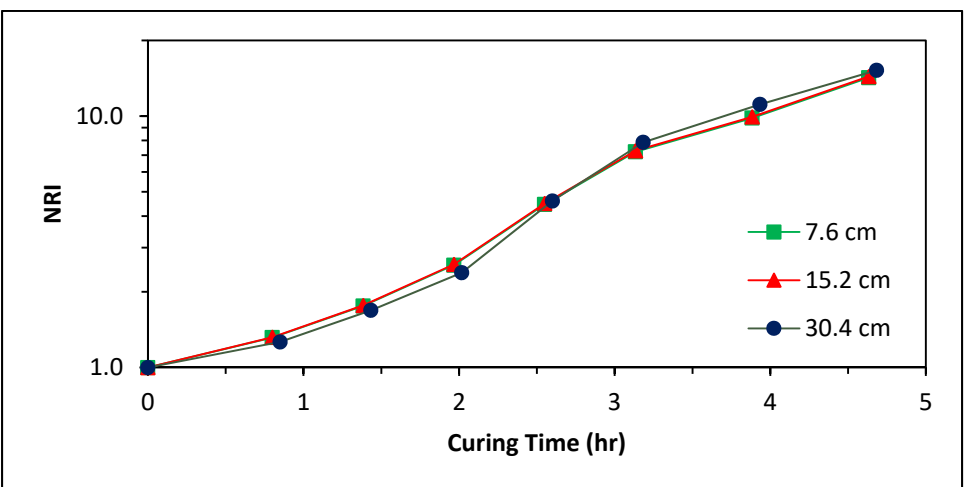


Figure 4.20: NRI vs. curing time at SR 827 in Angola: probes spaced at different distances.



Although setting greater distances between electrodes seems attractive at first glance, extending the distance between electrodes also increases the phase angle of the electrical measurement, as shown in Figure 4.21. From a measurement reliability perspective, it is preferable to keep the phase angle of the electrical measurement at the lowest possible value. The smallest distance of 7.6 cm between electrodes is better for maintaining the phase angle within a tolerable range (between 0 and 10 degrees) than the other two distances tested.

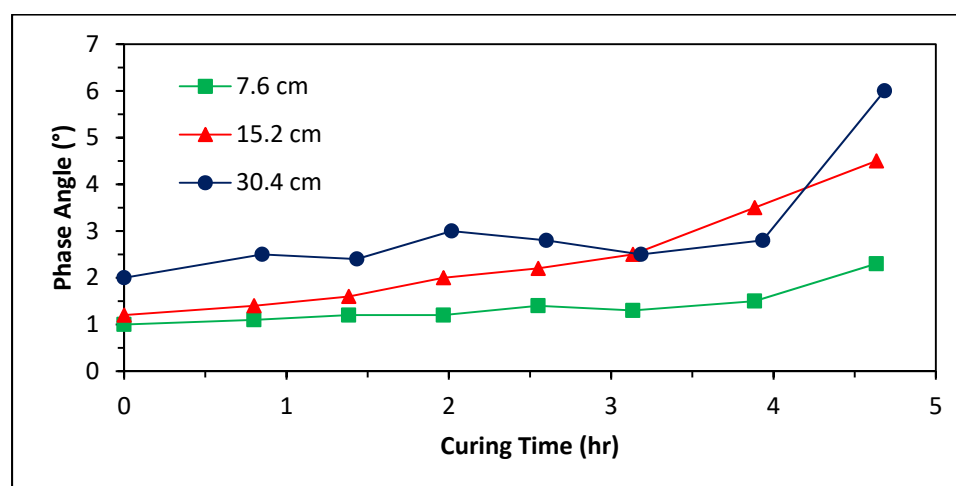
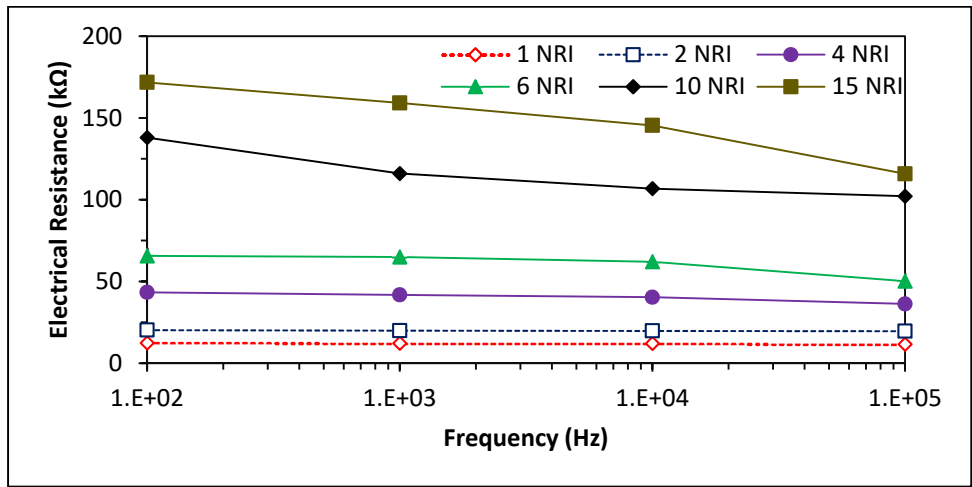


Figure 4.21: Phase angle vs. curing time at SR 827 in Angola: probes spaced at different distances.

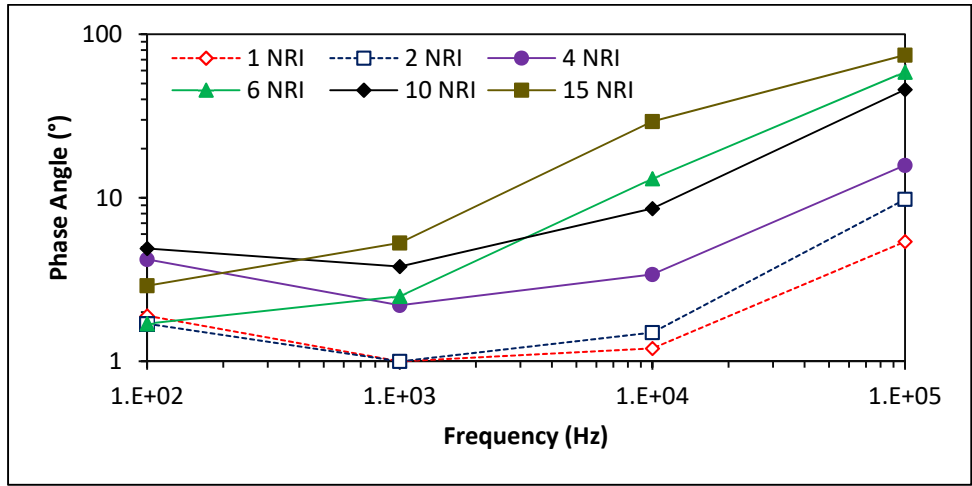
### 4.3.3 Frequency of Electrical Current

Figure 4.22 shows multiple frequency responses at different NRI values for the resistance measured at SR 352 in Oxford using a 7.6-cm two-point probe supported by plywood pads. The Bode plots highlight the importance of selecting the frequency that generates the minimum phase angle to guarantee measurement reliability. The results are comparable to the Bode plots obtained using sophisticated EIS measurements developed during the preliminary EIS testing in this study. As the chip seal system cures, the

frequency with the minimum phase angle tends to decrease (most likely the initial frequency is 1000 Hz and then shifts to 100 Hz).



(a)



(b)

Figure 4.22: Bode plots at SR 352 in Oxford: (a) electrical resistance vs. frequency and (b) phase angle vs. frequency.

#### 4.3.4 Two-point Probe Setting

Taking into consideration these observations, a 7.6-cm two-point probe using plywood pad supports is recommended for taking measurements. In this study, the felt and stainless steel washers were not sufficient to support the steel rod probes firmly and using a plastic spacer might jeopardize measurement accuracy.

Once the rolling protocol is completed, it is recommended the probes be embedded into the fresh chip seal. The probes should be fixed at a specific spot for the following reasons: to embed the probes thoroughly into the fresh chip seal system to provide a good connection between the asphalt emulsion and steel rods, to facilitate the monitoring of the increase in the electrical resistance measurements, and to reduce the amount of time required to take the measurements at different curing times. Considerable care must be exercised when setting the probes to guarantee that the steel rods penetrate the aggregate layer and are seated in the existing pavement, as shown in Figure 4.23.

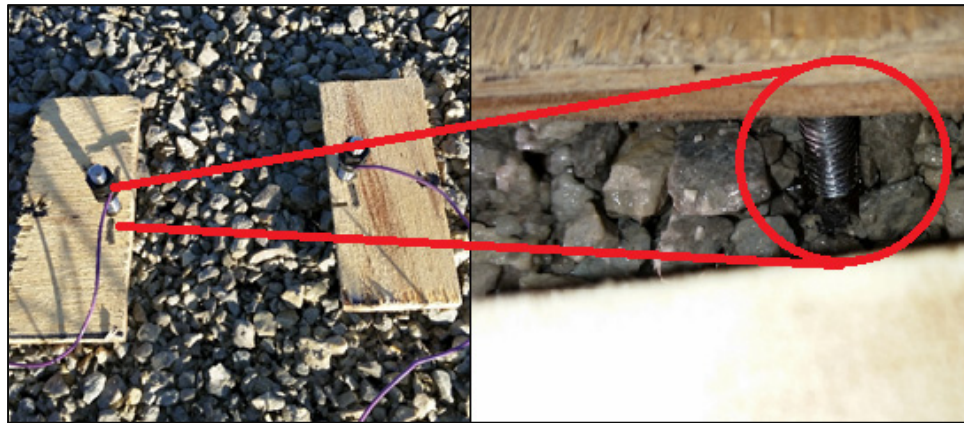


Figure 4.23: Setting probe in fresh chip seal system.

For the initial setting of the probes and additional resistance measurements, the top of the rods should be tapped gently to ensure that the position of the probes is appropriate (Figure 4.24). In this study, tapping the rods before each measurement was taken helped to achieve low phase angle values. A high phase angle value could be an indication of a poor electrical connection (i.e., emulsion-steel probe, steel probe-wire). The distance between probes was verified using a ruler. The steel rods can be easily removed after the chip seal system has sufficiently cured. Following these recommendations should lead to effective and reliable resistance measurements.



Figure 4.24: Tapping steel rod probes.

### 4.3.5 Chip Seal Curing Times

As shown in Figure 4.25, the curing times were quantified *in situ* as the time that was required for the initial resistance to increase by a factor of 10 (or NRI value greater than 10). In order to validate the methodology, the results were compared to the measured MCRs and WERs (Figure 4.26), as well as to the observed DP. Table 4.7 presents the curing times determined for each pavement section using 7.6-cm two-point probes supported by plywood pads. The curing times were quantified at chip seal projects carried out throughout the 2016 chip sealing season.

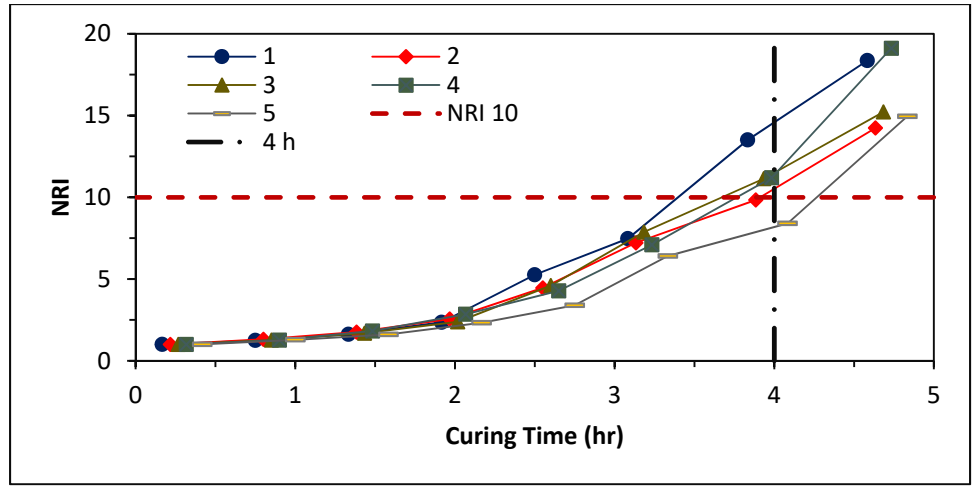


Figure 4.25: NRI vs. Curing time, measured at five-different spots on the fresh chip seal at SR 827 Angola.

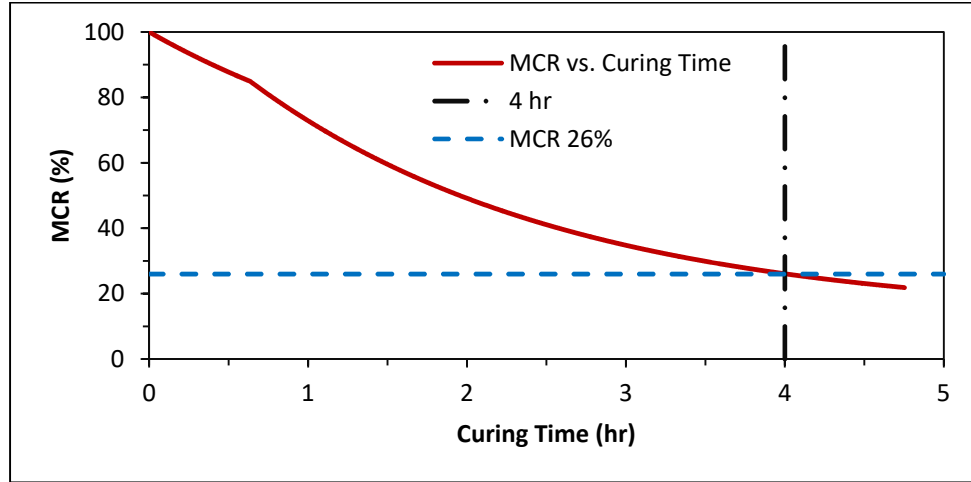


Figure 4.26: MCR vs. Curing time, plate sample (1) at SR 827 Angola.

Table 4.7: Quantified Chip Seal Curing Times at Field Sites

Pavement Section/ Date	Materials Applied	Curing Time (hr)	MCR (%)		WER (g/cm <sup>2</sup> -hr)		DP (%)
			Plate Sample		Plate Sample		
			1	2	1	2	
SR 352 Oxford/ 06-28-16	AE-90S SC 16 Limestone	4.0	19.0	22.0	0.003	0.001	5.0
SR 38 Kirklin/ 07-21-16	AE-90S SC 16 Gravel	3.8	21.0	19.0	0.002	0.003	5.0
US 52 Brookville/ 08-23-16	CRS-2P SC 11 Dolomite	4.0	16.0	15.0	0.002	0.002	5.0
US 52 Metamora/ 08-24-16	CRS-2P SC 11 Dolomite	3.5	20.0	22.0	0.004	0.010	5.0
SR 827 Angola/ 09-01-16	AE-90S SC 16 Dolomite	4.0	26.0	28.0	0.008	0.006	10.0

The curing times are in good agreement with chip seal construction guidelines that suggest that brooming generally can be performed within two to four hours after sealing (Caltrans, 2007). Furthermore, the curing times are within the critical moisture content range, i.e., between MCRs of 15 and 25 percent, which represents the amount of remaining moisture that corresponds to enough binder adhesive strength to allow sweeping and traffic on the newly placed surface. The results correlate well with low WERs and minimum aggregate DP. These findings validate the effectiveness of using electrical resistance measurements to quantify chip seal curing times.

#### 4.3.6 Quality Control Tool

From an asphalt emulsion product performance perspective, the measured curing times presented are in substantial contradiction with references in the literature that suggest chip seal curing times are reduced to one and one-half hours for polymer-modified asphalt emulsions, such as AE-90S and CRS-2P (Testa et al., 2014). This disagreement highlights the importance of measuring the actual curing time of each chip seal project, as several changeable variables can delayed the curing process.

Considering that an aggressive quality control testing program, combined with close inspection, can contribute to a chip seal project's success (Gransberg and James, 2005), the use of electrical resistance measurements can serve as a quality control tool for manufacturing and performance acceptance of asphalt emulsion products. Also, this measurement technique can help to use asphalt emulsion-cover aggregate combinations that ease the curing process, and thus improve chip seal performance.

## CHAPTER 5. SUMMARY, CONCLUSIONS, AND FUTURE WORK

### 5.1 Summary

This study investigated the potential for using electrical properties to quantify asphalt emulsion-based chip seal curing times. A robust experimental set-up that simulates surface treatment structures and ensures repeatable EIS experiments was established in order to conduct initial laboratory testing. The electrical properties of various asphalt emulsion and emulsion-aggregate combinations were monitored as the specimens cured. The results indicated that specimen thickness and asphalt emulsion application rate exert a noticeable effect on the material's electrical response.

The normalized approach (i.e., the NRI) formulated during the initial research phase was able to correlate the electrical properties with the amount of curing that occurred, despite the varied seal coat design components and aggregate dampness. The results supported the developed experimental set-up and the proposed electrical measurement concept. Stable electrical responses for various asphalt emulsion and cover aggregate combinations were observed.

The second phase of this research effort focused on transferring the initial findings to the field. Based on the fact that water is lost from a seal coat during the curing process, it was hypothesized that, when a sufficient amount of water is lost, the seal coat begins to gain sufficient adhesive strength to secure the aggregate in the seal coat.



Therefore, this phase of the study was designed to determine the relationships among the electrical resistance properties, the amount of moisture removed, and the mechanical performance of full-scale chip seal systems and laboratory specimens. The electrical resistance measurements indicated correlations with the water content (i.e., the WER) and the amount of aggregate loss experienced by a chip seal system under various field and laboratory conditions. Moreover, the proposed field measurement technique was shown to be simple, convenient, and portable.

In the third phase of the study, the electrical resistance measurement technique was implemented, validated, and calibrated at full-scale chip seal projects, based on the following criteria: measurement effectiveness, measurement reliability, and ease of use. Observations and recommendations with regard to the methodology were used to refine the measurement technique. Finally, the measurement technique was implemented to quantify the curing time of five full-scale chip seal projects.

## 5.2 Conclusions

The following conclusions can be drawn from this study:

1. A normalized resistance measurement can be used to quantify chip seal curing times. The NRI approach takes into account the factors that affect the electrical resistance measurements, such as material cross-sectional area, distance between probes, and material properties. Thus, the NRI is a reliable, quantifiable tool that can be used to determine when a fresh chip seal can withstand the forces of brooming or be opened to unrestricted traffic. Also, the NRI approach is capable

of capturing the factors (i.e. material properties, climatic conditions) that are associated with variable curing times within chip seal projects.

2. The NRI versus MCR relationships correlated with the strength gain versus moisture loss trends that are found in the literature. The findings from this study suggest that a normalized resistance measurement (i.e., the NRI value) indicates binder strength development. The field and laboratory experimental results agree that when the NRI value exceeds 10, a chip seal system has sufficiently cured and ample mechanical strength gains have been achieved to allow for brooming and opening to traffic.
3. The typical methodology currently used to determine when to allow brooms and traffic onto a fresh seal coat relies on critical moisture content. However, the findings of this study show that chip seal material properties and compatibility can significantly shift the critical moisture content at which the system experiences substantial mechanical strength gains as well as sharp electrical resistance increase. As an alternative, the NRI approach provides quantitative measurements that can be used to evaluate the chip seal curing process in a consistent and repeatable fashion.
4. Implementation of the methodology for full-scale chip seal systems shows that the curing time for the chip seal projects ranges from 3.5 to 4.0 hours. These curing times are in good agreement with chip seal construction guidelines that suggest that brooming generally can be performed within two to four hours after sealing. Also, the measured curing times are within the critical moisture content range, i.e.,

MCRs between 15 and 25 percent, which corresponds to adequate binder adhesive strength to allow brooms and traffic onto the newly placed surface.

5. This research has demonstrated that an electrical measurement technique can be employed to optimize chip seal construction practices. The implementation of the methodology should lead to more reliable and longer-lasting chip seals that will perform as designed. Additionally, application of this measurement technique as a quality control tool can ensure quality of materials used on the project, prevent minimal windshield claims and chip seal repair work, prevent unnecessary construction delays, provide safety for the public and construction workers and ensure a successful chip seal project.

### 5.3 Future Work

A natural progression of this research is to have field personnel use the resistance measurement technique during chip seal construction. Thus, future work should be focused on extending the understanding of chip seal curing by field inspectors, practitioners, and contractors, as well as collecting practical feedback from these users. Pilot projects and controlled brooming trials are needed to determine the appropriate location(s) and number of resistance measurements taken throughout a chip-sealed pavement section. Also, the operational implementation of brooming and opening a roadway to unrestricted traffic once the material has sufficiently cured based on the resistance measurement technique should be examined, as labor and equipment are required.

Additional field trials carried out by other state DOTs and highway agencies from around the world would be interesting to validate the findings of this study using different asphalt emulsions and cover aggregates under various climatic conditions. Finally, future studies must be performed to assess the impacts of this construction technique on the long-term performance of chip seals and life-cycle benefits.

Furthermore, the findings of this study can be extended to various other asphalt emulsion applications. Asphalts in their emulsified form are widely used for road construction and maintenance, but the current need for testing would tie together the asphalt emulsion products with their final application for performance (Kadmas, 2006). Uncertainties about asphalt emulsion workability and the development of early mechanical strength are still an inherent concern for any asphalt emulsion application, thus limiting the wider use of this paving material. Asphalt emulsions require minimum viscosity to prevent run-off, but the workability of the emulsified bitumen also must permit spraying, laying, and compaction using conventional construction equipment. Asphalt emulsion properties such as viscosity, homogeneity, and final residue directly affect workability and ultimate binder performance. These characteristics of bitumen emulsion need to be identified properly in the field to ensure the appropriateness of the emulsion for a specific use.

As an alternative, electrical resistance measurements show great potential to serve as a quality control tool for asphalt emulsion products. Future work should aim to establish whether handheld electrical devices can be employed to determine asphalt emulsion properties during construction. The use of electrical resistance measurements as a quality control and early-life performance assessment tool for asphalt emulsion paving

applications (i.e. tack coat, cold mix asphalt) would be extremely beneficial. A field measurement technique that characterizes the actual material being used for paving will guarantee the quality and performance of asphalt emulsion products.

## LIST OF REFERENCES

## LIST OF REFERENCES

- Alderson, A. 2009. "Update of the Austroads Sprayed Seal Design Method." Austroads Publication, No. APT-09-01, Sydney, Australia.
- Arizona Chapter Associated General Contractors (ACAGC). 2013. "Chip Seal Guide for Application and Construction." Pavement Preservation Committee, Phoenix, AZ.
- Asphalt Institute, Asphalt Emulsion Manufacturers Association (AEMA). 2008. "A Basic Asphalt Emulsion Manual." Manual Series No. 19, Third Edition, Lexington, KY.
- ASTM D7000. 2011. "Standard Test Method for Sweep Test of Bituminous Emulsion Surface Treatment Samples." ASTM International, West Conshohocken, PA.
- Banerjee, A. 2012. "Breaking and Curing Rates in Asphalt Emulsions." Ph.D. Dissertation, The University of Texas at Austin, Austin, TX.
- Banerjee, A, A de Fortier Smit, and JA Prozzi. 2012. "Modeling the effect of environmental factors on evaporative water loss in asphalt emulsions for chip seal applications." *Construction and Building Materials*, Vol 27(1), pp. 158–164.
- Baumgardner, G. 2006. "Asphalt Emulsion Manufacturing Today and Tomorrow." *Transportation Research Circular E-C102: Asphalt Emulsion Technology*, Washington, D.C., pp. 16-25.

- Brown, ER and Heitzman M. 2013. "Thin HMA Overlays for Pavement Preservation and Low Volume Asphalt Roads." National Center for Asphalt Technology, Auburn, AL.
- BSI. 2003. "Determination of Binder Aggregate Adhesivity by the Vialit Plate Shock Test Method." British Standard Institution, EN 12272-3, London, UK.
- Caltrans Division of Maintenance. 2014. "Caltrans Maintenance Technical Advisory Guide (MTAG)." Retrieved from Volume I - Flexible Pavement Preservation Second Edition Chapter 7 Chip Seals: <http://www.dot.ca.gov/hq/maint/FPMTAGChapter7-ChipSeals.pdf>
- Cole, MK and TJ Wood. 2014. "Effective Use of Chip Seals in Minnesota." TR News, January-February, Issue 290, pp.51-52.
- Connor, B. 1984. "Asphalt Surface Treatment and Sealing Parameters." Research Section, Division of Planning, Alaska Department of Transportation and Public Facilities, Fairbanks, AK.
- Federal Highway Administration (FHWA). 2003. "Pavement Preservation Compendium." Office of Asset Management, FHWA, Washington, D.C.
- Federal Highway Administration (FHWA). 2005. "Memorandum on Pavement Preservation Definitions." Office of Asset Management, FHWA, Washington, D.C.
- Galehouse, L, JS Moulthrop and RG Hicks. 2003. "Principles for Pavement Preservation: Definitions, Benefits, Issues and Barriers," TR News 228, pp. 4-9.



- Geoffroy, DN. 1996. "Synthesis of Highway Practice 223: Cost-effective Preventive Pavement Maintenance." Transportation Research Board, National Research Council, Washington, D.C.
- Gransberg, D and M Zama. 2002. "Comparing the Performance of Emulsion versus Hot Asphalt Cement Chip Seal Projects in the Texas Department of Transportation's Atlanta District." University of Oklahoma Transportation Research Report, Asphalt Emulsion Manufacturers Association Sponsored Research Report, Annapolis, MD.
- Gransberg, D, and DM James. 2005. "Synthesis 342: Chip Seal Best Practices, A Synthesis of Highway Practice." Transportation Research Board, National Research Council, Washington, D.C.
- Griffith, A., & Hunt, E. 2000. "Asphalt Cement Chip Seals in Oregon." Construction Report, Oregon Department of Transportation, Research Group, Salem, OR.
- Howard, IL, S Shuler, WS Jordan III, JM Hemsley, and K McGlumphy. 2011. "Correlation of Moisture Loss and Strength Gain in Chip Seals." Journal of the Transportation Research Board, No. 2207, pp. 49-57.
- Indiana Department of Transportation (INDOT). 2012. "Pavement Preservation." Fiscal Year 2012 Annual Report, Indianapolis, IN.
- Indiana Department of Transportation (INDOT). 2013. "Aggregate Properties." Standard and Specifications, Chapter 3, Indianapolis, IN.
- Indiana Department of Transportation (INDOT). 2015. "Aggregate for Seal Coat." 2016 Standard Specifications, Section 404 – Seal Coat (404-R-624), Indianapolis, IN.

- Indiana Department of Transportation (INDOT). 2016. "Chip Sealing." Maintenance Operations, Indianapolis, IN.
- James, A. 2006. "Overview of Asphalt Emulsion." Transportation Research Circular E-C102: Asphalt Emulsion Technology, Washington, D.C., pp. 1-15.
- Jordan III, W and I Howard. 2011. "Applicability of Modified Vialit Adhesion Test for Seal Treatment Specification." Journal of Civil Engineering and Architecture, Vol. 5, No. 3, pp. 215-223.
- Kadrmaz, A. 2006. "Emulsion Test Methods, Do We Need Them?" Transportation Research Circular E-C102: Asphalt Emulsion Technology, Washington, D.C., pp. 26-29.
- Layssi, H, P Ghods, A Alizadeh and M Salehi. 2015. "Electrical Resistivity of Concrete." Concrete International, May 2015, pp.41-46.
- Lee, J and T Shields. 2010. "Treatment Guidelines for Pavement Preservation." Joint Transportation Research Program, Indiana Department of Transportation and Purdue University, West Lafayette, IN.
- Lee, J, T Shields, and H Jun Ahn. 2011. "Performance Evaluation of Seal Coat Materials and Designs." Joint Transportation Research Program, Indiana Department of Transportation and Purdue University, West Lafayette, IN.
- Mahoney, JP, M Slater, C Keifenheim, J Uhlmeyer, T Moomaw and K Willoughby. 2014. "WSDOT Chip Seals—optimal timing, design and construction considerations." Washington State Transportation Center (TRAC), Washington State Department of Transportation, Olympia, WA.

- Moulthrop, J. 2003. "Pavement Preservation: Protecting the Investment." Northeast Asphalt User Producer Group (NEAUPG) Annual Meeting, Wilkes-Barre, PA.
- Needham, D. 1996. "Developments in Bitumen Emulsions Mixtures for Roads," Ph.D. dissertation, University of Nottingham, Nottingham, United Kingdom.
- New Zealand Transport Agency (NZTA). 2012. "Chip Seal Design in New Zealand." Wellington, New Zealand.
- North Carolina Department of Transportation (NCDOT). 2015. "Chip Seal Best Practices Manual." Raleigh, NC.
- Padfield, J, J Handy and J Stephens. 2014. "Seal Coat Productivity." Joint Transportation Research Program, Indiana Department of Transportation and Purdue University, West Lafayette, IN.
- Read, J and Whiteoak, D. 2010. "Chapter 6 Bitumen Emulsions." The Shell Bitumen Handbook Fifth Edition, Thomas Telford Publishing, London, pp. 91 – 118.
- Road Surface Treatments Association (RSTA). 2014. "Code of Practice for Surface Dressing." Association of Directors of Environment, Economy, Planning and Transport, Wolverhampton, UK.
- Shahidi, S. 2013. "An Electrochemical Impedance Spectroscopic Diagnostic Device for Characterization of Liquid-Liquid Systems and Phase Separation Detection in Emulsions." M. Sc. Dissertation, Department of Mechanical Engineering, University of Alberta, Edmonton, Alberta.
- Shuler, S. 1999. "Design and Construction of Chip Seals for High Traffic Volume." Flexible Pavement Rehabilitation and Maintenance, ASTM Special Technical Publication, Issue 1348, pp. 96-114.

- Shuler, S. 2011. "When to Broom or Remove Traffic Control Safely on Fresh Emulsified Asphalt Chip Seals." *Journal of the Transportation Research Board*, Issue 2235, pp. 82-87.
- Shuler, S, A Lord, A Epps-Martin and D Hoyt. 2011. "Manual for Emulsion-Based Chip Seals for Pavement Preservation." NCHRP Report 680, Transportation Research Board, Washington, D.C.
- Singh, Y. 2013. "Electrical Resistivity Measurements: A Review." *International Journal of Modern Physics: Conference Series*, International Conference on Ceramics, Vol 22, pp. 745-756, Bikaner, India.
- Sinha, KC, S Labi, M Rodriguez, G Tine, and R Dutta. 2005. "Procedures for the Estimation of Pavement and Bridge Preservation Costs for Fiscal Planning." Joint Transportation Research Program, Indiana Department of Transportation and Purdue University, West Lafayette, IN.
- Sowa, J, P Sheng, M Zhou, T Chen, A Serres, and M Sieben. 1995. "Electrical properties of bitumen emulsions." *Fuel*, Vol. 74, No. 8, pp. 1176 - 1179.
- Spragg, RP. 2013. "The rapid assessment of transport properties of cementitious materials using electrical methods." Master Degree Dissertation, Purdue University, West Lafayette, IN.
- Stamm, AJ. 1927. "The Electrical Resistance of Wood as a Measure of Its Moisture Content." *Industrial and Engineering Chemistry*, Vol 19(9), pp. 1021-1025.

- Takamura, K and A James. 2015. "Paving with Asphalt Emulsions." *Advances in Asphalt Materials, Road and Pavement Construction*, Woodhead Publishing Series in Civil and Structural Engineering, Number 56, Elsevier Ltd, United Kingdom, pp. 393-426.
- Testa, DM and M Hossain. 2014. "Kansas Department of Transportation 2014 Chip Seal Manual." Kansas State University Transportation Center, Kansas Department of Transportation, Topeka, KS.
- Texas Department of Transportation (TxDOT). 2003. "Seal Coat and Surface Treatment Manual." Austin, TX.
- Tompkins, B. 2013. "How To Develop and Implement a Successful In-House Chip Seal Program." Purdue Road School, West Lafayette, IN.
- Victorian State Road Authority (VICROADS). 2004. "Bituminous Sprayed Surfacing Manual." General Manager - Road System Management VicRoads, Kew, Australia.
- Washington State Department of Transportation (WSDOT). 2003. "Asphalt Seal Coats." Washington State Technology Transfer (T2) Center, Olympia, WA.
- Waters, EH. 1974. "Determining the moisture content on concrete: the use of electrical resistance methods." *Building Science*, Vol 9(4), pp. 289-297.
- Wegman, D. 1991. "Design and Construction of Seal Coats." Minnesota Department of Transportation, Mendota Heights, MN.
- Williams, THL. 1980. "An automatic electrical resistance soil-moisture measuring system." *Journal of Hydrology*, Vol 46(3), pp. 385-390.

- Wood, TJ, DW Janisch, and FS Gaillard. 2006. "Minnesota Seal Coat Handbook 2006." Minnesota Department of Transportation, Maplewood, MN.
- Wood, TJ, and R Olson. 2007. "Rebirth of Chip Sealing in Minnesota." Journal of the Transportation Research Board, No. 1989, Transportation Research Board of the National Academies, Washington, D.C., pp. 260–264.
- Yaacob, H, FL Chang, M Rosli Hainin, and RP Jaya. 2015. "Curing of Asphalt Emulsified Tack Coat Subjected to Malaysian Weather Conditions." Journal of Materials in Civil Engineering, Vol 27(4), pp. 1-10.

## APPENDICES

## Appendix A. INDOT's Chip Seal Aggregate Gradation

Table A.1: INDOT's Chip Seal Aggregate Gradation

Sieve size (mm)	Percent passing (%)			
	SC 11	SC 12	SC 13	SC 16
12.5	100	100	100	100
9.50	75 - 95	95 - 100	100	94 - 100
4.75	10 - 30	50 - 80	80 - 90	15 - 45
2.36	0 - 10	0 - 35	8 - 12	
1.18			0 - 2	0 - 4
0.60				
Decant	0 - 1.5	0 - 1.5	0 - 1.5	0 - 1.5



## Appendix B. Sweep Test Specimens

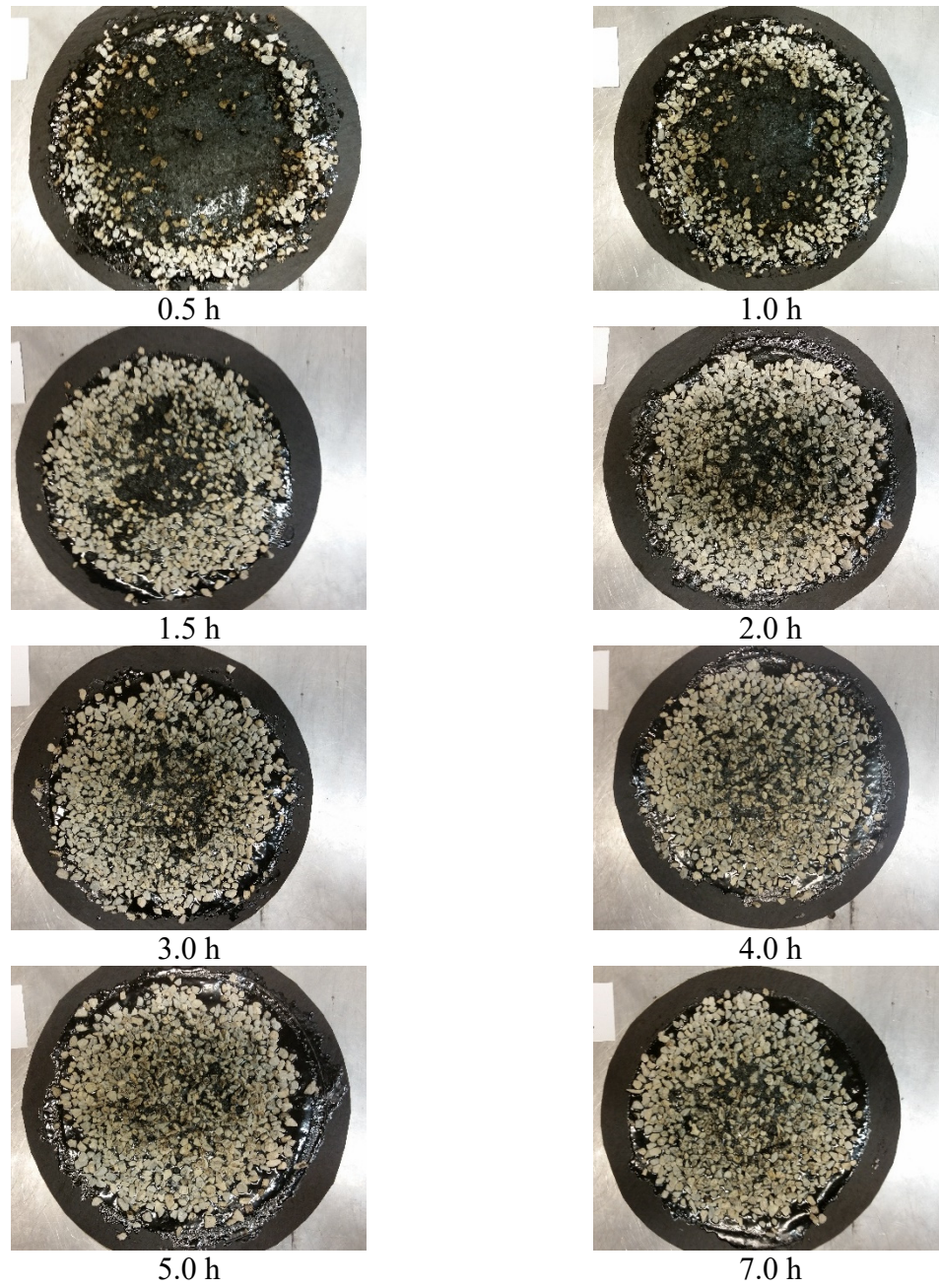


Figure B.1: AE-90S SC 16 Limestone.

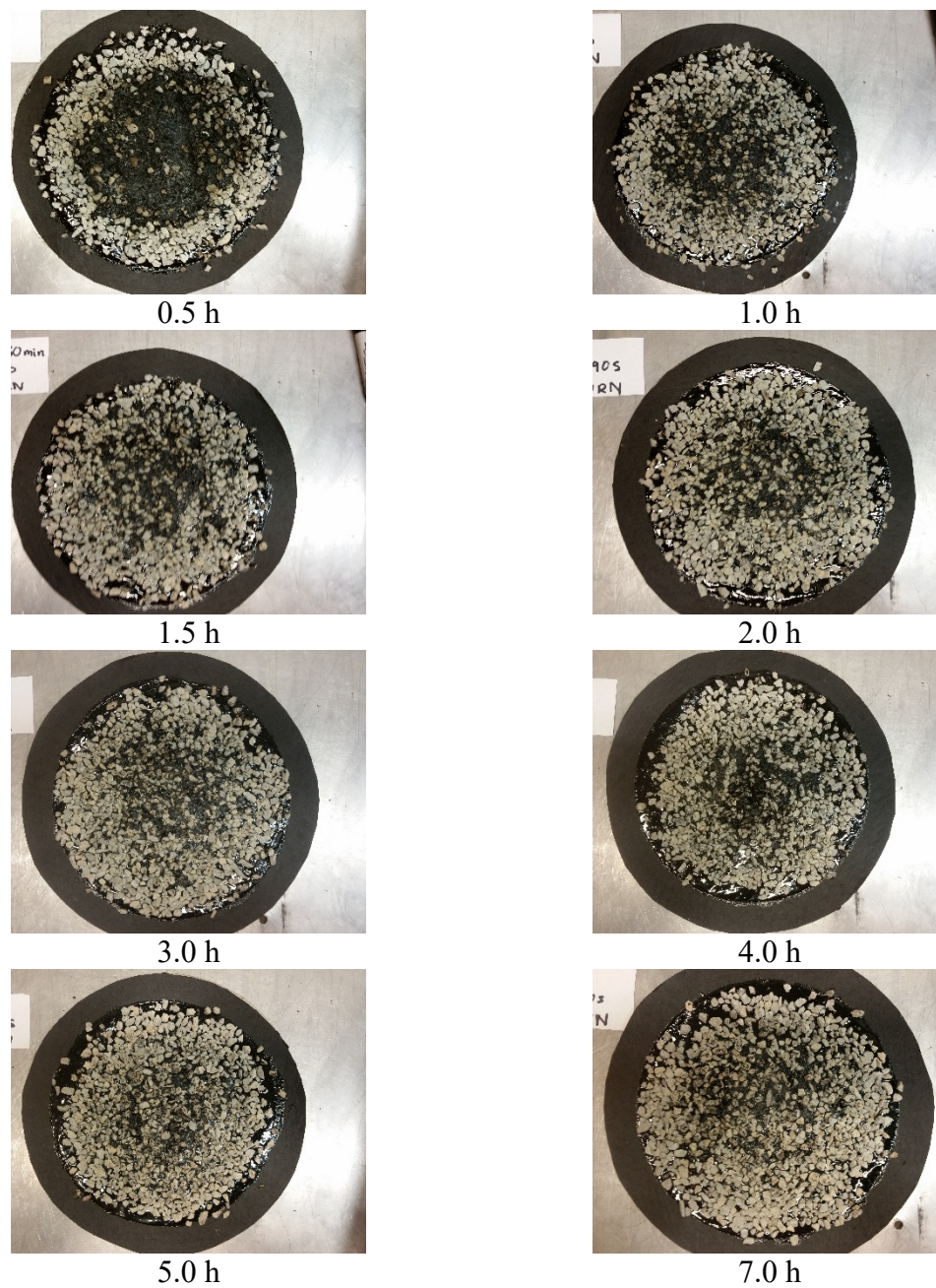
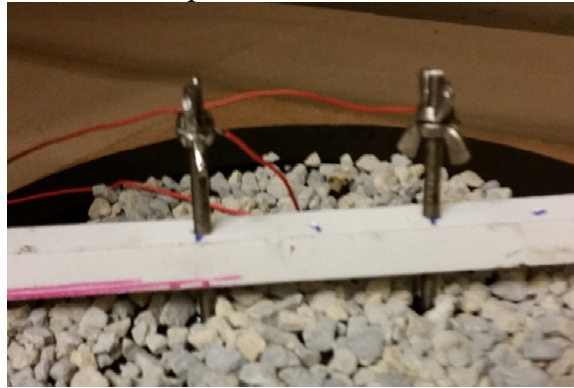


Figure B.2: AE-90S SC 16 Dolomite.





Specimens at oven.



Two-point probe.



Sweep Test.

Figure B.3: AE-90S SC 11 Limestone.

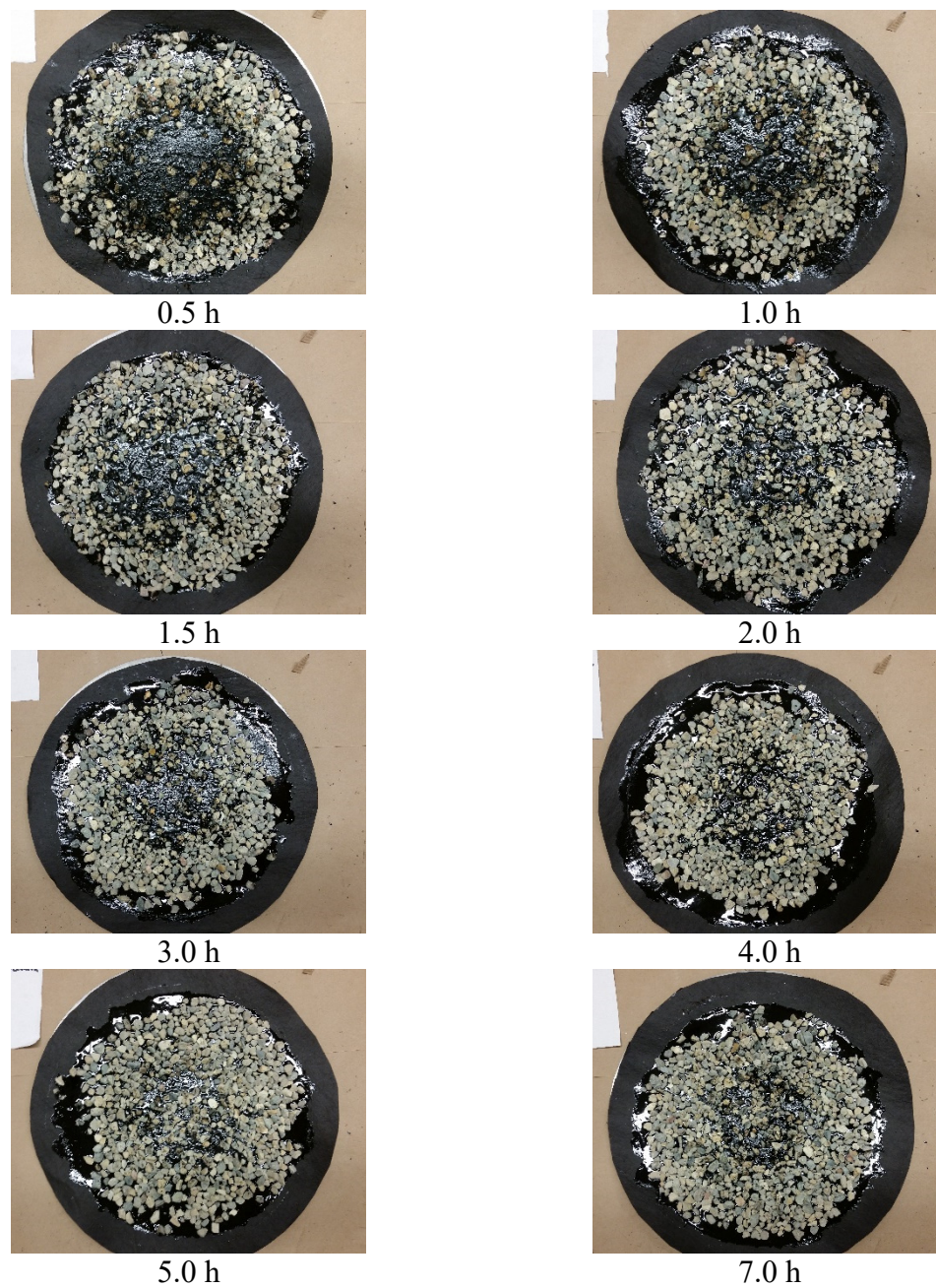


Figure B.4: AE-90S SC 16 Gravel.



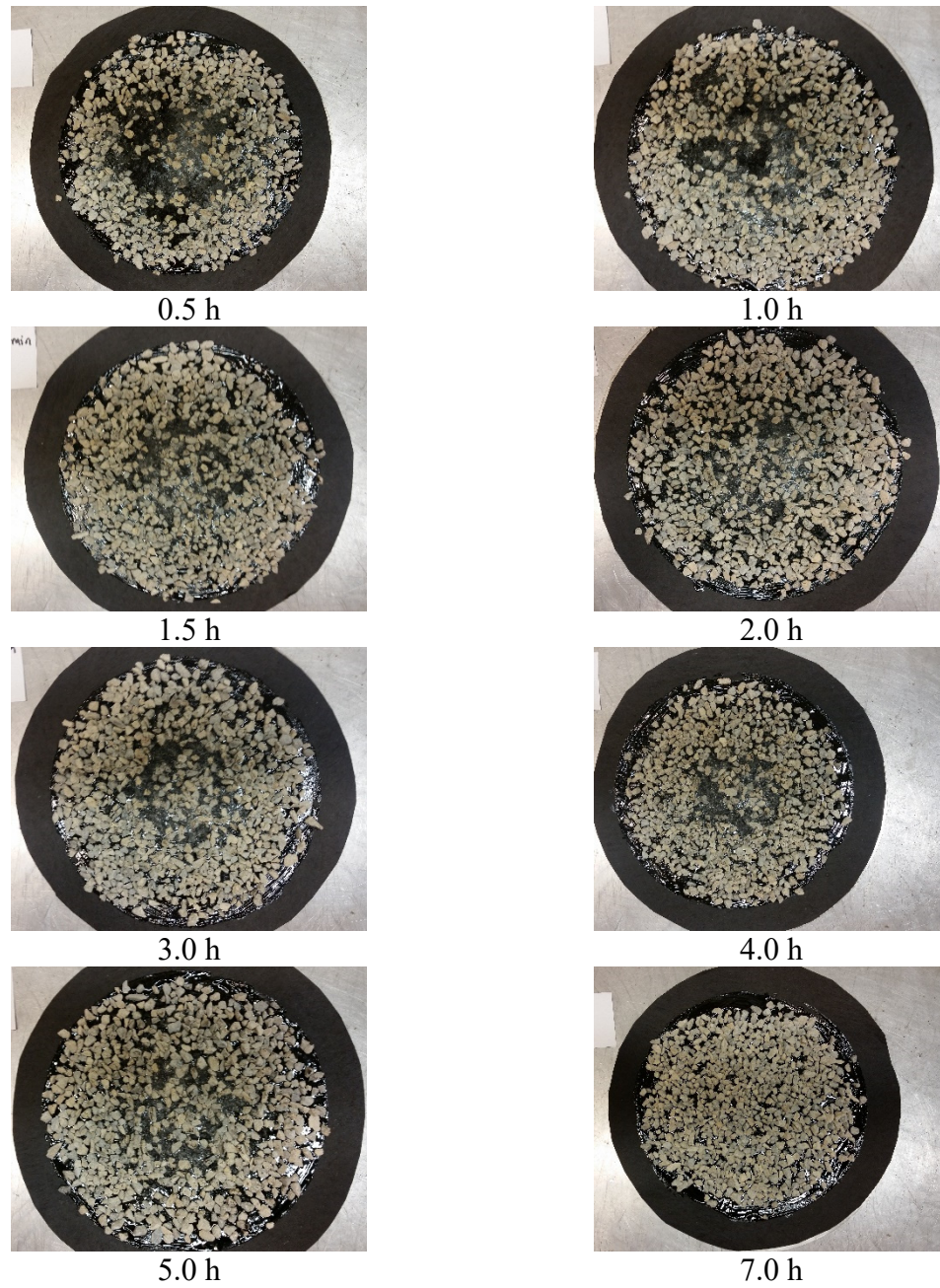


Figure B.5: CRS-2P SC 16 Limestone.

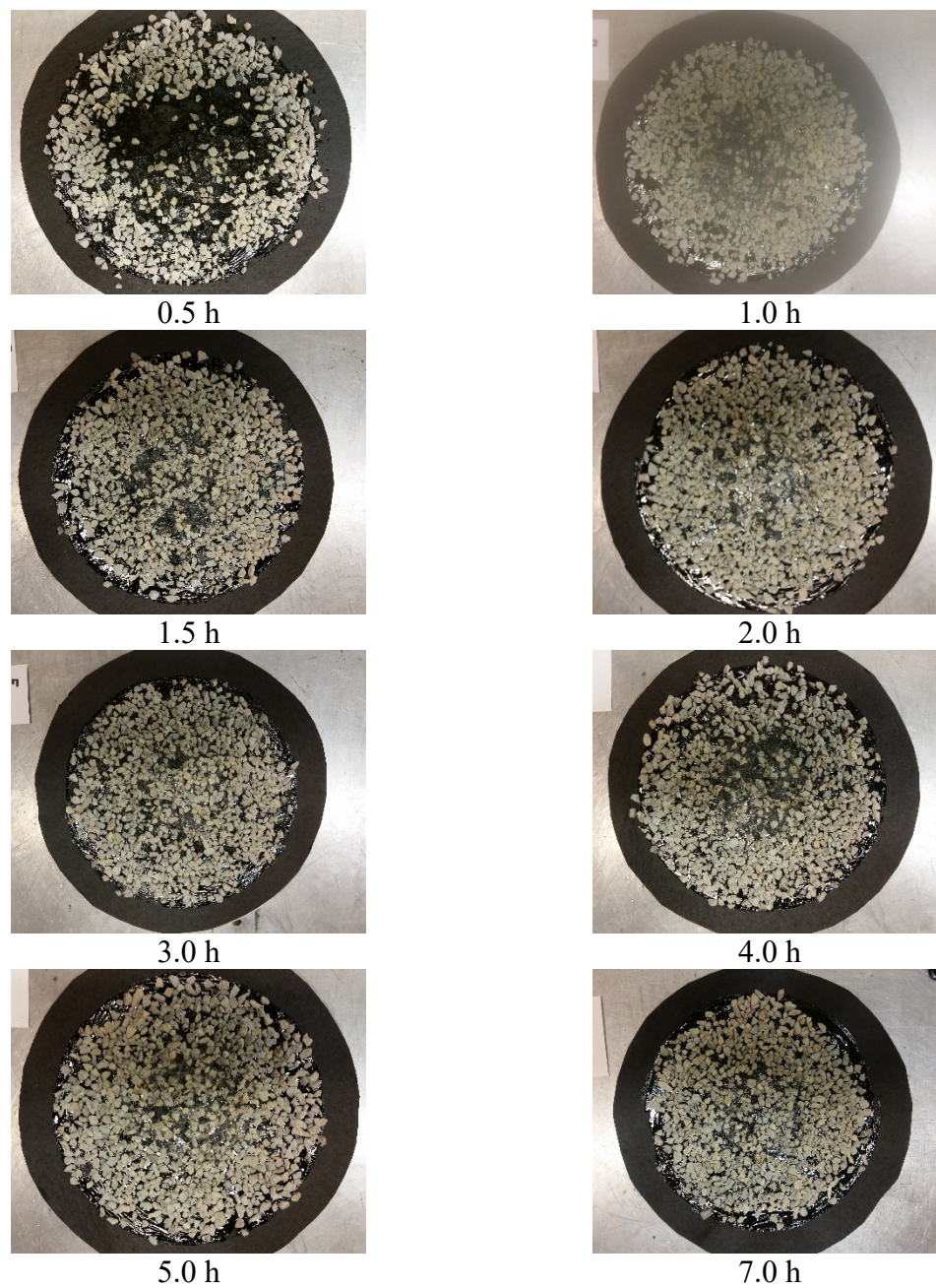


Figure B.6: CRS-2P SC 16 Dolomite.



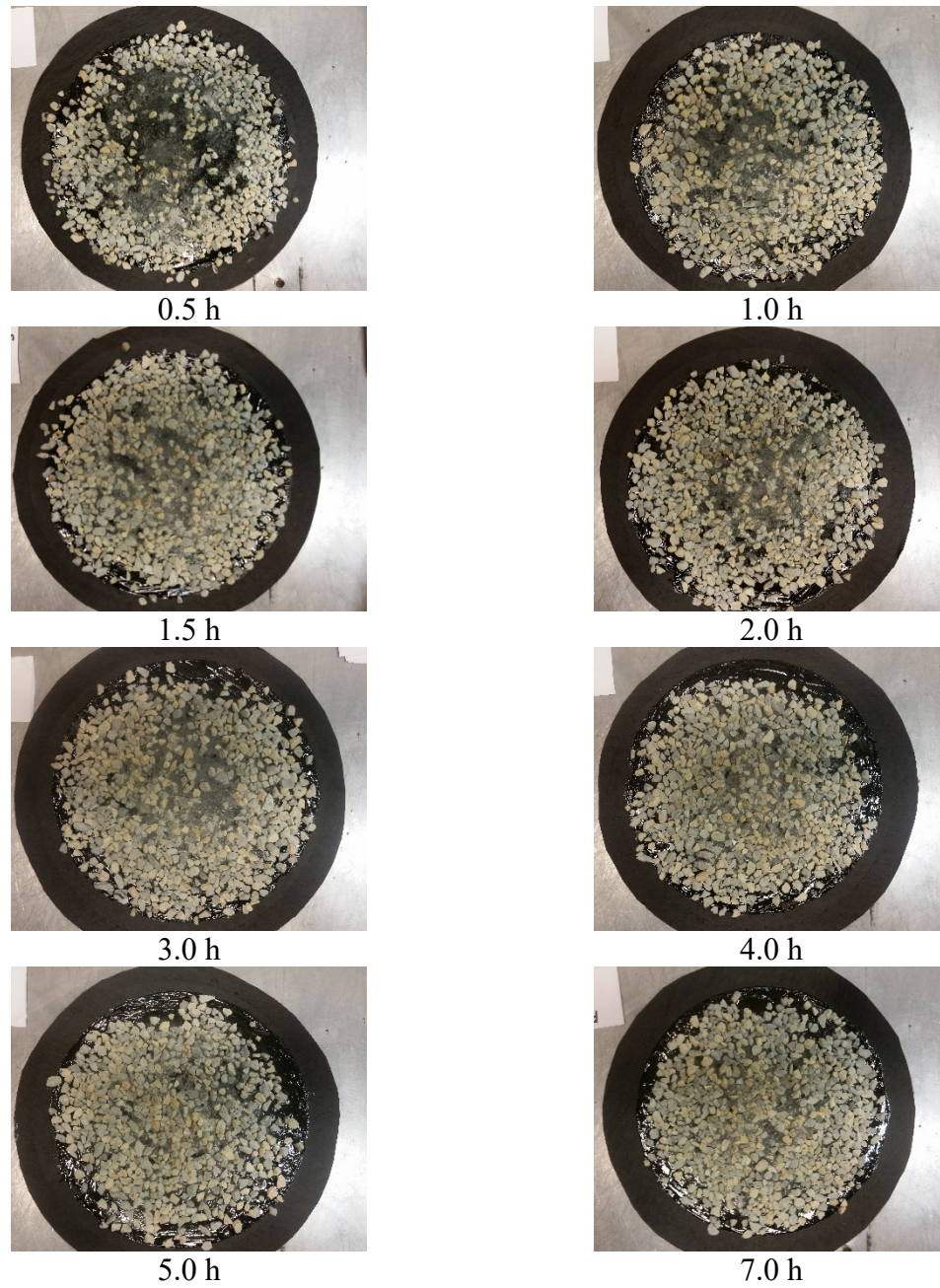


Figure B.7: CRS-2P SC 11 Limestone.

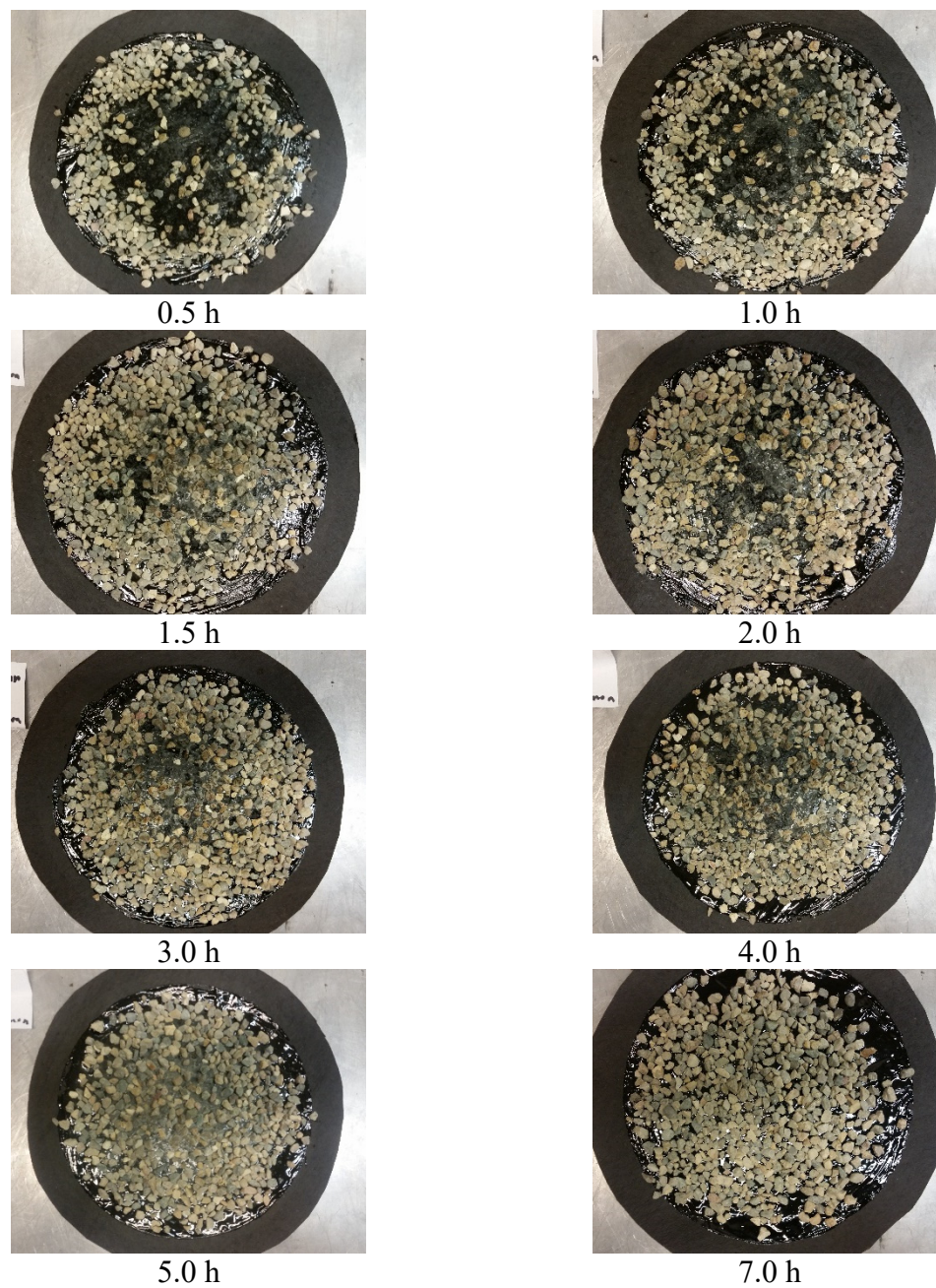


Figure B.8: CRS-2P SC 16 Gravel.



## Appendix C. Vialit Test Specimens

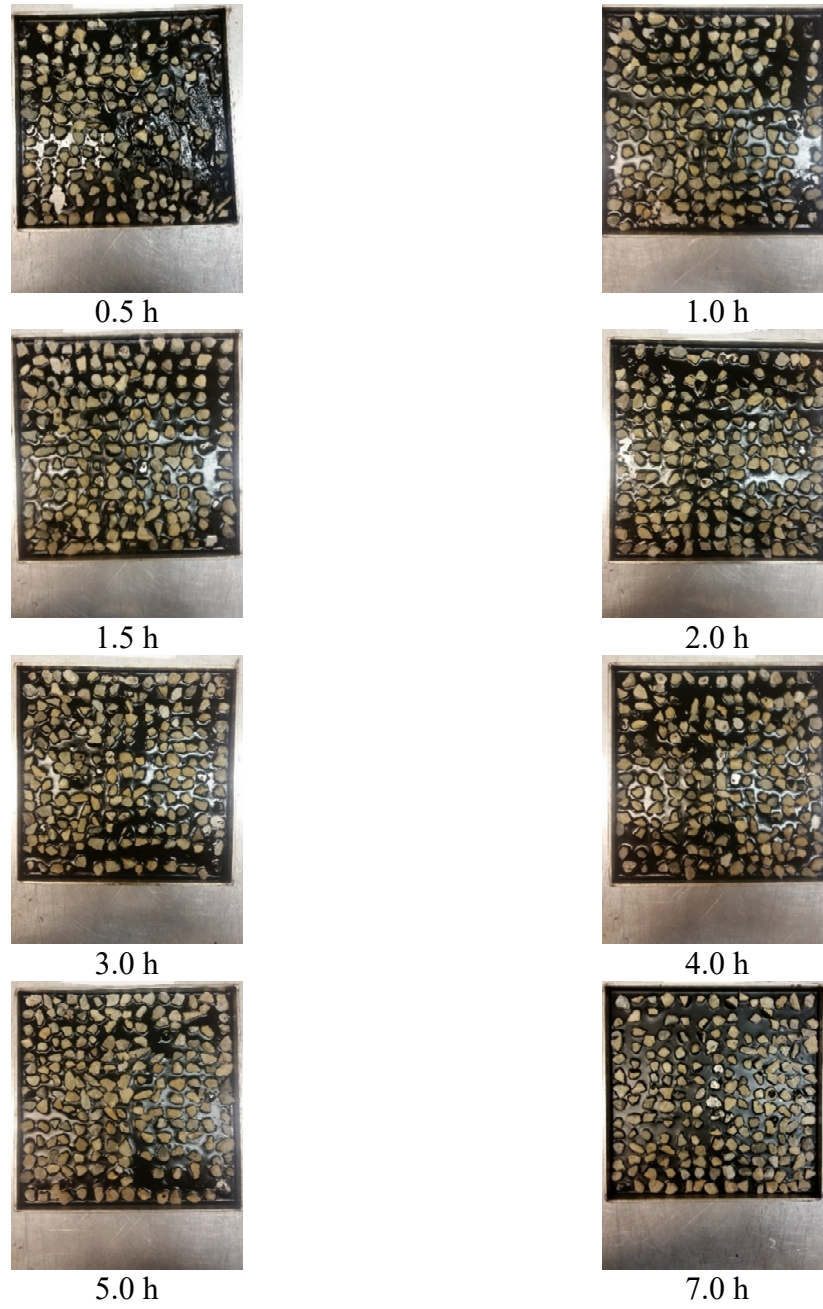


Figure C.1: AE-90S SC 16 Limestone.

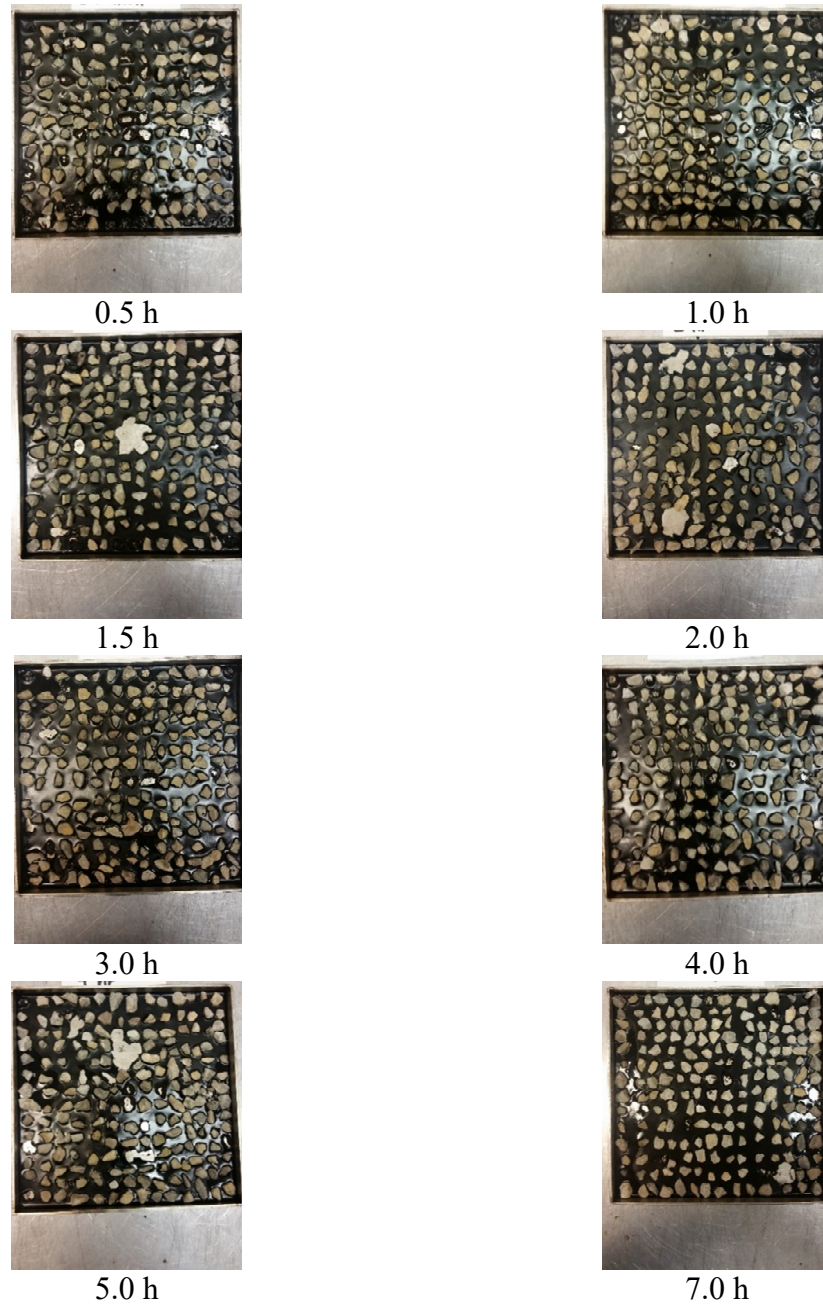


Figure C.2: AE-90S SC 16 Dolomite.

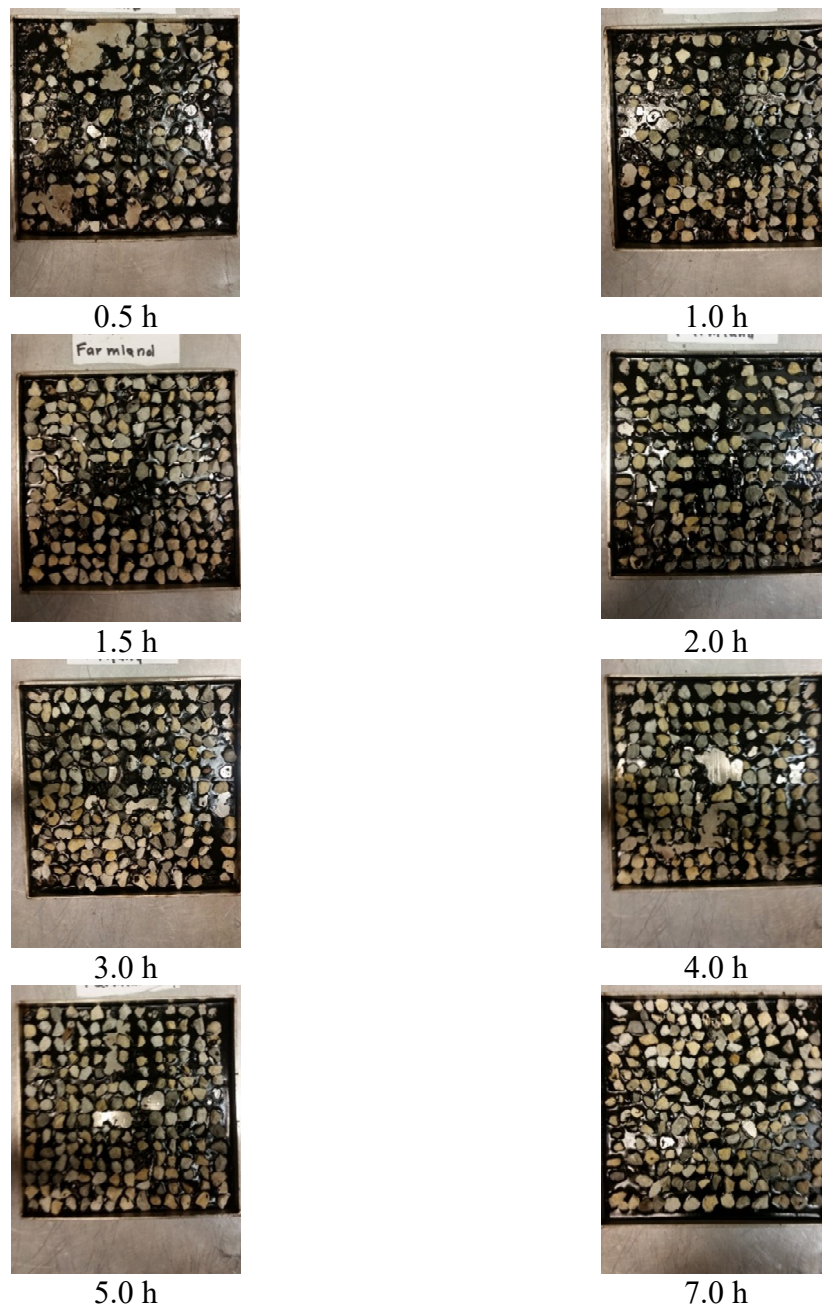


Figure C.3: AE-90S SC 11 Limestone.



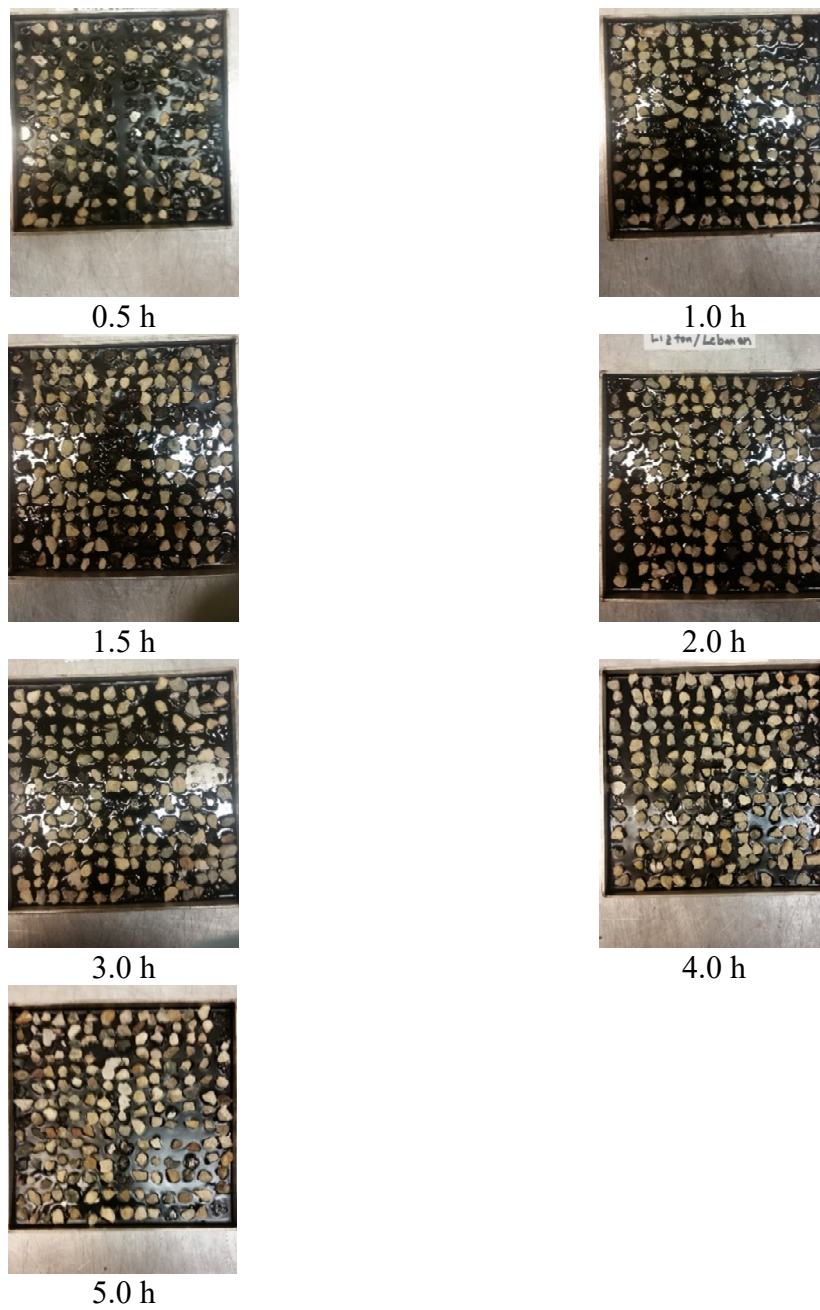


Figure C.4: AE-90S SC 11 Gravel.

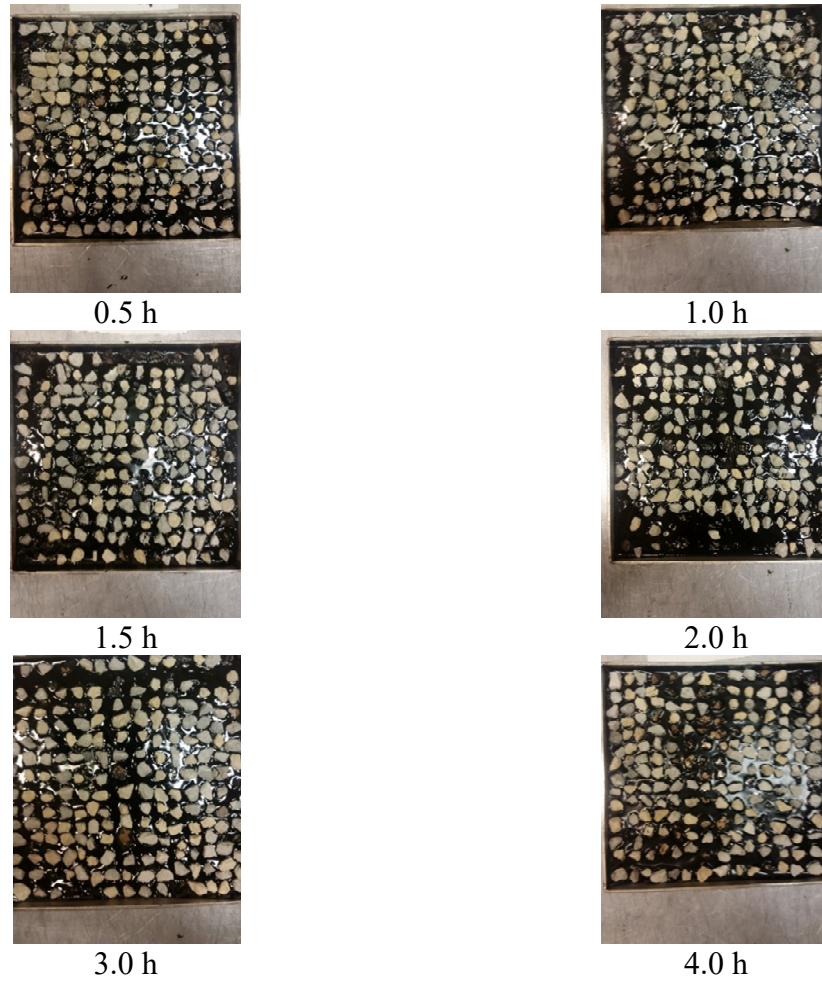


Figure C.5: CRS-2P SC 11 Limestone.

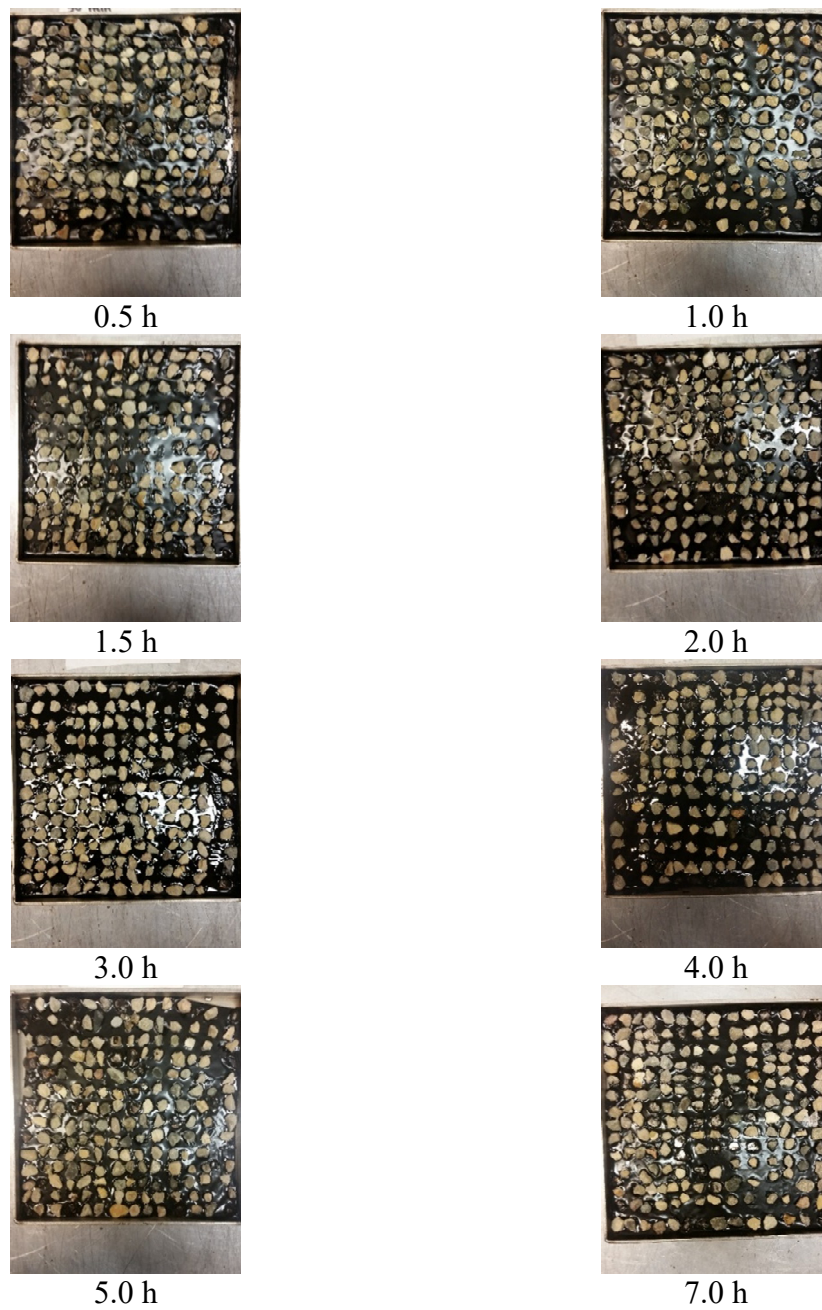


Figure C.6: CRS-2P SC 16 Gravel.